CCSP Synthesis and Assessment Product 1.2

Past Climate Variability and Change in the Arctic and at High Latitudes

Chapter 5 — Temperature and Precipitation History of the Arctic

Chapter Lead Authors:

Gifford Miller, University of Colorado, Boulder, CO

Julie Brigham-Grette, University of Massachusetts, Amherst , MA

Contributing Authors:

Lesleigh Anderson, U.S.Geological Survey

Henning Bauch, GEOMAR, University of Kiel

Mary Anne Douglas, University of Alberta

Mary E. Edwards, University of Southampton

Scott Elias, Royal Holloway, University of London

Bruce Finney, University of Alaska-Fairbanks

Svend Funder, University of Copenhagen

Timothy Herbert, Brown University

Larry Hinzman, University of Alaska-Fairbanks

Darrell Kaufman, University of Northern Arizona

Glen MacDonald, University of California-Los Angeles

Alan Robock, Rutgers University

Mark Serreze, University of Colorado

John Smol, Queen's University

Robert Spielhagen, GEOMAR, University of Kiel

Alexander P. Wolfe, University of Alberta

Eric Wolff, British Antarctic Survey

ABSTRACT

The Arctic has undergone dramatic changes in temperature and precipitation during the Cenozoic Era, the past 65 million years (m.y.) of Earth history. Arctic summer temperature changes during this interval exceeded global average temperature changes during both warm times and cold times, which supports the concept of Arctic amplification. (Strong positive feedbacks—processes that amplify the effects of a change in the controls on global temperature—produce larger changes in temperature in the Arctic than elsewhere). Warm times in the past, those periods when the Arctic was either mildly or substantially warmer than at present in either summer or winter season, help to constrain scenarios for future warming in the Arctic. Past warm times are rarely ideal analogues of future warming because the boundary conditions (such as continental positions and topography) during past times of exceptional warmth were quite different. Nevertheless, paleoclimate records help to define the climate sensitivity of the planet and to quantify Arctic amplification.

At the start of the Cenozoic, 65 million years ago (Ma), the planet was ice free; there was no sea ice in the Arctic Ocean and neither a Greenland nor an Antarctic ice sheet. General cooling through the Cenozoic is attributed mainly to a slow decrease in greenhouse gases in the atmosphere. As the Arctic cooled, high-elevation mountain glaciers formed as did seasonal sea ice in the Arctic Ocean, but a detailed record of changes in the Arctic is available only for the last few million years. A global warm period that affected both seasons in the middle Pliocene, about 3.5 Ma, is well represented in the Arctic; at that time extensive deciduous forests occupied lands that

now support only polar desert and tundra. Global oceanic and atmospheric circulation was substantially reorganized between 3 and 2.5 Ma, and that reorganization was accompanied by the development of the first continental ice sheets throughout North America and Eurasia. Icebergs from these ice sheets delivered rock fragments into the central North Atlantic Ocean. This change marks the onset of the Quaternary Period (2.6–0 Ma), generally equated with “ice-age” time. From about 2.7 to about 0.8 Ma, the ice sheets came and went about every 41 thousand years (k.y.), the same timing as changes in the ongoing tilt of Earth’s axis. Ice sheets grew when Earth’s tilt was at a minimum, and they melted when tilt was at a maximum. For the past 800 k.y., ice sheets have grown larger and ice age times have been longer, lasting about 100 ka; those icy intervals have been separated by brief warm periods of about 10 k.y. duration. The cause of this shift is debated. The relatively warm interval during which human civilization developed is the most recent of these 10 k.y. warm intervals, the Holocene (about 11.5–0 ka). During the penultimate warm interval, about 130–120 ka, solar energy in summer in the northern high latitudes was greater than at any time in the current warm interval. As a consequence, the Arctic summer was about 5°C warmer than at present and almost all glaciers melted completely except for the Greenland Ice Sheet, and even it was reduced in size substantially from its present extent. Although sea ice is difficult to reconstruct, the evidence suggests that the central Arctic Ocean retained some permanent ice cover or was periodically ice free, even though the flow of warm Atlantic water into the Arctic Ocean may have been greater than during the present warm interval.

The last glacial maximum peaked about 20 ka when parts of the Arctic were as much as 20°C colder than at present. Ice recession was well underway by 16 ka, and most of the Northern Hemisphere ice sheets had melted by 7 ka. Solar energy due to Earth's proxity to the Sun in summer rose in the Arctic steadily from 20 ka to a maximum (10% higher than at present) about 11 ka and has been decreasing since then, as the precession of the equinoxes has tilted the Northern Hemisphere farther from the sun in summer. The extra energy received in early Holocene summers warmed summers throughout the Arctic about 1°–3°C above 20th century averages, enough to completely melt many small glaciers throughout the Arctic (although the Greenland Ice Sheet was only slightly smaller than present). Summer sea ice limits were substantially smaller than their 20th century average, and the flow of Atlantic water into the Arctic Ocean was substantially greater. As summer solar energy decreased in the second half of the Holocene, glaciers re-established or advanced, sea ice extended, and the flow of warm Atlantic water into the Arctic Ocean diminished. Late Holocene cooling reached its nadir during the Little Ice Age (about 1250–1850 AD), when most Arctic glaciers reached their maximum Holocene extent. During the warming of the past century and a half, glaciers have receded throughout the Arctic, terrestrial ecosystems have advanced northward, and perennial Arctic Ocean sea ice has diminished.

Paleoclimate reconstructions of Arctic temperatures, compared with global temperature changes during four key intervals in the past 4 m.y., allow a quantitative estimate of Arctic amplification. These data suggest that Arctic temperature change is three to four times as large as the global average temperature change during both warm and cold intervals. If global warming forecasts are correct, this relation indicates that Arctic temperatures are likely to increase dramatically in the next century.

5.1 Introduction

Recent instrumental records show that during the last few decades, temperatures throughout much of the far north have risen more rapidly than temperatures in lower latitudes and usually about twice as fast (Delworth and Knutson, 2000; Knutson et al., 2006). The remarkable reduction in Arctic Ocean summer sea ice in 2007 (Figure 5.1) has outpaced the most recent predictions from available climate models (Stroeve et al., 2008), but it is in concert with widespread reductions in glacier length, increased borehole temperatures, increased coastal erosion, changes in vegetation and wildlife habitats, the northward migration of marine life, and degradation of permafrost. On the basis of the past century's trend of increasing greenhouse gases, climate models forecast continuing warming into the foreseeable future (Figure 5.2) and a continuing amplification in the Arctic of global changes (Serreze and Francis, 2006). As outlined by the Arctic Climate Impact Assessment (ACIA, 2004), the sensitivity of the Arctic to changed forcing is due to strong positive feedbacks in the Arctic climate system (see Chapter 4.3). These feedbacks strongly amplify changes to the climate of the Arctic and also affect the global climate system.

FIGURE 5.1 NEAR HERE

FIGURE 5.2 NEAR HERE

Because strong Arctic feedbacks act on climate changes caused by either nature or by humans, natural variability and human-caused changes are large in the Arctic, and separating them requires understanding and characterization of its natural variability. The short time interval for which instrumental data are available in the Arctic is not sufficient to characterize that natural variability, so a paleoclimatic perspective is required.

This chapter focuses primarily on the history of temperature and precipitation in the Arctic. These topics are important in their own right, and they also set the stage for understanding the histories of the Greenland Ice Sheet and the Arctic sea ice, which are described in Chapters 7 (Greenland Ice Sheet) and 8 (sea ice). Because of the great interest in rates of change, and because of some technical details in extracting rate of change from the broad history of temperature or precipitation, careful consideration of rates of change is deferred to Chapter 6 (past rates of Arctic climate change).

Before providing the history of temperature and precipitation in the Arctic, this chapter supplements the discussion in Chapter 4 (paleoclimate concepts) on forcings, feedbacks, and proxies by providing additional information on those aspects particularly relevant to the histories of temperature and precipitation in the Arctic. The climate history of the past 65 m.y. is then summarized; it focuses on temperature and precipitation changes that span the full range of the Arctic's natural climate variability and response under different forcings. We place special emphasis on relevant intervals in the past with a mean climate state warmer than our own. Where possible, we discuss causes of these changes. From these summaries, it is possible to estimate the magnitude of polar amplification and to characterize how the Arctic system responds to global warm times.

5.2 Feedbacks Influencing Arctic Temperature and Precipitation

The most commonly used measure of the climate is the mean surface air temperature **(**Figure 5.3**)**, which is influenced by climate forcings and climate feedbacks. As discussed with references in Chapter 4.2, important forcings during the past several millennia have been changes in the distribution of solar radiation that resulted from features of Earth's orbit; volcanism; and changes in atmospheric greenhouse-gas concentrations. On longer time scales (tens of millions of years), the long-term increase in the solar constant (a 30% increase in the past 4600 m.y.) was important, and the redistribution of continental landmasses caused by plate motions also affected the planetary energy balance.

FIGURE 5.3 NEAR HERE

How much the temperature changes in response to a forcing of a given magnitude (or in response to the net magnitude of a set of forcings in combination) depends on the sum of all of the feedbacks. Feedbacks may act in days or less or endure for millions of years. The focus here is on faster feedbacks. For example, a warming may have many causes (such as brighter sun, higher concentration of greenhouse gases in the atmosphere, less blocking of the sun by volcanoes). Whatever the cause, warmer air moving over the ocean tends to entrain more water vapor, which itself is a greenhouse gas, so more water vapor in the atmosphere leads to a further rise in global mean surface temperature (Pierrehumbert et al., 2007). The discussion below focuses on those feedbacks that are especially linked to the Arctic. We include several processes linked to ice-age cycling here, because of the dominant role of northern land in supporting ice-sheet growth, although ice-age processes (like some of the other processes discussed below) clearly extend well beyond the Arctic.

5.2.1 Ice-albedo feedback

Ice and snow present highly reflective surfaces. The albedo of a surface is defined as the reflectivity of that surface to the wavelengths of solar radiation. Fresh ice and snow have the highest albedo of any widespread surfaces on the planet (Figure 5.4), so it is apparent that changes in the seasonal and areal distribution of snow and ice will exert strong influences on the planetary energy balance (Peixoto and Oort, 1992). Open ocean, on the other hand, has a low albedo; it absorbs almost all solar energy when the sun angle is high. Changes in albedo are most important in the Arctic summer, when solar radiation is at a maximum, whereas changes in the winter albedo have little influence on the energy balance because little solar radiation reaches the surface then. In general, warming reduces ice and snow whereas cooling allows them to extend, so the changes in ice and snow act as positive feedbacks to amplify climate changes (e.g., Lemke et al., 2007).

FIGURE 5.4 NEAR HERE

5.2.2 Ice-insulation feedback

In addition to its effects on albedo, sea ice also causes a positive insulation feedback, primarily in the wintertime. Ice effectively blocks heat transfer between relatively warm ocean (at or above the freezing point of seawater) and cold atmosphere (which, in the Arctic winter, averages –40°C (Chapman and Walsh, 2007). If sea ice is thinned by warming, then the ocean heats the overlying atmosphere in winter months, amplifying that warming.

Feedbacks involving snow insulation of the ground may also be important, through their effects on vegetation and on permafrost temperature and its influence on storage or release of greenhouse gases, as described in the next subsections (e.g., Ling and Zhang, 2007).

5.2.3 Vegetation feedbacks

A related terrestrial feedback involves changing vegetation. A warming climate can cause tundra to give way to shrub vegetation. However, the shrub vegetation has a lower albedo than tundra, and the shrubs thus cause further warming (Figure 5.5) (Chapin et al., 2005; Goetz et al., 2007). Interactions involving the boreal forest and deciduous forest can also be important. When, as a result of warming, deciduous forest replaces evergreen boreal forest, then winter surface albedo increases—an example of a negative feedback to the warming climate.(Bonan et al., 1992; Rivers and Lynch, 2004).

FIGURE 5.5 NEAR HERE

5.2.4 Permafrost feedbacks

Additional but poorly understood feedbacks in the Arctic involve changes in the extent of permafrost and how changes in cloud cover interact both with permafrost and with the release of carbon dioxide and methane from the land surface. Feedbacks between permafrost and climate became widely recognized only in recent decades (building on the works of Kvenvolden, 1988; 1993; MacDonald, 1990, and Haeberli et al., 1993. As permafrost thaws under a warmer summer climate (Figure 5.6), it may release much more greenhouse gases such as CO_2 and methane from the decomposition of organic matter previously sequestered in permafrost and in widespread Arctic yedoma deposits (e.g., Vörösmarty, 2001; Thomas et al., 2002, Smith et al., 2004, Archer, 2007; Walter et al., 2007). Because CO_2 and methane are greenhouse gases, atmospheric temperature is likely to increase in turn, a positive feedback. Walter et al. (2007) suggest that methane bubbling from the thawing of newly formed thermokarst lakes across parts of the Arctic during deglaciation may account for as much as 33–87% of the increase in atmospheric methane measured in ice cores. Such a release would have contributed a strong positive feedback to warming during the last deglaciation, and it likely continues today (Walter et al., 2006).

FIGURE 5.6 NEAR HERE

5.2.5 Freshwater balance feedbacks and thermohaline circulation

The Arctic Ocean is almost completely surrounded by continents (Figure 5.7). Because precipitation is low over the ice-covered ocean (Serreze et al., 2006), the freshwater input to the Arctic Ocean largely derives from the runoff from large rivers in Eurasia and North America and by the inflow of relatively low-salinity Pacific water through the Bering Strait. The Yenisey, Ob, and Lena are among the nine largest rivers on Earth, and there are several other large rivers, such as the Mackenzie, that feed into the Arctic Ocean (see Vörösmarty et al., 2008). The freshwater discharged by these rivers maintains low salinities on the broad, shallow, and seasonally ice-free seas bordering the Arctic Ocean. The largest of these border the Eurasian continent, where they serve as the dominant area in the Arctic Ocean in which sea ice is produced (for some fundamentals on Arctic sea ice, see Barry et al., 1993). Sea ice forms along the Eurasian margin and then drifts toward Fram Strait; transit time is 2–3 years in the current regime. In the Amerasian part of the Arctic Ocean, the clockwise-rotating Beaufort Gyre is the dominant ice-drift feature (see Figure 8.1).

However, the transport pathway for most of the freshwater entering the Arctic Ocean is the ocean's surface layer (its upper 50 m) (e.g., Schlosser et al., 2000). Low-salinity surface waters are exported from the Arctic Ocean to the northern North Atlantic (Nordic Seas) through western Fram Strait, after which they follow the east coast of Greenland and exit the Nordic Seas through Denmark Strait. A smaller volume of freshwater flows out through the inter-island channels of the Canadian Arctic Archipelago, and it eventually reaches the North Atlantic through the Labrador Sea. The low-saline outflow from the Arctic Ocean is compensated by a relatively warm inflow of saline Atlantic water through eastern Fram Strait. Despite its warmth, Atlantic water has sufficient density due to its high salinity that it is forced to sink beneath the colder, but much fresher, surface water upon entering the Arctic Ocean. North of Svalbard, Atlantic water spreads as a boundary current into the Arctic Basin and forms the Atlantic Water Layer (Morison et al., 2000). The strong vertical gradients of salinity and temperature in the Arctic Ocean produce a relatively stable stratification. However, recent observations have shown that in some areas in the Eurasian part of the Arctic Ocean, the warm Atlantic layer is in direct contact with the surface mixed layer (Rudels et al., 1996; Steele and Boyd, 1998; Schauer et al., 2002), thereby promoting vertical heat transfer to the Arctic atmosphere in winter. In recent decades circum-Arctic glaciers and ice sheets have been losing mass (more snow and ice melting in summer than accumulates as snow in winter) (Dowdeswell et al., 1997; Rignot and Thomas, 2002; Meier et al., 2007), and since the 1930s river runoff to the Arctic Ocean has been increasing (Peterson et al., 2002). Both factors increase the export of freshwater from the Arctic Ocean (Peterson et al., 2006). Recent studies suggest that changes in river runoff strongly influence the stability of Arctic Ocean stratification (Steele and Boyd, 1998; Martinson and Steele, 2001; Björk et al., 2002; Boyd et al., 2002; McLaughlin et al., 2002; Schlosser et al., 2002).

In the North Atlantic, primarily in the Nordic Seas and the Labrador Sea, wintertime cooling of the relatively warm and salty waters increases its density. The denser waters then sink and flow southward to participate in the global thermohaline circulation ("thermo" for temperature and "haline" for salt, the two components that determine density. This circulation system also is referred to as the meridional overturning circulation (MOC)). Continuing surface inflow from the south, which replaces the water sinking in the Nordic and Labrador Seas, promotes persistent open water rather than sea ice in these regions. In turn, this lack of sea ice promotes notably warmer conditions, especially in wintertime, over and near the North Atlantic and extending downwind across Europe and beyond (Seager et al., 2002). Salt rejected from sea ice growing nearby also may contribute to increasingly dense sea water and to its sinking.

If the surface waters are made sufficiently less salty by an increase in freshwater from runoff of melting ice or from direct precipitation, then the rate of sinking of those surface waters will diminish or stop (e.g., Broecker et al., 1985). Results of numerical models indicate that if freshwater runoff into the Arctic Ocean and the North Atlantic increases as surface waters warm in the northern high latitudes, then the thermohaline irculation in the North Atlantic will weaken, with consequences for marine ecosystems and energy transport (e.g., Rahmstorf, 1996, 2002; Marotzke, 2000; Schmittner, 2005).

Reducing the rate of North Atlantic thermohaline circulation may have global as well as regional effects (e.g., Obata, 2007). Oceanic overturning is an important mechanism for transferring atmospheric CO_2 to the deep ocean. Reducing the rate of deep convection in the ocean would allow a higher proportion of anthropogenic CO_2 to remain in the atmosphere. Similarly, a slowdown in thermohaline circulation would reduce the turnover of nutrients from the deep ocean, with potential consequences across the Pacific Ocean.

5.2.6 Feedbacks during glacial-interglacial cycles

The growth and melting of immense ice sheets, which at their peak size covered approximately 30% of the modern global land area including the modern sites of New York and Chicago, were paced by the orbital variations often called Milankovitch forcings (e.g., Imbrie et al., 1993) described in Chapter 4 (paleoclimate concepts). There is little doubt that the orbital forcings drove this glacial-interglacial cycling, but a remarkably rich and varied literature debates the detailed mechanisms (see, e.g., Roe, 1999).

The generally accepted explanation of the glacial-interglacial cycling is that ice sheets grew when limited summer sunshine at high northern latitudes allowed survival of accumulated snow, and ice sheets shrank when abundant summer sunshine in the north melted the ice. The north is more important than the south because the Antarctic has remained ice covered during this cycling of the last million years and more, and there is no other high-latitude land in the south on which ice sheets could grow.

The increased reflectivity produced by expanded ice contributed to cooling. This effect is the ice-albedo feedback as described above, but with slower response controlled by the flow of the great ice sheets. Atmospheric dust was more abundant in the ice ages than in the intervening warm interglacials, and that additional ice-age dust contributed to cooling by blocking sunlight. The changes in Earth's orbit and ice-sheet growth led to complex changes in the ocean-atmosphere system that shifted carbon dioxide from the air to the ocean and reduced the atmospheric greenhouse effect. The carbon-dioxide changes lagged behind the orbital forcing, and thus carbon dioxide was clearly a feedback, but the large global cooling of the ice ages has been successfully explained only if the reduced greenhouse effect is included (Jansen et al., 2007). By analogy, overspending a credit card induces debt, which is made larger by interest payments on that debt. The interest payments clearly lag the debt in time and did not cause the debt, but they contribute to the size of the debt, and the debt cannot be explained quantitatively unless the interest payments are included.

Abrupt climate changes have been associated with the ice-age cycles. The most prominent and best known of these are linked to jumps in the wintertime extent of sea ice in the North Atlantic, which in turn were linked to changes in the large-scale circulation of the ocean (e.g., Alley, 2007), as described in the previous section. The associated temperature changes were very large around the North Atlantic (as much as 10°C or more) but much smaller in remote regions, and they were in the opposite direction in the far south (northern cooling was accompanied by slight southern warming). Hence, the globally averaged temperature changes were small and were probably linked primarily to ice-albedo feedback and small changes in the strength of the greenhouse effect. As reviewed by Alley (2007), the large ice-age ice sheets seem to have both triggered these abrupt swings and created conditions under which triggering was easier. Although such events may remain possible, they are less likely without the large ice sheet on Canada.

5.2.7 Arctic Amplification

The positive feedbacks outlined above amplify the Arctic response to climate forcings. The ice-albedo feedback is potentially strong in the Arctic because it hosts so much snow and ice (see Serreze and Francis, 2006 for additional discussion); if conditions are too warm for snow to form, no ice-albedo feedback can exist. Climate models initialized from modern or similar conditions and forced in various ways are in widespread agreement that global temperature trends are amplified in the Arctic and that the largest changes are over the Arctic Ocean during the cold season (autumn through spring) (e.g., Manabe and Stouffer, 1980; Holland and Bitz, 2003; Meehl et al., 2007). Summer changes over the Arctic Ocean are relatively damped, although summer changes over Arctic lands may be substantial (Serreze and Francis, 2006). The strong wintertime changes over the Arctic Ocean are linked to the insulating character of sea ice.

Think first of an unperturbed climate in balance on annual time scales. During summer, solar energy melts the sea ice cover. As the ice cover melts, areas of open water are exposed. The albedo of the open water is much lower than that of sea ice, so the open water gains heat. Because much of the solar energy goes into melting ice and warming the ocean, the surface air temperature does not rise much and, indeed, over the melting ice it stays fairly close to the freezing point. Through autumn and winter, when little or no solar energy is received, this ocean heat is released back to the atmosphere. The formation of sea ice itself further releases heat back to the atmosphere.

However, if the climate warms (e.g., through the effects of higher greenhouse gas concentrations) then the summer melt season lengthens and intensifies, and more areas of low-albedo open water form in summer and absorb solar radiation. As more heat is gained in the upper ocean, more heat is released back to the atmosphere in autumn and winter; this additional heat is expressed as a rise in air temperature. Furthermore, because the ocean now contains more heat, the ice that forms in autumn and winter is thinner than before. This thinner ice melts more easily in summer and produces even more low-albedo open water that absorbs solar radiation, meaning even larger releases of heat to the atmosphere in autumn and even thinner ice the next spring, and so on. The process can also work in reverse. An initial Arctic cooling melts less ice during the summer and creates less low-albedo open water. If less summer heat is gained in the ocean, then less heat is released back to the atmosphere in autumn and winter, and air temperatures further fall.

Although the albedo feedback over the ocean seems to dominate, an albedo feedback over land is much more direct. Under a warming climate, snow melts earlier in spring and thus low-albedo tundra, shrub, and forest cover is exposed earlier and fosters further spring warming. Similarly, later autumn snow cover will foster further autumn warming. More snow-free days produce a longer period of surface warming and imply warmer summers. Again, the process can work in reverse: initial cooling leads to more snow cover, fostering further cooling. Collectively, these processes result in stronger net positive feedbacks to forced temperature change (regardless of forcing mechanism) than is typical globally, thereby producing “Arctic amplification”.

During longer time intervals, an ice sheet such as the Laurentide Ice Sheet on North America can grow, or an ice sheet such as that on Greenland can melt. This growth or melting in turn influences albedo, freshwater fluxes to the ocean, broad patterns of atmospheric circulation, greenhouse-gas storage or release in the ocean and on land, and more.

5.3 Proxies of Arctic Temperature and Precipitation

Temperature and precipitation are especially important climate variables. Climate change is typically driven by changes in key forcing factors, which are then amplified or retarded by regional feedbacks that affect temperature and precipitation (section 5.2 and 4.2). Because feedbacks have strong regional variability, spatially variable responses to hemispherically symmetric forcing are common throughout the Arctic (e.g., Kaufman et al., 2004). Consequently, spatial patterns of temperature and precipitation must be reconstructed regionally.

Reconstructing temperature and precipitation in pre-industrial times requires reliable proxies (see section 4.3 for a general discussion of proxies) that can be used to derive qualitative or, preferably, quantitative estimates of past climates. To capture the expected spatial variability, proxy climate reconstructions must be spatially distributed and span a wide range of geological time. In general, the use of several proxies to reconstruct past climates provides the most robust evidence for past changes in temperature and precipitation.

5.3.1 Proxies for Reconstruction of Temperature

5.3.1a Vegetation/pollen records

Estimates of past temperature from data that describe the distribution of vegetation (primarily fossil pollen assemblages but also plant macrofossils such as fruits and seeds) may be relative (warmer or colder) or quantitative (number of degrees of change). Most information pertains to the growing season, because plants are dormant in the winter and so are less influenced by climate than during the growing season (but see below). For example, evidence of boreal forest vegetation (the presence of one or more boreal tree species) would be more strongly associated with warmer growing seasons than would evidence of treeless tundra—and the general position of northern treeline today approximates the location of the July 10 °C isotherm.

Indicator species are species with well studied and relatively restricted modern climatic ranges. The appearance of these species in the fossil record indicates that a certain climate milestone was reached, such as exceeding a minimum summer temperature threshold for successful growth or a winter minimum temperature of freezing tolerance (Figure 5.8). This methodology was developed early in Scandinavia (Iversen, 1944); Matthews et al. (1990) used indicator species to constrain temperatures during the last interglaciation in northwest Canada, and Ritchie et al. (1983) used indicator species to highlight early Holocene warmth in northwest Canada. The technique has been used extensively with fossil insect assemblages.

FIGURE 5.8 NEAR HERE

Methodologies for the numerical estimation of past temperatures from pollen assemblages follow one of two approaches. The first is the inverse-modeling approach, in which fossil data from one or more localities are used to provide temperature estimates for those localities (this approach also underlies the relative estimates of temperature described above). A modern “calibration set”’ of data (in this case, pollen assemblages) is related by equations to observed modern temperature, and the functions thus obtained are then applied to fossil data. This method has been developed and applied in Scandinavia (e.g., Seppä et al., 2004). A variant of the inverse approach is analogue analysis, in which a large modern dataset with assigned climate data forms the basis for comparison with fossil spectra. Good matches are derived statistically, and the resulting set of analogues provides an estimate of the past mean temperature and accompanying uncertainty (Anderson et al., 1989; 1991).

Inverse modeling relies upon observed modern relationships. Some plant species were more abundant in the past than they are today, and the fossil pollen spectra they produced may have no recognizable modern counterpart—so-called "'no-analogue"' assemblages. Outside the envelope of modern observations, fossil pollen spectra, which are described in terms of pollen abundance, cannot be reliably related to past climate. This problem led to the adoption of a second approach to estimating past temperature (or other climate variable) called forward modeling. The pollen data are not used to develop numerical values but are used to test a "hypothesis" about the status of past temperature (a key ingredient of climate). The hypothesis may be a conceptual model of the status of past climate, but typically it is represented by a climate-model simulation for a given time in the past. The climate simulation drives a vegetation model that assigns vegetation cover on the basis of bioclimatic rules (such as the winter minimums or required warmth of summer growing temperatures mentioned above). The resultant map is compared with a map of past vegetation developed from the fossil data. The philosophy of this approach is described by Prentice and Webb (1998). Such data and models have been compared for the Arctic by Kaplan et al. (2003) and Wohlfahrt et al. (2004). The great advantage of this approach is that underlying the model simulation are hypothesized climatic mechanisms; those mechanisms allow not only the description but also an explanation of past climate changes.

5.3.1b Dendroclimatology

Seasonal differences in climate variables such as temperature and precipitation throughout many parts of the world, including the high latitudes, are known to produce annual rings that reflect distinct changes in the way trees grow and respond, year after year, to variations in the weather (Fritts, 1976). Alternating light and dark bands (couplets) of low-density early wood (spring and summer) and higher density late wood (summer to late summer) have been used for decades to reproduce long time series of regional climate change thought to directly influence the production of meristematic cells in the trees' vascular cambium, just below the bark. Cambial activity in many parts of the northern boreal forests can be short; late wood may start production in late June and annual-ring width is complete by early August (e.g., Esper and Schweingruber, 2004). Fundamental to the use of tree rings is the fact that the average width of a tree ring couplet reflects some combination of environmental factors, largely temperature and precipitation, but it can also reflect local climatic variables such as wind stress, humidity and soil properties (see Bradley, 1999, for review).

The extraction of a climate signal from ring width and wood density (dendroclimatology), relies on the identification and calibration of regional climate factors and on the ability to distinguish local climate influences from regional noise (Figure 5.9). How sites for tree sampling are selected is also important depending upon the climatological signal of interest. Trees in marginal growth sites, perhaps on drier substrates or near an ecological transition, may be ideally most sensitive to minor changes in temperature stress or moisture stress. On the other hand, trees in less-marginal sites may reflect conditions of more widespread change. In the high latitudes, research is commonly focused on trees at both the latitude and elevation limits of tree growth or of the forest-tundra ecotone.

FIGURE 5.9 NEAR HERE

Pencil-sized increment cores or sanded trunk cross sections are routinely used for stereomicroscopic examination and measurement (Figure 5.10). A number of tree species are examined, most commonly varieties of the genera *Larix* (larch), *Pinus* (pine), and *Picea* (spruce). Raw ring-width time series are typically generated at a resolution of 0.01 mm along one or more radii of the tree, and these data are normalized for changes in ring width that reflect the natural increase in tree girth (a young tree produces wider rings). Ring widths for a number of trees are then averaged to produce a master curve for a particular site. The replication of many time series throughout a wide area at a particular site permits extraction of a climate-related signal and the elimination of anomalous ring biases caused by changes in competition or the ecology of any particular tree. Abrupt growth that caused a large change in ring width (Figure 5.9) can only be causually evaluated based on forest-site characteristics; that is, if the change isn’t replicated in nearby trees, it’s probably not related to climate.

FIGURE 5.10 NEAR HERE

Dendroclimatology is statistically laborious, and a variety of approaches are used by the science community. Ring widths or ring density must first be calibrated by a response-function analysis in which tree growth and monthly climatic data are compared for the instrumental period. Once this is done, then cross-dated tree ring series reaching back millennia can be used as predictors of past change. Principal-components analysis, along with some form of multiple regression analysis, is commonly used to identify key variables. A comprehensive review of statistical treatments is beyond the scope of this report, but summaries can be found in Fritts (1976), Briffa and Cook (1990), Bradley (1999, his Chapter 10), and Luckman (2007).

5.3.1c Marine isotopic records

The oxygen isotope composition of the calcareous shells of planktic foraminifers accurately records the oxygen isotope composition of ambient seawater, modulated by the temperature at which the organisms built their shells (Epstein et al., 1953; Shackleton, 1967; Erez and Luz, 1982; Figure 5.11). (The term $\delta^{18}O$ refers to the proportion of the heavy isotope, ^{18}O, relative to the lighter, more abundant isotope, ^{16}O.) However, the low horizontal and vertical temperature variability found in Arctic Ocean surface waters (less than –1°C) has little effect on the oxygen isotope composition of *N. pachyderma* (sin.) (maximum 0.2‰, according to Shackleton, 1974). Because meteoric waters, discharged into the ocean by precipitation and (indirectly) by river runoff, have considerably lower $\delta^{18}O$ values than do ocean waters, a reasonable correlation can be interpreted between salinity and the oxygen isotope composition of Arctic surface waters despite the complications of seasonal sea ice (Bauch et al., 1995; LeGrande and Schmidt, 2006). Accordingly, the spatial variability of surface-water salinity in the Arctic Ocean is recorded today by the $\delta^{18}O$ of planktic foraminifers (Spielhagen and Erlenkeuser, 1994; Bauch et al., 1997).

FIGURE 5.11 NEAR HERE

The $\delta^{18}O$ values of planktic foraminifers in cores of ancient sediment from the deep Arctic Ocean vary considerably in on millennial time scales (e.g., Aksu, 1985; Scott et al., 1989; Stein et al., 1994; Nørgaard-Pedersen et al., 1998; 2003; 2007a,b; Polyak et al., 2004; Spielhagen et al., 2004; 2005). The observed variability in foraminiferal $\delta^{18}O$ commonly exceeds the change in the isotopic composition of seawater that results merely from storing, on glacial-interglacial time scales, isotopically light freshwater in glacial ice sheets (about 1.0–1.2‰ $\delta^{18}O$) (Fairbanks, 1989; Adkins et al., 1997; Schrag et al. 2002). Changes with time in freshwater balance of the near-surface waters, and in the temperature of those waters, are both recorded in the $\delta^{18}O$ values of foraminifer shells. Moreover, in cases where independent evidence of a regional warming of surface waters is available (e.g., in the eastern Fram Strait during the last glacial maximum; Nørgaard-Pedersen et al., 2003), this warming is thought to have been caused by a stronger influx of saline Atlantic Water. Because salinity influences $\delta^{18}O$ of foraminfer shells from the Arctic Ocean more than temperature does, it is difficult to reconstruct temperatures in the past on the basis of systematic variations in calcite $\delta^{18}O$ in Arctic Ocean sediment cores.

5.3.1d Lacustrine isotopic records

Isotopic records preserved in lake sediment provide important paleoclimatic information on landscape change and hydrology. Lakes are common in high-latitude landscapes, and sediment deposited continuously provides uninterrupted, high-resolution records of past climate (Figure 5.12).

FIGURE 5.12 NEAR HERE

Oxygen isotope ratios in precipitation reflect climate processes, especially temperature (see 5.3.1e). The oxygen isotope ratios of shells and other materials in lakes primarily reflect ratios of the lake water. The isotopic ratios in the lake water are dominantly controlled by the isotopic ratios in precipitation—unless evaporation from the lake is sufficiently rapid, compared with inflow of new water, to shift the isotopic ratios towards heavier values by preferentially removing isotopically lighter water. Those lakes that have streams entering and leaving (open lakes) have isotopic ratios that are generally not affected much by evaporation, as do some lakes supplied only by water flow through the ground (closed lakes). These lakes allow isotopic ratios of shells and other materials in them to be used to reconstruct climate, especially temperature. However, some closed lakes are affected notably by evaporation, in which case the isotopic ratios of the lake are at least in part controlled by lake hydrology. Unless independent evidence of lake hydrology is available, quantitative interpretation of $\delta^{18}O$ is difficult. Consequently, $\delta^{18}O$ is normally combined with additional climate proxies to constrain other variables and strengthen interpretations. For example, in rare cases, ice core records that are located near lakes can provide an oxygen isotope record for direct comparison (Fisher et al., 2004; Anderson and Leng, 2004; Figure 5.13). Oxygen isotope ratios are relatively easy to measure on carbonate shells or other carbonate materials. Greater difficulty, which limits the accuracy (i.e., the time-resolution) of the records, is associated with analyses of oxygen isotopes in silica from diatom shells (Leng and Marshall, 2004) and in organic matter (Sauer et al., 2001; Anderson et al., 2001). Additional uncertainty arises with organic matter because its site of origin is unknown: although some of it grew in the lake, some was also washed in and may have been stored on the landscape for an indeterminate time previously.

FIGURE 5.13 NEAR HERE

5.3.1e Ice cores

The most common way to deduce temperature from ice cores (Figures 5.13 and 5.14) is through the isotopic content their water, i.e., the ratio of $H_2{}^{18}O$ to $H_2{}^{16}O$, or of HDO to H_2O (where D is deuterium, ^2H). The ratios are expressed as $\delta^{18}O$ and δD respectively, relative to standard mean ocean water (SMOW). Pioneering studies (Dansgaard, 1964) showed how $\delta^{18}O$ is related to climatic variables in modern precipitation. At high latitudes both $\delta^{18}O$ and δD are generally, with some caveats, considered to represent the mean annual temperature at the core site, and the use of both measures together offers additional information about conditions at the source of the water vapor (e.g., Dansgaard et al., 1989). Recent work by Werner et al. (2000), however, demonstrates that changes in the seasonal cycle of precipitation over the ice sheets can affect measurements of ice-core temperature.

FIGURE 5.14 NEAR HERE

The underlying idea is that an air mass loses water vapor by condensation as it travels from a warm source to a cold (polar) site. This point is easily shown by the nearly linear relationship between precipitation and temperature over modern ice sheets (Figure 5.15). Water that contains the heavy isotopes has a lower vapor pressure, so the heavy isotope preferentially condenses into rain or snow, and the air mass becomes progressively depleted of the heavy isotope it moves to colder sites. It can easily be shown from spatial surveys (Johnsen et al., 1989) and, indeed, from modeling studies using models enabled with water isotopes (e.g., Hoffmann et al., 1998; Mathieu et al., 2002) that a good spatial relationship between temperature and water isotope ratio exists. The relationship is

$$\delta = aT + b$$

where T is mean annual surface temperature, and δ is annual mean $\delta^{18}O$ or δD value in precipitation in the polar regions, and the slope, a, has values typically around 0.6 for Greenland $\delta^{18}O$.

FIGURE 5.15 NEAR HERE

Temperature is not the only factor that can affect isotopic ratios. Changes in the season when snow falls, in the source of the water vapor, and other things are potentially important (Jouzel et al., 1997; Werner et al., 2000) (Figure 5.16). For this reason, it is common whenever possible to calibrate the isotopic ratios using additional paleothermometers. For short intervals, instrumental records of temperature can be compared with isotopic ratios (e.g., Shuman et al., 1995). The few comparisons that have been done (summarized in Jouzel et al., 1997) tend to show δ/T gradients that are slightly lower than the spatial gradient. Accurate reconstructions of past temperature, but with low time resolution, are obtained from the use of borehole thermometry. The center of the Greenland ice sheet has not finished warming from the ice age, and the remaining cold temperatures reveal how cold the ice age was (Cuffey et al., 1995; Johnsen et al., 1995). Additional paleothermometers are available that use a thermal diffusion effect. In this effect, gas isotopes are separated slightly when an abrupt temperature change at the surface creates a temperature difference between the surface and the region a few tens of meters down, where bubbles are pinched off from the interconnected pore spaces in old snow (called firn). The size of the gas-isotope shift reveals the size of an abrupt warming, and the number of years between the indicators of an abrupt change in the ice and in the bubbles trapped in ice reveals the temperature before the abrupt change—if the snowfall rate before the abrupt change is known (Severinghaus et al., 1998; Severinghaus and Brook, 1999; Huber et al., 2006). These methods show that the value of the δ/T slope produced by many of the large changes recorded in Greenland ice cores was considerably less (typically by a factor of 2) than the spatial value, probably because of a relatively larger reduction in winter snowfall in colder times (Cuffey et al., 1995; Werner et al., 2000; Denton et al., 2005). The actual temperature changes were therefore larger than would be predicted by the standard calibration.

FIGURE 5.16 NEAR HERE

In summary, water isotopes in polar precipitation are a reliable proxy for mean annual air temperature, but for quantitative use, some means of calibrating them is required. They may be calibrated either against instrumental data by using an alternative estimate of temperature change, or through modeling, even for ice deposited during the Holocene (Schmidt et al., 2007).

5.3.1f Fossil assemblages and sea surface temperatures

Different species live preferentially at different temperatures in the modern ocean. Modern observations can be used to learn the preferences of species. If we assume that species maintain their preferences through time, then the mathematical expression of these preferences plus the history of where the various species lived in the past can then be used to interpret past temperatures (Imbrie and Kipp, 1971; CLIMAP, 1981). This line of reasoning is primarily applied to near-surface (planktic) species, and especially to foraminifers, diatoms, and dinoflagellates. The presence or absence and the relative abundance of species can be used. Such methods are now commonly supported by sea-surface temperature estimates using emerging biomarker techniques outline below.

5.3.1g Biogeochemistry

Within the past decade, two new organic proxies have emerged that can be used to reconstruct past ocean surface temperature. Both measurements are based on quantifying the proportions of biomarkers—molecules produced by restricted groups of organisms—preserved in sediments. In the case of the "$U^{k'}_{37}$ index" (Brassell et al., 1986 ; Prahl et al., 1988), a few closely related species of coccolithophorid algae are entirely responsible for producing the 37-carbon ketones ("alkenones") used in the paleotemperature index, whereas crenarcheota (archea) produce the tetra-ether lipids that make up the TEX_{86} index (Wuchter et al., 2004). Although the specific function that the alkenones and glycerol dialkyl tetraethers serve for these organisms is unclear, the relationship of the biomarker $U^{k'}_{37}$ index to temperature has been confirmed experimentally in the laboratory (Prahl et al., 1988) and by extensive calibrations of modern surface sediments to overlying surface ocean temperatures (Muller et al., 1998, Conte et al., 2006, Wuchter et al., 2004).

Biomarker reconstructions have several advantages for reconstructing sea surface conditions in the Arctic. First, in contrast to $\delta^{18}O$ analyses of marine carbonates (outlined above), the confounding effects of salinity and ice volume do not compromise the utility of biomarkers as paleotemperature proxies (a brief discussion of caveats in the use of $U^{k'}_{37}$ is given below). Both the $U^{k'}_{37}$ and TEX_{86} proxies can be measured reproducibly to high precision (analytical errors correspond to about 0.1°C for $U^{k'}_{37}$ and 0.5°C for TEX_{86}), and sediment extractions and gas or liquid chromatographic detections can be automated for high sampling rates. The abundances of biomarkers also provide insights into the composition of past ecosystems, so that links between the physical oceanography of the high latitudes and carbon cycling can be assessed. And lastly, organic biomarkers can usually be recovered from Arctic sediments that do not preserve carbonate or siliceous microfossils. It should be noted, however, that the harsh conditions of the northern high latitudes mean that the organisms producing the alkenone and tetraethers may have been excluded at certain times and places; thus, continuous records cannot be guaranteed.

The principal caveats in using biomarkers for paleotemperature reconstructions come from ecological and evolutionary considerations. Alkenones are produced by algae that are restricted to the region of abundant light (the photic zone), so paleotemperature estimates based on them apply to this layer, which approximates the sea surface temperature. In the vast majority of the ocean, the alkenone signal recorded by sediments closely correlates with mean annual sea-surface temperature (Muller et al., 1998; Conte et al., 2006; Figure 5.17). However, in the case of highly seasonal high-latitude oceans, the temperatures inferred from the alkenone $U^{k'}_{37}$ index may better approximate summer surface temperatures than mean annual sea-surface temperature. Furthermore, past changes in the season of production could bias long-term time series of past temperatures that are based on the $U^{k'}_{37}$ proxy. Depending on water column conditions, past production could have been highly focused toward a short (summer?) or a more diffuse (late spring–early fall?) productive season. A survey of modern surface sediments in the North Atlantic (Rosell-Mele et al., 1995) shows that the seasonal bias in alkenone unsaturation is not important except at high (greater than 65°N.) latitudes (Rosell-Mele et al., 1995). A possible additional complication with the $U^{k'}_{37}$ proxy is that in the Nordic Seas an additional alkenone (of the 37:4 type) is common, although it is rare or absent in most of the world ocean including the Antarctic. The relatively fresh and cold waters of the Nordic Seas may affect alkenone production by the usual species, or they may affect the mixture of species that produce alkenone. Regardless, this oddity suggests caution in applying the otherwise robust global calibration of alkenone unsaturation to Nordic Sea surface temperature (Rosell-Mele and Comes, 1999).

FIGURE 5.17 NEAR HERE

In contrast to the near-surface restriction of the algae producing the $U^{k'}_{37}$ proxy, the marine crenarcheota that produce the tetraether membrane lipids used in the TEX_{86} index can range widely through the water column. In situ analyses of particles suspended in the water column show that the tetraether lipids are most abundant in winter and spring months in many ocean provinces (Wuchter et al., 2005) and are present in large amounts below 100 m depth. However, it appears that the chemical basis for the TEX_{86} proxy is fixed by processes in the upper lighted (photic) zone, so that the sedimentary signal originates near the sea surface (Wuchter et al., 2005), just as for the $U^{k'}_{37}$ proxy. No studies have yet been conducted to assess how high-latitude seasonality affects the TEX_{86} proxy.

As for many other proxies, use of these biomarker proxies is based on the assumption that the modern relation between organic proxies and temperature was the same in the past. The two modern (and genetically closely related) species producing the alkenones in the $U^{k'}_{37}$ proxy can be traced back in time in a continuous lineage to the Eocene (about 50 Ma), and alkenone occurrences coincide with the fossil remains of the ancestral lineage in the same sediments (Marlowe et al., 1984). One might suppose that past evolutionary events in the broad group of algae that includes these species might have produced or eliminated other species that generated these chemicals but with a different relation to temperature. However, other such species would cause jumps in climate reconstructions at times of evolutionary events in the group, and no such jumps are observed. The TEX_{86} proxy can be applied to marine sediments 70–100 million years old. The working assumption is, therefore, that both organic proxies can be applied accurately to sediments containing the appropriate chemicals.

Because these biomarker proxies depend on changes in relative abundance of chemicals, it is important that natural processes after death of the producing organisms do not preferentially break down one chemical and thus change the ratio. Fortunately, the ratio appears to be stable (Prahl et al., 1989; Grice et al., 1998, Teece et al., 1998; Herbert, 2003; Schouten et al., 2004). An additional complication is that sediments can be moved around by ocean currents, so that the material sampled at one place might have been produced in another place under different climate conditions (Thomsen et al., 1998; Ohkouchi et al., 2002). Ordinarily, lengthy transport of biomarkers into a depositional site is rare and volumes are small compared with the supply from the productive ocean above, so that the proxy indeed records local climate. However, at some times and places, the Arctic has been comparatively unproductive, so that transport from other parts of the ocean, or from land in the case of the TEX_{86} proxy, may have been important (Weijers et al., 2006).

5.3.1h Biological proxies in lakes

Lakes and ponds are common in most Arctic regions and provide useful records of climate change (Smol and Cumming, 2000; Cohen, 2003; Schindler and Smol, 2006; Smol 2008). Many different biological climate proxies are preserved in Arctic lake and pond sediments (Pienitz et al., 2004). Diatom shells (Douglas et al., 2004) and remains of non-biting midge flies (chironomid head capsules; Bennike et al., 2004) are among the biological indicators most commonly used to reconstruct ancient Arctic climate (Figure 5.18). The approach generally used by those who study the history of lakes (paleolimnologists) is first to identify useful species— those that grow only within a distinct range of conditions. Then, the modern conditions preferred by these indicator species are determined, as are the conditions beyond which these indicator species cannot survive. (Typically used are surface sediment calibration sets or training sets to which are applied statistical approaches such as canonical correspondence analysis and weighted averaging regression and calibration; see Birks, 1998.) The resulting mathematical relations (or transfer functions such as those used in marine records) are then used to reconstruct the environmental variables of interest, on the basis of the distribution of indicator assemblages preserved in dated sediment cores (Smol, 2008). Where well-calibrated transfer functions are not available, such as for some parts of the Arctic, less-precise climate reconstructions are commonly based on the known ecological and life-history characteristics of the organisms.

FIGURE 5.18 NEAR HERE

Ideally, sedimentary characteristics would be linked directly to key climatic variables such as temperature (e.g., Pienitz and Smol, 1993; Joynt and Wolfe, 2001; Bigler and Hall, 2003; Bennike et al., 2004; Larocque and Hall, 2004;Woller et al. 2004, Finney et al., 2004, other chapters in Pienitz et al., 2004; Barley et al., 2006; Weckström et al., 2006;). However, lake sediments typically record conditions in the lake that are only indirectly related to climate (Douglas and Smol, 1999). For example, lake ecosystems are strongly influenced by the length of the ice-free versus the ice-covered season, by the sun-blocking effect of any snow cover on ice (Figure 5.19) (e.g., Smol, 1988; Douglas et al., 1994; Sorvari and Korhola, 1998; Douglas and Smol, 1999; Sorvari et al., 2002; Rühland et al., 2003; Smol and Douglas, 2007a) and by the existence or absence of a seasonal layer of warm water near the lake surface that remains separate from colder waters beneath (Figure 5.20). Shells and other features in the lake sediment record the species living in the lake and conditions under which they grew. These factors rather directly reflect the ice and snow cover and lake stratification and only indirectly reflect the atmospheric temperature and precipitation that control the lake conditions.

FIGURE 5.19 NEAR HERE

FIGURE 5.20 NEAR HERE

5.3.1i Insect proxies.

Insects are common and typically are preserved well in Arctic sediment. Because many insect types live only within narrow ranges of temperature or other environmental conditions, the remains of particular insects in old sediments provides useful information on past climate.

Calibrating the observed insect data to climate involves extensive modern and recent studies, together with careful statistical analyses. For example, fossil beetles are typically related to temperature using what is known as the Mutual Climatic Range method (Elias et al., 1999; Bray et al., 2006). This method quantitatively assesses the relation between the modern geographical ranges of selected beetle species and modern meteorological data. A “climate envelope” is determined, within which a species can thrive. When used with paleodata, the method allows for the reconstruction of several parameters such as mean temperatures of the warmest and coldest months of the year.

5.3.1j Sand dunes When plant roots anchor the soil, sand cannot blow around to make dunes. In the modern Arctic, and especially in Alaska (Figure 5.21) and Russia, sand dunes are forming and migrating in many places where dry, cold conditions restrict vegetation. During the last glacial interval and at some other times, dunes formed in places that now lack active dunes and indicate colder or drier conditions at those earlier times (Carter, 1981; Oswald et al., 1999; Beget, 2001; Mann et al., 2002). Some wind-blown mineral grains are deposited in lakes. The rate at which sand and silt are deposited in lakes increases as nearby vegetation is removed by cooling or drying, so analysis of the sand and silt in lake sediments provides additional information on the climate (e.g., Briner et al., 2006).

FIGURE 5.21 NEAR HERE

5.3.2 Proxies for Reconstruction of Precipitation

In the case of sand dunes described above, separating the effects of changing temperature from those of changing precipitation may be difficult, but additional indicators such as insect fossils in lake sediments may help by constraining the temperature. In general, precipitation is more difficult to estimate than is temperature, so reconstructions of changes in precipitation in the past are less common, and typically less quantitative, than are reconstructions of past temperature changes.

5.3.2a Vegetation-derived precipitation estimates Different plants live in wet and dry places, so indications of past vegetation provide estimates of past wetness. Plants do not respond primarily to rainfall but instead to moisture availability. Availability is primarily controlled in most places by the difference between precipitation and evaporation, although some soils carry water downward so efficiently that dryness occurs even without much evaporation.

Much modern tundra vegetation grows where precipitation exceeds evaporation. Plants such as *Sphagnum* (bog moss), cotton-grass (*Eriophorum*), and cloudberry (*Rubus chamaemorus*) indicate moist growing conditions. In contrast, grasses dominate dry tundra and polar semi-desert. Such differences are evident today (Oswald et al., 2003) and can be reconstructed from pollen and larger plant materials (macrofossils) in sediments. Some regions of Alaska and Siberia retain sand dunes that formed in the last glacial maximum but are inactive today; typically, those regions are near areas that had grasses then but now have plants requiring greater moisture (Colinvaux, 1964; Ager and Brubaker, 1985; Lozhkin et al. 1993; Goetcheus and Birks 2001, Zazula et al., 2003).

In Arctic regions, snow cover may allow persistence of shrubs that would be killed if exposed during the harsh winter. For example, dwarf willow can survive if snow depths exceed 50 cm (Kaplan et al., 2003). Siberian stone pine requires considerable winter snow to weigh down and bury its branches (Lozhkin et al, 2007). The presence of these species therefore indicates certain minimum levels of winter precipitation.

Moisture levels can also be estimated quantitatively from pollen assemblages by means of formal techniques such as inverse and forward modeling, following techniques also used to estimate past temperatures. Moisture-related transfer functions have been developed, in Scandinavia for example (Seppä and Hammarlund, 2000). Kaplan et al. (2003) compared pollen-derived vegetation with vegetation derived from model simulations for the present and key times in the past. The pollen data indicated that model simulations for the Last Glacial Maximum tended to be “too moist”—the simulations generated shrub-dominated biomes whereas the pollen data indicated drier tundra dominated by grass.

5.3.2b Lake-level derived precipitation estimates In addition to their other uses in paleoclimatology as described above, lakes act as natural rain gauges. If precipitation increases relative to evaporation, lakes tend to rise, so records of past lake levels provide information about the availability of moisture.

Most of the water reaching a lake first soaked into the ground and flowed through spaces as groundwater, before it either seeped directly into the lake or else came back to the surface in a stream that flowed into the lake. Smaller amounts of water fall directly on the lake or flow over the land surface to the lake without first soaking in (e.g., MacDonald et al., 2000b). Lakes lose water to streams (“overflow”), as outflow into groundwater, and by evaporation. If water supply to a lake increases, the lake level will rise and the lake will spread. This spread will increase water loss from the lake by increasing the area for evaporation, by increasing the area through which groundwater is leaving and the “push” (hydraulic head) causing that outflow, and perhaps by forming a new outgoing stream or increasing the size of an existing stream. Thus, the level of a lake adjusts in response to changes in the balance between precipitation and evaporation in the region feeding water to the lake (the catchment). Because either an increase in precipitation or a reduction in evaporation will cause a lake level to rise, an independent estimate of either precipitation or evaporation is required before one can estimate the other on the basis of a history of lake levels (Barber and Finney, 2000).

Former lake levels can be identified by deposits such as the fossil shoreline they leave (Figure 5.22); sometimes these deposits are preserved under water and can be recognized in sonar surveys or other data, and these deposits can usually be dated. Furthermore, the sediments of the lake may retain a signature of lake-level fluctuations: coarse-grained material generally lies near the shore and finer grained materials offshore (Digerfeldt, 1988), and these too can be identified, sampled, and dated (Abbott et al., 2000).

FIGURE 5.22 NEAR HERE

For a given lake, modern values of the major inputs and outputs can be obtained empirically, and a model can then be constructed that simulates lake-level changes in response to changing precipitation and evaporation. Allowable pairs of precipitation and evaporation can then be estimated for any past lake level. Particularly in cases where precipitation is the primary control of water depth, it is possible to model lake level responses to past changes in precipitation (e.g., Vassiljev, 1998; Vassiljev et al., 1998). For two lakes in interior Alaska, this technique suggested that precipitation now was as much as 50% lower than at the time of the Last Glacial Maximum (about 20 ka) (Barber and Finney, 2000).

Biological groups living within lakes also leave fossil assemblages that can be interpreted in terms of lake level by comparing them with modern assemblages. In all cases, factors other than water depth (e.g., conductivity and salinity) likely influence the assemblages (MacDonald et al., 2000b), but these factors may themselves be indirectly related to water depth. Aquatic plants, which are represented by pollen and macrofossils, tend to dominate from nearshore to moderate depths, and shifts in the abundance of pollen or seeds in one of more sediment profiles can indicate relative water-level changes (Hannon and Gaillard, 1997; Edwards et al., 2000). Diatom and chironomid (midge) assemblages may also be related quantitatively to lake depth by means of inverse modeling and the transfer functions used to reconstruct past lake levels (Korhola et al., 2000; Ilyashuk et al., 2005).

The great variety of lakes, and the corresponding range of sedimentary indicators, requires that field scientists be broadly knowledgeable in selecting which lakes to study and which techniques to use in reconstructions. For some important case studies, see Hannon and Gaillard, 1997; Abbott et al., (2000), Edwards et al., (2000), Korhola et al., 2000; Pienitz et al., (2000), Anderson et al., (2005), and Ilyashuk et al., 2005).

5.3.2c Precipitation estimates from ice cores. Ice cores provide a direct way of recording the net accumulation rate at sites with permanent ice. The initial thickness of an annual layer in an ice core (after mathematically accounting for the amount of air trapped in the ice) is the annual accumulation. Most ice cores are drilled in cold regions that produce little meltwater or runoff. Furthermore, sublimation or condensation and snow drift generally account for little accumulation, so that accumulation is not too different from the precipitation (e.g., Box et al., 2006). The thickness of layers deeper in the core must be corrected for the thinning produced as the ice sheet spreads and thins under its own weight, but for most samples this correction can be made with much accuracy by using simple ice flow models (e.g., Alley et al., 1993; Cuffey and Clow, 1997).

The annual-layer thickness can be recorded using any component that varies regularly with a defined seasonal cycle. Suitable components include visible layering (e.g. Figure 5.14a), which responds to changes in snow density or impurities (Alley et al., 1997), the seasonal cycle of water isotopes (Vinther et al., 2006), and seasonal cycles in different chemical species (e.g. Rasmussen et al., 2006). Using more than one component gives extra security to the combined output of counted years and layer thicknesses.

Although the correction for strain (layer thinning) increases the uncertainty in estimates of absolute precipitation rate deeper in ice cores, estimates of changes in relative accumulation rate along an ice core can be considered reliable (e.g., Kapsner et al., 1995). Because the accumulation rate combines with the temperature to control the rate at which snow is transformed to ice, and because the isotopic composition of the trapped air (Sowers et al., 1989) and the number of trapped bubbles in a sample (Spencer et al., 2006) record the results of that transformation, then accumulation rates can also be estimated from measurements of these parameters plus independent estimation of past temperature using techniques described above.

5.4 Arctic Climate over the past 65 Ma

During the past 65 m.y. (the Cenozoic), the Arctic has experienced a greater change in temperature, vegetation, and ocean surface characteristics than has any other Northern Hemisphere latitudinal band (e.g., Sewall and Sloan, 2001; Bice et al., 2006; and see results presented below). Those times when the Arctic was unusually warm offer insights into the feedbacks within the Arctic system that can amplify changes imposed from outside the Arctic regions. Below we summarize the evidence for Cenozoic history of climate in the Arctic, and we focus especially on warm times by using climate and environmental proxies outlined in section 5.3.

5.4.1 Early Cenozoic and Pliocene Warm Times

Records of the $\delta^{18}O$ composition of bottom-dwelling foraminifers from the global ocean document a long-term cooling of the deep sea during the past 70 m.y. (Figure 4.8; Zachos et al., 2001) and the development of large Northern Hemisphere continental ice sheets at 2.6–2.9 Ma (Duk-Rodkin et al., 2004). As discussed below and in Chapter 6 (past rates of Arctic climate change), Arctic climate history is broadly consistent with the global data reported by Zachos et al. (2001): general cooling and increase in ice was punctuated by short-lived and longer lived reversals, by variations in cooling rate, and by additional features related to growth and shrinkage of ice once the ice was well established. A detailed Arctic Ocean record that is equivalent to the global results of Zachos et al. (2001) is not yet available, and because the Arctic Ocean is geographically somewhat isolated from the world ocean (e.g., Jakobsson and MacNab, 2006), the possibility exists that some differences would be found. Emerging paleoclimate reconstructions from the Arctic Ocean derived from recently recovered sediment cores on the Lomonosov Ridge (Backman et al., 2006; Moran et al., 2006) shed new light on the Cenozoic evolution of the Arctic Basin, but the data have yet to be fully integrated with the evidence from terrestrial records or with the sketchy records from elsewhere in the Arctic Ocean (see Chapter 8, Arctic sea ice).

Data clearly show warm Arctic conditions during the Cretaceous and early Cenozoic. For example, late Cretaceous (70 Ma) Arctic Ocean temperatures of 15°C (compared to near-freezing temperatures today) are indicated by TEX_{86}-based estimates (Jenkyns et al., 2004). The same indicator shows that peak Arctic Ocean temperatures near the North Pole rose from about 18°C to more than 23°C during the short-lived Paleocene-Eocene thermal maximum about 55 Ma (Figure 5.23) (Moran et al., 2006; also see Sluijs et al., 2006; 2008). This rise was synchronous with warming on nearby land from a previous temperature of about 17°C to peak temperature during the event of about 25°C (Weijers et al., 2007). By about 50 Ma, Arctic Ocean temperatures were about 10°C and relatively fresh surface waters were dominated by aquatic ferns (Brinkhuis et al., 2006). Restricted connections to the world ocean allowed the fern-dominated interval to persist for about 800,000 years; return of more-vigorous interchange between the Arctic and North Altantic oceans was accompanied by a warming in the central Arctic Ocean of about 3°C (Brinkhuis et al., 2006). On Arctic lands during the Eocene (55–34 Ma), forests of *Metasequoia* dominated a landscape characterized by organic-rich floodplains and wetlands quite different from the modern tundra (McKenna, 1980; Francis, 1988; Williams et al., 2003).

FIGURE 5.23 NEAR HERE

Terrestrial evidence shows that warm conditions persisted into the early Miocene (23–16 Ma), when the central Canadian Arctic Islands were covered in mixed conifer-hardwood forests similar to those of southern Maritime Canada and New England today (Whitlock and Dawson, 1990). *Metasequoia* was still present although less abundant than in the Eocene. Still younger, deposits known as the Beaufort Formation and tentatively dated to about 8–3 Ma (and thus within Miocene to Pliocene times) record an extensive riverside forest of pine, birch, and spruce, which lived throughout the Canadian Arctic Archipelago before geologic processes formed many of the channels that now divide the islands.

The relatively warm climates of the earlier Cenozoic altered to the colder times of the Quaternary Ice Age, which was marked by cyclic growth and shrinkage of extensive land ice, during the Pliocene (5–1.8 Ma). Climate changed although continental configurations remained similar to those of the present, and most Pliocene plant and animal species were similar to those that remain today. A well-documented warm period in the middle Pliocene (about 3 Ma), just before the planet transitioned into the Quaternary ice age, supported forests that covered large regions near the Arctic Ocean that are currently polar deserts. Fossils of *Arctica islandica* (a marine bivalve that does not live near seasonal sea ice) in marine deposits as young as 3.2 Ma on Meighen Island at 80°N., likely record the peak Pliocene mean warmth of the ocean (Fyles et al., 1991). As compared with recent conditions, warmer conditions then are widely indicated (Dowsett et al., 1994). At a site on Ellesmere Island, application of a novel technique for paleoclimatic reconstruction based on ring-width and isotopic measurements of wood suggests mean-annual temperatures 14°C warmer than recently (Ballantyne et al., 2006). Additional data from records of beetles and plants indicate mid-Pliocene conditions as much as 10°C warmer than recently for mean summer conditions, and even larger wintertime warming to a maximum of 15°C or more (Elias and Matthews, 2002).

Much attention has been focused on learning the causes of the slow, bumpy slide from Cretaceous hothouse temperatures to the recent ice age. As discussed below, changes in greenhouse-gas concentrations appear to have played the dominant role, and linked changes in continental positions, in sea level, and in oceanic circulation also contributed.

Based on general circulation models of climate, Barron et al. (1993) found that continental position had little effect on temperature difference between Cretaceous and modern temperatures (also see Poulsen et al., 1999 and references therein). Years later, Donnadieu et al. (2006), using more sophisticated climate modeling, found that continental motions and their effects on atmospheric and oceanic circulation modified global average temperature by almost 4°C from Early to Late Cretaceous; this result does not compare directly with modern conditions, but it does suggest that continental motions can notably affect climate. However, despite much effort, modeling does not indicate that the motion of continents by itself can explain either the long-term cooling trend from the Cretaceous to the ice age or the “wiggles” within that cooling.

The direct paleoclimatic data provide one interesting perspective on the role of oceanic circulation in the warmth of the later Eocene. When the Arctic Ocean was filled with water ferns living in “brackish” water (less salty than normal marine water) in an ocean that was ice-free or nearly so, the oceanic currents reaching the near-surface Arctic

Ocean must have been greatly weakened relative to today for the fresh water to persist. Thus, heat transport by oceanic currents cannot explain the Arctic-Ocean warmth of that time. The resumption of stronger currents and normal salinity was accompanied by a warming of about 3°C (Brinkhuis et al., 2006), important but not dominant in the temperature difference between then and now.

As discussed in section 4.2.4, the atmospheric CO_2 concentration has changed during tens of millions of years in response to many processes, and especially to those processes linked to plate tectonics and perhaps also to biological evolution. Many lines of proxy evidence (see Royer, 2006) show that atmospheric CO_2 was higher in the warm Cretaceous than it was recently, and that it subsequently fell in parallel with the cooling (Figure 5.24). Furthermore, models find that the changing CO_2 concentration is sufficient to explain much of the cooling (e.g., Bice et al., 2006; Donnadieu et al., 2006).

FIGURE 5.24 NEAR HERE

A persistent difficulty is that models driven by reconstructed CO_2 tend to underestimate Arctic warmth (e.g., Sloan and Barron, 1992). Many possible explanations have been offered for this situation: underestimation of CO_2 levels (Shellito et al., 2003; Bice et al., 2006); an enhanced greenhouse effect from polar stratospheric clouds during warm times (Sloan and Pollard, 1998; Kirk-Davidoff et al., 2002); changed planetary obliquity (Sewall and Sloan, 2004); reduced biological productivity that provided fewer cloud-condensation nuclei and thus fewer reflective clouds (Kump and Pollard, 2008); and greater heat transport by tropical cyclones (Korty et al., 2008). Several of these mechanisms use feedbacks not normally represented in climate models and that serve to amplify warming in the Arctic. Consideration of the literature cited above and of additional materials points to some combination of stronger greenhouse-gas forcing (see Alley, 2003 for a review) and to stronger long-term feedbacks than typically are included in models, rather than to large change in Earth's orbit, although that cannot be excluded.

It is thought that greenhouse gases were the primary control on Arctic temperature changes because the warmth of the Paleocene-Eocene Thermal Maximum took place in the absence of any ice—and therefore the absence of any ice-albedo or snow-albedo feedbacks. As described above (see Sluijs et al., 2008 for an extensively referenced summary of the event together with new data pertaining to the Arctic), this thermal maximum was achieved by a rapid (within a few centuries or less), widespread warming coincident with a large increase in atmospheric greenhouse-gas concentrations from a biological source (whether from sea-floor methane, living biomass, soils, or other sources remains debated). Following the thermal maximum, the anomalous warmth decayed more slowly and the extra greenhouse gases dissipated for tens of thousands of years, to roughly 100,000 years ago. The event in the Arctic seems to have been positioned within a longer interval of restricted oceanic circulation into the Arctic Ocean (Sluijs et al., 2008), and it was too fast for any notable effect of plate tectonics or evolving life. The reconstructed CO_2 change thus is strongly implicated in the warming (e.g., Zachos et al., 2008).

Taken very broadly, the Arctic changes parallel the global ones during the Cenozoic, except that changes in the Arctic were larger than globally averaged ones (e.g., Sluijs et al., 2008). The global changes parallel changing atmospheric carbon-dioxide concentrations, and changing CO_2 is the likely cause of most of the temperature change (e.g., Royer, 2006; Royer et al., 2007).

The well-documented warmth of the Pliocene is not fully explained. This interval is recent enough that continental positions were substantially the same as today. As reviewed by Jansen et al. (2007), many reconstructions show notable Arctic warmth but little low-latitude change; however, recent work suggests the possibility of low-latitude warmth as well (Haywood et al., 2005). Reconstructions of Pliocene atmospheric CO_2 concentration (reviewed by Royer, 2006) generally agree with each other within the considerable uncertainties, but they allow values above, similar to, or even below the typical levels just before major human influence. Data remain equivocal on whether the ocean transported more heat during Pliocene warmth (reviewed by Jansen et al., 2007). The high-latitude warmth thus may have originated primarily from changes in greenhouse-gas concentrations in the atmosphere, or from changes in oceanic or atmospheric circulation, or from some combination, perhaps with a slight possibility that other processes also contributed.

5.4.2 The Early Quaternary: Ice-Age Warm Times

A major reorganization of the climate system occurred between 3.0 and 2.5 Ma. As a result, the first continental ice sheets developed in the North American and Eurasian Arctic and marked the onset of the Quaternary Ice Ages (Raymo, 1994). For the first 1.5–2.0 Ma, ice age cycles appeared at a 41 k.y. interval, and the climate oscillated between glacial and interglacial states (Figure 5.25). A prominent but apparently short-lived interglacial (warm interval) about 2.4 Ma is recorded especially well in the Kap

København Formation, a 100-m-thick sequence of estuarine sediments that covered an extensive lowland area near the northern tip of Greenland (Funder et al., 2001).

FIGURE 5.25 NEAR HERE

The rich and well-preserved fossil fauna and flora in the Kap København Formation (Figure 5.26) record warming from cold conditions into an interglacial and then subsequent cooling during 10,000–20,000 years. During the peak warmth, forest trees reached the Arctic Ocean coast, 1000 kilometers (km) north of the northernmost trees today. Based on this warmth, Funder et al. (2001) suggested that the Greenland Ice Sheet must have been reduced to local ice caps in mountain areas (Figure 5.26a) (see Chapter 7, Greenland Ice Sheet). Although finely resolved time records are not available throughout the Arctic Ocean at that time, by analogy with present faunas along the Russian coast, the coastal zone would have been ice-free for 2 to 3 months in summer. Today this coast of Greenland experiences year-round sea ice, and models of diminishing sea ice in a warming world generally indicate long-term persistence of summertime sea ice off these shores (e.g., Holland et al., 2006). Thus, the reduced sea ice off northern Greenland during deposition of the Kap København Formation suggests a widespread warm time in which Arctic sea ice was much diminished.

FIGURE 5.26 NEAR HERE

During Kap København times, precipitation was higher and temperatures were warmer than at the peak of the current interglacial about 7 ka, and the temperature difference were larger during winter than during summer. Higher temperatures during deposition of the Kap København were not caused by notably greater solar insolation, owing to the relative repeatability of the Milankovitch variations during millions of years (e.g., Berger et al., 1992). As discussed above, uncertainties in estimation of atmospheric carbon-dioxide concentration, ocean heat transport, and perhaps other factors at the time of the Kap København Formation are sufficiently large to preclude strong conclusions about the causes of the unusual warmth.

Potentially correlative records of warm interglacial conditions are found in deposits on coastal plains along the northern and western shores of Alaska. High sea levels during interglaciations repeatedly flooded the Bering Strait, and they rapidly modified the configuration of the coastlines, altered regional continentality (isolation from the moderating influence of the sea), and reinvigorated the exchange of water masses between the North Pacific, Arctic, and North Atlantic oceans. Since the first submergence of the Bering Strait about 5.5–5 Ma (Marincovich and Gladenkov, 2001), this marine gateway has allowed relatively warm Pacific water from as far south as northern Japan to reach as far north as the Beaufort Sea (Brigham-Grette and Carter, 1992). The Gubik Formation of northern Alaska records at least three warm high sea stands in the early Quaternary (Figure 5.27). During the Colvillian transgression, about 2.7 Ma, the Alaskan Coastal Plain supported open boreal forest or spruce-birch woodland with scattered pine and rare fir and hemlock (Nelson and Carter, 1991). Warm marine conditions are confirmed by the general character of the ostracode fauna, which includes

Pterygocythereis vannieuwenhuisei (Brouwers, 1987), an extinct species of a genus whose modern northern limit is the Norwegian Sea and which, in the northwestern Atlantic Ocean, is not found north of the southern cold-temperate zone (Brouwers, 1987). Despite the high sea level and relative warmth indicated by the Colvillian transgression, erratics (rocks not of local origin) in Colvillian deposits southwest of Barrow, Alaska, indicate that glaciers then terminated in the Arctic Ocean and produced icebergs large enough to reach northwest Alaska at that time.

FIGURE 5.27 NEAR HERE

Subsequently, the Bigbendian transgression (about 2.5 Ma) was also warm, as indicated by rich molluscan faunas such as the gastropod *Littorina squalida* and the bivalve *Clinocardium californiense* (Carter et al., 1986). The modern northern limit of both of these mollusk species is well to the south (Norton Sound, Alaska). The presence of sea otter bones suggests that the limit of seasonal ice on the Beaufort Sea was restricted during the Bigbendian interval to positions north of the Colville River and thus well north of typical 20th-century positions (Carter et al., 1986); modern sea otters cannot tolerate severe seasonal sea-ice conditions (Schneider and Faro, 1975).

The youngest of these early Quaternary events of high sea level is the Fishcreekian transgression (about 2.1–2.4 Ma), suggested to be the same age as the Kap Kobenhavn Formation on Greenland (Brigham-Grette and Carter, 1992). However, age control is not complete, and Brigham (1985) and Goodfriend et al. (1996) suggested that the Fishcreekian could be as young as 1.4 Ma. This deposit contains several mollusk species that currently are found only to the south. Moreover, sea otter remains and the intertidal gastropod *Littorina squalida* at Fish Creek suggest that perennial sea ice was absent or severely restricted during the Fishcreekian transgression (Carter et al., 1986). Correlative deposits rich in mollusk species that currently live only well to the south are reported from the coastal plain at Nome, Alaska (Kaufman and Brigham-Grette, 1993).

The available data clearly indicate episodes of relatively warm conditions that correlate with high sea levels and reduced sea ice in the early Quaternary. The high sea levels suggest melting of land ice (see Chapter 7, Greenland Ice Sheet). Thus the correlation of warmth with diminished ice on land and at sea (see Chapter 8, Arctic sea ice)—indicated by recent instrumental observations, model results, and data from other time intervals—is also found for this time interval. Improved time resolution of histories of forcing and response will be required to assess the causes of the changes, but estimates of forcings indicate that they were relatively moderate and thus that the strong Arctic amplification of climate change was active in these early Quaternary events.

5.4.3 The Mid-Pleistocene Transition: 41 ka and 100 ka worlds

Since the late Pliocene, the cyclical waxing and waning of continental ice sheets have dominated global climate variability. The variations in sunshine caused by features of Earth's orbit have been very important in these ice-sheet changes, as described in Chapter 4 (paleoclimate concepts).

After the onset of glaciation in North America about 2.7 Ma (Raymo, 1994), ice grew and shrank as Earth's obliquity (tilt) varied in its 41 k.y. cycle. But between 1.2 and 0.7 Ma, the variations in ice volume became larger and slower, and an approximately

100-k.y. period has dominated especially during the last 700 k.y. or so (Figure 5.25). Although Earth's eccentricity varies with an approximately 100-k.y. period, this variation does not cause as much change in sunshine in the key regions of ice growth as did the faster cycles, so the reasons for the dominant 100-k.y. period in ice volume remain obscure. Roe and Allen (1999) assessed six different models of this behavior and found that all fit the data rather well. The record is still too short to allow the data to demonstrate the superiority of any one model.

Models for the 100-k.y. variability commonly assign a major role to the ice sheets themselves and especially to the Laurentide Ice Sheet on North America, which dominated the total global change in ice volume (e.g., Marchant and Denton, 1996). For example, Marshall and Clark (2002) modeled the growth and shrinkage of the Laurentide Ice Sheet and found that during growth the ice was frozen to the bed beneath and unable to move rapidly. After many tens of thousands of years, ice had thickened sufficiently that it trapped Earth's heat and thawed the bed, which allowed faster flow. Faster flow of the ice sheet lowered the upper surface, which allowed warming and melting (see Chapter 7, Greenland Ice Sheet). Behavior such as that described could cause the main variations of ice volume to be slower than the main variations in sunshine caused by Earth's orbital features, and the slow-flowing ice might partly ignore the faster variations in sunshine until the shift to faster flow allowed a faster response. Note that this explanation remains a hypothesis, and other possibilities exist. Alternative hypotheses require interactions in the Southern Ocean between the ocean and sea ice and between the ocean and the atmosphere (Gildor et al., 2002). For example, Toggweiler (2008) suggested that because of the close connection between the southern westerly winds and meridional overturning circulation in the Southern Ocean, shifts in wind fields may control the exchange of CO_2 between the ocean and the atmosphere. Carbon models support the notion that weathering and the burial of carbonate can be perturbed in ways that alter deep ocean carbon storage and that result in 100 k.y. CO_2 cycles (Toggweiler, 2008). Others have suggested that 100 k.y. cycles and CO_2 might be controlled by variability in obliquity cycles (i.e., two or three 41 k.y. cycles (Huybers, 2006) or by variable precession cycles (altering the 19 k.y. and 23 k.y. cycles (Raymo, 1997)). Ruddimann (2006) recently furthered these ideas but suggested that since 900 ka, CO_2-amplified ice growth continued at the 41 k.y. intervals but that polar cooling dampened ice ablation. His CO_2-feedback hypothesis suggests a mechanism that combines the control of 100 k.y. cycles with precession cycles (19 k.y. and 23 k.y.) and with tilt cycles (41 k.y.). The cause of the switch in the length of climate cycles from about 41 k.y. to about 100 k.y, known as the mid-Pleistocene transition, also remains obscure. This transition is of particular interest because it does not seem to have been caused by any major change in Earth's orbital behavior, and so the transition may reflect some fundamental threshold within the climate system.

The mid-Pleistocene transition may be related to continuation of the gradual global cooling from the Cretaceous, as described above (Raymo et al., 1997; 2006; Ruddiman, 2003). If, for example, the 100-k.y. cycle requires that the Laurentide Ice Sheet grow sufficiently large and thick to trap enough of Earth's heat to thaw the ice-sheet bed (Marshall and Clark, 2002), then long-term cooling may have reached the threshold at which the ice sheet became large enough.

However, such a cooling model does not explain the key observation (Clark et al., 2006) that the ice sheets of the last 700 k.y. configured a larger volume (Clark et al.,

2006) into a smaller area (Boellstorff, 1978; Balco et al., 2005a,b) than was true of earlier ice sheets. Clark and Pollard (1998) used this observation to argue that the early Laurentide Ice Sheet must have been substantially lower in elevation than in the late Pleistocene, possibly by as much as 1 km. Clark and Pollard (1998) suggested that the tens of millions of warm years back to the Cretaceous and earlier had produced thick soils and broken-up rocks below the soil. When glaciations began, the ice advanced over these water-saturated soils, which deformed easily. Just as grease on a griddle allows batter poured on top to spread easily into a wide, thin pancake, deformation of the soils beneath the growing ice (Alley, 1991) would have produced an extensive ice sheet that did not contain a large volume of ice. As successive ice ages swept the loose materials to the edges of the ice sheet, and as rivers removed most of the materials to the sea, hard bedrock was exposed in the central region. And, just as the bumps and friction of an ungreased waffle iron slow spreading of the batter to give a thicker, not-as-wide breakfast than on a greased griddle, the hard, bumpy bedrock produced an ice sheet that did not spread as far but which contained more ice.

Other hypotheses also exist for these changes. A complete explanation of the onset of extensive glaciation on North America and Eurasia as well as Greenland about 2.8 Ma, or of the transition from 41 k.y. to 100 k.y. ice age cycles, remains the object of ongoing investigations.

5.4.4 A link between ice volume, atmospheric temperature and greenhouse gases

The globally-averaged temperature change during one of the large 100-k.y. ice-age cycles was about 5°–6°C (Jansen et al., 2007). The larger changes were measured in the Arctic and close to the ice sheets, such as a change of 21°–23°C atop the Greenland ice sheet (Cuffey et al., 1995). The total change in sunshine reaching the planet during these cycles was near zero, and the orbital features served primarily to move sunshine from north to south and back, or from equator to poles and back, depending on the cycle considered (see Chapter 4, paleoclimate concepts).

As discussed by Jansen et al. (2007), and in section 5.2.6 above, many factors probably contributed to the large temperature change despite very small global change in total sunshine. Cooling produced growth of reflective ice that reduced the amount of sunshine absorbed by the planet. Complex changes especially in the ocean reduced atmospheric carbon dioxide, and both oceanic and terrestrial changes reduced atmospheric methane and nitrous oxide, all of which are greenhouse gases; the changes in carbon dioxide were most important. Various changes produced additional dust that blocked sunshine from reaching the planet (e.g., Mahowald et al., 2006). Cooling caused regions formerly forested to give way to grasslands or tundra that also reflected more sunshine. While Earth's orbit features drove the ice-age cycles, these feedbacks are required to provide quantitatively accurate explanations of the changes.

The relation between climate and carbon dioxide has been relatively constant for at least 650,000 years (Siegenthaler et al., 2005), and the growth and shrinkage of ice, cooling and warming of the globe, and other changes have repeated along similar although not identical paths. However, some of the small differences between successive cycles are of interest, as discussed next.

5.4.5 Marine Isotopic Stage 11 – a long interglaciation

Following the mid-Pleistocene transition, the growth and decay of ice sheets followed a 100 k.y. cycle: brief, warm interglaciations lasted about 10 k.y., after that ice progressively extended, and then the icy interval terminated rapidly by the transition into the next warm interglaciation (e.g., Kellogg, 1977; Ruddiman et al., 1986; Jansen et al., 1988; Bauch and Erlenkeuser, 2003; Henrich and Baumann, 1994). As discussed above, this 100 k.y. cycle may be linked to the 100 k.y. variation of the eccentricity, or out-of-roundness, of Earth's orbit about the sun, although other explanations are possible.

The eccentricity exhibits an additional cycle of just greater than 400,000 years, such that the orbit goes from almost round to more eccentric to almost round in about 100,000 years, but the maximum eccentricity reached in this 100,000-year cycle increases and decreases within a 400,000-year cycle (Berger and Loutre, 1991; Loutre, 2003). When the orbit is almost round, there is little effect from Earth's precession, which determines whether Earth is closer to the sun or farther from the sun during a particular season such as northern summer. About 400,000 years ago, during marine isotope stage (MIS) 11, the 400,000-year cycle caused a nearly round orbit to persist. The interglacial of MIS 11 lasted longer then previous or subsequent interglacials (see Droxler et al., 2003 and references therein; Kandiano and Bauch, 2007; Jouzel et al., 2007), perhaps because the summer sunshine (insolation) at high northern latitudes did not become low enough at the end of the first 10,000 years of the interglacial to allow ice growth at high northern latitudes—because the persistently nearly round orbit (i.e., of low eccentricity) prevented adequate cooling during northern summer (Figure 5.28).

FIGURE 5.28 NEAR HERE

As discussed in Chapter 7 (Greenland Ice Sheet), indications of Arctic and subarctic temperatures at this time versus more-recent interglacials are inconsistent (also see Stanton-Frazee et al., 1999; Bauch et al., 2000; Droxler and Farrell, 2000; Helmke and Bauch, 2003). Sea level seems to have been higher at this time than at any time since, and data from Greenland are consistent with notable shrinkage or loss of the ice sheet accompanying the notable warmth, although the age of this shrinkage is not constrained well enough to be sure that the warm time recorded was indeed MIS 11 (Chapter 7).

5.4.6 Marine Isotopic Stage (MIS) 5e: The Last Interglaciation

The warmest millennia of at least the past 250,000 years occurred during MIS 5, and especially during the warmest part of that interglaciation, MIS 5e (e.g., McManus et al., 1994; Fronval and Jansen, 1997; Bauch et al., 1999; Kukla, 2000). At that time global ice volumes were smaller than they are today, and Earth's orbital parameters aligned to produce a strong positive anomaly in solar radiation during summer throughout the Northern Hemisphere (Berger and Loutre, 1991). Between 130 and 127 ka, the average solar radiation during the key summer months (May, June, and July) was about 11% greater than solar radiation at present throughout the Northern Hemisphere, and a slightly greater anomaly, 13%, has been measured over the Arctic. Greater solar energy in summer, melting of the large Northern Hemisphere ice sheets, and intensification of the

North Atlantic Drift (Chapman et al., 2000; Bauch and Kandiano, 2007) combined to reduce Arctic Ocean sea ice, to allow expansion of boreal forest to the Arctic Ocean shore throughout large regions, to reduce permafrost, and to melt almost all glaciers in the Northern Hemisphere (CAPE Project Members, 2006).

High solar radiation in summer during MIS 5e, amplified by key boundary-condition feedbacks (especially sea ice, seasonal snow cover, and atmospheric water vapor; see above), collectively produced summer temperature anomalies 4°–5°C above present over most Arctic lands, substantially above the average Northern Hemisphere summer temperature anomaly (0°–2°C above present; CLIMAP Project Members, 1984; Bauch and Erlenkeuser, 2003). MIS 5e demonstrates the strength of positive feedbacks on Arctic warming (CAPE Project Members, 2006; Otto-Bleisner et al., 2006).

5.4.6a Terrestrial MIS 5e records At high northern latitudes, summer temperatures exert the dominant control on glacier mass balance, unless they are accompanied by strong changes in precipitation (e.g., Oerlemans, 2001; Denton et al., 2005; Koerner, 2005). Summer temperature is also the most effective predictor of most biological processes, although seasonality and the availability of moisture may influence some biological parameters such as dominance by evergreen or by deciduous vegetation (Kaplan et al., 2003). For these reasons, most studies of conditions during MIS 5e have focused on reconstructing summer temperatures. Terrestrial MIS 5e climate, especially, has been reconstructed from diagnostic assemblages of biotic proxies preserved in lake, peat, river, and shallow marine archives and from isotopic changes preserved in ice cores and carbonate deposits in lakes. Estimated winter and summer temperatures, and hence seasonality, are well constrained for Europe but are poorly known for most other **sectors** [please define "sector"]; likewise, precipitation reconstructions are limited to qualitative estimates in most cases where they are available, and they are not available for most regions.

During MIS 5e, all sectors of the Arctic had summers that were warmer than at present, but the magnitude of warming differed from one place to another (Figure 5.29) (CAPE Last Interglacial Project Members, 2006). Positive summer temperature anomalies were largest around the Atlantic sector, where summer warming was typically 4°–6°C. This anomaly extended into Siberia, but it decreased from Siberia westward to the European sector (0°–2°C), and eastward toward Beringia (2°–4°C). The Arctic coast of Alaska had sea-surface temperatures 3°C above recent values and considerably less summer sea ice than recently, but much of interior Alaska had smaller anomalies (0°–2°C) that probably extended into western Canada. In contrast, northeastern Canada and parts of Greenland had summer temperature anomalies of about 5°C and perhaps more (see Chapter 7 for a discussion of Greenland).

FIGURE 5.29 NEAR HERE

Precipitation and winter temperatures are more difficult to reconstruct for MIS 5e than are summer temperatures. In northeastern Europe, the latter part of MIS 5e was characterized by a marked increase in winter temperatures. A large positive winter temperature anomaly also occurred in Russia and western Siberia, although the timing is not as well constrained (Troitsky, 1964; Gudina et al., 1983; Funder et al., 2002).

Qualitative precipitation estimates for most other sectors indicate wetter conditions than in the Holocene.

5.4.6b Marine MIS 5e records Low sedimentation rates in the central Arctic Ocean and the rare preservation of carbonate fossils limit the number of sites at which MIS 5e can be reliably identified in sediment cores. MIS 5e sediments from the central Arctic Ocean usually contain high concentrations of planktonic (surface-dwelling) foraminifers and coccoliths, which indicate a reduction in summer sea-ice coverage that permitted increased biological productivity (Gard, 1993; Spielhagen et al., 1997; 2004; Jakobsson et al., 2000; Backman et al., 2004; Polyak et al., 2004; Nørgaard-Pedersen et al., 2007a,b). However, occasional dissolution of carbonate fossils complicates the interpretation of microfossil concentrations. Also, marine sediments from MIS 5a, slightly younger and cooler than MIS 5e, sometimes have higher microfossil concentrations than do MIS 5e sediments (Gard, 1986; 1987).

Arctic Ocean sediment cores recently recovered from the Lomonosov Ridge, north of Greenland, have revived the discussion of MIS 5e conditions in the Arctic Ocean. Unusually high concentrations of a subpolar foraminifer species, one which usually dwells in waters with temperatures well above freezing, were found in MIS 5e zones and interpreted to indicate warm interglacial conditions and much reduced sea-ice cover in the interior Arctic Ocean (Nørgaard-Pedersen et al., 2007a,b). Interpretation of these and other microfossils is complicated by the strong vertical stratification in the Arctic Ocean; today, warm Atlantic water (temperatures greater than 1°C) is in most areas isolated from the atmosphere by a relatively thin layer of cold (less than 1°C) fresher water; this cold water limits the transfer of heat to the atmosphere. It is not always possible to determine whether warm-water foraminifers found in marine sediment from the Arctic Ocean lived in warm waters that remained isolated from the atmosphere below the cold surface layer, or whether the warm Atlantic water had displaced the cold surface layer and was interacting with the atmosphere and affecting its energy balance.

Landforms and fossils from the western Arctic and Bering Strait indicate vastly reduced sea ice during MIS 5 (Figure 5.30). The winter sea-ice limit is estimated to have been as much as 800 km farther north than its average 20th-century position, and summer sea ice may at times have been absent (Brigham-Grette and Hopkins, 1995). These reconstructions are consistent with the northward migration of treeline by hundreds of kilometers throughout much of Alaska and nearby Chukotka and with the elimination of tundra from Chukotka to the Arctic Ocean coast (Lozhkin and Anderson, 1995).

FIGURE 5.30 NEAR HERE

Sufficient data are not yet available to allow unambiguous reconstruction of MIS 5e conditions in the central Arctic Ocean. Key uncertainties are related to the extent and duration of Arctic Ocean sea ice. The vertical structure of the upper 500 m of the water column is also climatically important but poorly known, in particular whether the strong vertical stratification characteristic of the modern regime persisted throughout MIS 5e, or whether reduced sea ice and changes in the hydrologic cycle and winds destabilized this stratification and allowed Atlantic water to reside at the surface in larger areas of the Arctic Ocean.

5.4.7 MIS 3 Warm Intervals

The temperature and precipitation history of MIS 3 (about 70–30 ka) is difficult to reconstruct because of the paucity of continuous records and the difficulty in providing a secure time frame. The $\delta^{18}O$ record of temperature change over the Greenland ice sheet and other ice-core data show that the North Atlantic region experienced repeated episodes of rapid, high-magnitude climate change, that temperatures rapidly increased by as much as 15°C (reviewed by Alley, 2007 and references therein), and that each warm period lasted several hundred to a few thousand years. These brief climate excursions are found not only in the Greenland Ice Sheet but are also recorded in cave sediments in China (Wang et al., 2001; Dykoski, et al., 2005) and in high-resolution marine records off California (Behl and Kennett, 1996), and in the Caribbean Sea's Cariaco Basin (Hughen et al., 1996.), the Arabian Sea (Schulz et al., 1998) and the Sea of Okhotsk (Nürnberg and Tiedmann, 2004), among many other sites. The ice-core records from Greenland contain indications of climate change in many regions on the same time scale (for example, the methane trapped in ice-core bubbles was in part produced in tropical wetlands and was essentially all produced beyond the Greenland ice sheet; Severinghaus et al., 1998). These ice-core records demonstrate clearly that the climate-change events were synchronous throughout widespread areas, and that the ages of events from many regions agree within the stated uncertainties. These events were thus hemispheric to global in nature (see review by Alley, 2007) and are considered a sign of large-scale coupling between the ocean and the atmosphere (Bard, 2002). The cause of these events is still debated. However, Broecker and Hemming (2001) and Bard (2002) among others suggested that they were likely the result of major and abrupt reorganizations of the ocean's thermohaline circulation, probably related to ice sheet instabilities that introduced large quantities of fresh water into the North Atlantic (Alley, 2007). Such large and abrupt oscillations, which were linked to changes in North Atlantic surface conditions and probably to the large-scale oceanic circulation, persisted into the Holocene (MIS 1); the youngest was only about 8.2 ka (Alley and Ágústdóttir, 2005). However, it appears that the abrupt 8.2 ka cooling was linked to an ice-age cause, a catastrophic flood from a very large lake that had been dammed by the melting Laurentide Ice Sheet.

Within MIS 3, land ice was somewhat reduced compared with the colder times of MIS 2 and MIS 4, but Arctic temperatures generally were much lower and ice more extensive than in MIS 1 (with certain exceptions). Sea level was lower at that time, the coastline was well offshore in many places, and the increased continentality may have contributed to warmer summertime temperatures that presumably were offset by colder wintertime temperatures.

For example, on the New Siberian Islands in the East Siberian Sea, Andreev et al. (2001) documented the existence of graminoid-rich tundra thought to have covered wide areas of the emergent shelf while summer temperatures were perhaps as much as 2°C warmer than during the 20th century. At Elikchan 4 Lake in the upper Kolyma drainage, the sediment record contains at least three intervals (especially one about 38 ka) when summer temperatures and treeline reached late Holocene conditions (Anderson and Lozhkin, 2001). Insect faunas nearby in the lower Kolyma are thought to have thrived in summers that were 1°–4.5°C warmer than recently for similar intervals of MIS 3 Alfimov et al., 2003). In general, variable paleoenvironmental conditions were typical of the traditional Karaginskii-MIS 3 period throughout Arctic Russia; however, stratigraphic confusion within the limits of radiocarbon-dating precludes the widespread correlation of events.

Relative warmth during MIS 3 appears to have been strongest in eastern Beringia; some evidence suggests that between 45 and 33 ka temperatures were only 1°–2°C lower than at present (Elias, 2007). The warmest interval in interior Alaska is known as the Fox Thermal Event, about 40–35 ka, which was marked by spruce forest tundra (Anderson and Lozhkin, 2001). Yet in the Yukon forests were most dense a little earlier, about 43–39 ka. In general (Anderson and Lozhkin, 2001), the warmest interstadial interval in all of Beringia possibly was 44–35 ka; it is well represented in proxies from interior sites and little or no vegetation response in areas closest to Bering Strait. Climatic conditions in eastern Beringia appear to have been harsher than modern conditions for all of MIS 3. In contrast, MIS 3 climates of western Beringia achieved modern or near modern conditions during several intervals. Moreover, although the transition from MIS 3 to MIS 2 was clearly marked by a transition from warm-moist to cold-dry conditions in western Beringia, this transition is absent or subtle in all but a few records in Alaska (Anderson and Lozhkin, 2001).

5.4.8 MIS 2, The Last Glacial Maximum (30 to 15 ka)

The last glacial maximum was particularly cold both in the Arctic and globally, and it provides useful constraints on the magnitude of Arctic amplification (see below). During peak cooling of the last glacial maximum, planetary temperatures were about 5°–6°C lower than at present (Farrera et al., 1999; Braconnot et al., 2007, Jansen et al., 2007), whereas Arctic temperatures in central Greenland were depressed more than 20°C (Cuffey et al., 1995; Dahl-Jensen et al., 1998)and similarly in Beringia (Elias et al., 1996).

5.4.9 MIS 1, The Holocene: The Present Interglaciation

In the face of rising solar energy in summer that was tied to orbital features and to rising greenhouse gases, Northern Hemisphere ice sheets began to recede from near their largest extent shortly after 20 ka, and the rate of recession noticeably increased after about 16 ka (see, e.g., Alley et al., 2002 for the timing of various events during the deglaciation). Most coastlines became ice-free before 12 ka, and ice continued to melt rapidly as summer insolation reached a peak (about 9% above modern insolation) about 11 ka. The transition from MIS 2 to MIS 1, which marks the start of the Holocene interglaciation, is commonly placed at the abrupt termination of the cold event called the Younger Dryas; that termination recently was estimated at about 11.7 ka (Rasmussen et al., 2006).

A wide variety of evidence from terrestrial and marine archives indicates that peak Arctic summertime warmth was achieved during the early Holocene, when most regions of the Arctic experienced sustained temperatures that exceeded observed 20th century values. This period of peak warmth, which is geographically variable in its timing, is generally referred to as the Holocene Thermal Maximum. The ultimate driver of the warming was orbital forcing, which produced increased summer solar radiation across the Northern Hemisphere. At 70°N., insolation in June now is near a local minimum (the maximum was recorded about 11–12 ka). June insolation about 4 ka was about 15 W/m^2 larger than recently, and June insolation at the Holocene peak was about 45 W/m^2 larger than recently, for a total change of about 10% (Figure 5.31; Berger and Loutre, 1991). Winter (January) insolation about 11 ka was only slightly lower than today, in large part because there is almost zero insolation that far north in January.

FIGURE 5.31 NEAR HERE

By 6 ka, sea level and ice volumes were close to those observed more recently, and climate forcings such as atmospheric carbon-dioxide concentration differed little from pre-industrial conditions (e.g., Jansen et al., 2007). (The exception is that far-northern summer insolation steadily decreased throughout the Holocene.) High-resolution (decades to centuries) archives containing many climate proxies are available for most of the Holocene throughout the Arctic. Consequently, the mid- to late-Holocene record allows evaluation of the range of natural climate variability and of the magnitude of climate change in response to relatively small changes in forcings.

5.4.9a The Holocene Thermal Maximum

Many of the Arctic paleoenvironmental records for the Holocene Thermal Maximum appear to have recorded primarily summertime conditions. Many different proxies have been exploited to derive these reconstructions by use of biological indicators such as pollen, diatoms, chironomids, dinoflagellate cysts, and other microfossils; elemental and isotopic geochemical indexes from lacustrine sediments, marine sediments, and ice cores; borehole temperatures; and age distributions of radiocarbon-dated tree stumps north of (or above) current treeline, marine mollusks, and whale bones (Kaufman et al., 2004).

A recent synthesis of 140 Arctic paleoclimatic and paleoenvironmental records extending from Beringia westward to Iceland (Kaufman et al., 2004) outlines the nature of the Holocene Thermal Maximum in the western Arctic (Figure 5.32). Fully 85% of the sites included in the synthesis contained evidence of a Holocene thermal maximum. Its average duration extended from 2100 years in Beringia to 3500 years in Greenland. The interval 10–4 ka contains the greatest number of sites recording Holocene Thermal Maximum conditions and the greatest spatial extent of those conditions in the western Arctic (Figure 5.32b). In the western Arctic the timing of this thermal maximum begins and ends along a strong geographic gradient (Figure 5.32c). The thermal maximum began first in Beringia, where warmer-than-present summer conditions became established at 14–13 ka. Intermediate ages for its initiation (10–8 ka) are apparent in the Canadian Arctic islands and in central Greenland. The Holocene Thermal Maximum on Iceland occurred a bit later, 8–6 ka. The onset on Svalbard was earlier, by 10.8 ka (Svendsen and Mangerud, 1997). The latest general onset (7–4 ka) of Holocene Thermal Maximum conditions affected the continental portions of central and eastern Canada experienced. Similarly, the earliest termination of the Holocene Thermal Maximum occurred in Beringia, although most regions registered summer cooling by 5 ka. Much of the pattern of the onset of the Holocene Thermal Maximum can be explained at least in part by proximity to cold winds blowing off the melting Laurentide Ice Sheet in Canada, which depressed temperatures nearby until the ice melted back. Milankovitch cycling has also been suggested to explain the spatial variability of the Holocene Thermal Maximum (Maximova and Romanovsky, 1988).

FIGURE 5.32 NEAR HERE

Records for sea-ice conditions in the Arctic Ocean and adjacent channels have been developed by radiocarbon-dating indicators including the remains of open-water proxies such as whales and walrus, warm-water marine mollusks, and changes in the microfauna preserved in marine sediments. These reconstructions, presented in more detail in Chapter 8 (Arctic sea ice), parallel the terrestrial record for the most part. The data demonstrate that an increased mass of warm Atlantic water moved into the Arctic Ocean beginning about 11.5 ka. It peaked about 8–5 ka which, coupled with increased summer insolation, decreased the area of perennial sea-ice cover during the early Holocene. Decreased sea-ice cover in the western Arctic during the early Holocene also may be indicated by changes in concentrations of sodium from sea salt in the Penny Ice Cap (eastern Canadian Arctic; Fisher et al., 1998) and the Greenland Ice Sheet (Mayewski et al., 1997). In most regions, perennial sea ice increased in the late Holocene, although it has been suggested that sea ice declined in the Chukchi Sea (de Vernal et al., 2005), possibly in response to changing rates of Atlantic water inflow in Fram Strait.

As summer temperatures increased through the early Holocene, in North America treeline expanded northward into regions formerly mantled by tundra, although the northward extent appears to have been limited to perhaps a few tens of kilometers beyond its recent position (Seppä et al., 2003; Gajeswski and MacDonald, 2004). In contrast, treeline advanced much farther across the Eurasian Arctic. Tree macrofossils (Kremenetski et al., 1998; MacDonald et al., 2000a,b; 2007) collected at or beyond the current treeline indicate that tree genera such as birch (*Betula*) and larch (*Larix*) advanced beyond the modern limits of treeline across most of northern Eurasia between 11 and 10 ka (Figures 5.33 and 5.34). Spruce (*Picea*) advanced slightly later than the other two genera. Interestingly, pine (*Pinus*), which now forms the conifer treeline in Fennoscandia and the Kola Peninsula, does not appear to have established appreciable forest cover at or beyond the present treeline in those regions at the far west of Europe until around 7 ka (MacDonald et al. 2000a). However, quantitative reconstructions of temperature from the Kola Peninsula and adjacent Fennoscandia suggest that summer temperatures were warmer than modern temperatures by 9 ka (Seppä and Birks, 2001; 2002; Hammarlund et al., 2002; Solovieva et al., 2005), and the development of extensive pine cover at and north of the present treeline appears to have been delayed relative to this warming. In the Taimyr Peninsula of Siberia and across nearby regions, the most northerly limit reached by trees during the Holocene was more than 200 km north of the current treeline. The treeline appears to have begun its retreat across northern Eurasia about 4 ka. The timing of the Holocene Thermal Maximum in the Eurasian Arctic overlaps the widest expression of the Holocene Thermal Maximum in the western Arctic (Figure 5.33), but it differs in two respects. The timing of onset and termination in Eurasia show much less variability than in North America, and the magnitude of the treeline expansion and retreat is far greater in the Eurasian Arctic. Fossil pollen and other indicators of vegetation or temperature from the northern Eurasian margin also support the contention of a prolonged warming and northern extension of treeline during the early through middle

Holocene (see for example Hyvärinen, 1975; Seppä, 1996; Clayden et al., 1997; Velichko et al., 1997; Kaakinen and Eronen, 2000; Pisaric et al., 2001; Seppä and Birks, 2001, 2002; Gervais et al., 2002; Hammarlund et al., 2002; Solovieva et al., 2005).

FIGURE 5.33 NEAR HERE

FIGURE 5.34 NEAR HERE

Changes in landforms suggest that during the early to middle Holocene, permafrost in Siberia degraded. A synthesis of Russian data by Astakhov (1995) indicates that melting permafrost was apparent north of the Arctic Circle only in the European North, not in Siberia. In the Siberian North, permafrost partially thawed only very locally, and thawing was almost entirely confined to areas under thermokarst lakes that actively formed there during the early through middle Holocene. Areas south of the Arctic Circle appear to have experienced deep thawing (100–200 m depth) from the early Holocene until about 4–3 ka, when cooler summer conditions led permafrost to develop again. The deep thawing and subsequent renewal of surface permafrost in these regions produced an extensive thawed layer sandwiched between shallow (20–80 m deep) more recently frozen ground and deeper Pleistocene permafrost throughout much of northwestern Siberia.

Quantitative estimates of the Holocene Thermal Maximum summer temperature anomaly along the northern margins of Eurasia and adjacent islands typically range from 1° to 3°C. The geographic position of northern treeline across Eurasia is largely controlled by summer temperature and the length of the growing season (MacDonald et al., 2007), and in some areas the magnitude of treeline displacement there suggests a summer warming equivalent of 2.5°–7.0°C (see for example Birks, 1991; Wohlfarth et al., 1995; MacDonald et al., 2000a; Seppä and Birks, 2001, 2002; Hammarlund et al., 2002; Solovieva et al., 2005). Sea-surface temperature anomalies during the Holocene Thermal Maximum were as much as 4°–5°C higher than during the late Holocene for the eastern North Atlantic sector and adjacent Arctic Ocean (Salvigsen, 1992; Koç et al., 1993). Anomalies in summer temperature in the western Arctic during the Holocene Thermal Maximum ranged from 0.5° to 3°C (mean, 1.65°C). The largest anomalies were in the North Atlantic sector (Kerwin et al., 1999; Kaufman et al., 2004; Flowers et al., 2008).

5.4.9b Neoglaciation

Many climate proxies are available to characterize the overall pattern of Late Holocene climate change. Following the Holocene Thermal Maximum, most proxy summer temperature records from the Arctic indicate an overall cooling trend through the late Holocene. Cooling is first recognized between 6 and 3 ka, depending on the threshold for change of each particular proxy. Records that exhibit a shift by 6–5 ka typically reflect intensified summer cooling about 3 ka (Figure 5.34).

Summer cooling during the second half of the Holocene led to the expansion of mountain glaciers and ice caps around the Arctic. The term “Neoglaciation” is widely applied to this episode of glacier growth, and in some cases re-formation, following the maximum glacial retreat during the Holocene Thermal Maximum (Porter and Denton, 1967). The former extent of glaciers is inferred from dated moraines and proglacial sediments deposited in lakes and marine settings. For example, ice-rafted detritus (Andrews et al., 1997) and the glacial geologic record (Funder, 1989) indicate that outlet glaciers of the Greenland Ice Sheet advanced during 6–4 ka (see Chapter 7, Greenland Ice Sheet). Multiproxy records from 10 glaciers or glaciated areas in Norway show evidence for increased activity by 5 ka (Nesje et al., 2001; Nesje et al., 2008). Major advances of outlet glaciers of northern Icelandic ice caps begin by 5 ka (Stötter et al., 1999; Geirsdottir et al., in press). In the European Arctic, glaciers expanded on Franz Josef Land (Lubinski et al., 1999) and Svalbard (Svendsen and Mangerud, 1997) by 4 ka, although sustained growth primarily began around 3 ka. An early Neoglacial advance of mountain glaciers is registered in Alaska, most prominently in the Brooks Range, the highest-latitude mountains in the state (Ellis and Calkin, 1984; Calkin, 1988). In southwest Alaska, mountain glaciers in the Ahklun Mountains did not reform until about 3 ka (Levy et al., 2003). Neoglacial advances began in Arctic Canada by 5 ka(Miller et al., 2005)

Additional evidence of Neoglacial seasonal cooling comes from several localities: a reduction in melt layers in the Agassiz Ice Cap (Koerner and Fisher, 1990) and in Greenland (Alley and Anandakrishnan, 1995); the decrease in $\delta^{18}O$ values in ice cores such as those from the Devon Island (Fisher, 1979) and Greenland (Johnsen et al., 1992) and indications of cooling from borehole thermometry (Cuffey et al., 1995); the retreat of large marine mammals and warm-water-dependent mollusks from the Canadian Arctic (Dyke and Savelle, 2001); the southward migration of the northern treeline across central Canada (MacDonald et al., 1993), Eurasia (MacDonald et al., 2000b), and Scandinavia (Barnekow and Sandgren, 2001); the expansion of sea-ice cover along the shores of the

Arctic Ocean on Ellesmere Island (Bradley, 1990), in Baffin Bay (Levac et al., 2001), and in the Bering Sea (Cockford and Frederick, 2007); and the shift in vegetation communities inferred from plant macrofossils and pollen around the Arctic (Bigelow et al., 2003). The assemblage of microfossils and the stable isotope ratios of foraminifers indicate a shift toward colder, lower salinity conditions about 5 ka along the East Greenland Shelf (Jennings et al., 2002) and the western Nordic seas (Koç and Jansen, 1994), suggesting increased influx of sea ice from the Arctic. Where quantitative estimates of temperature change are available, they generally indicate that summer temperature decreased by 1°–2°C during this initial phase of cooling.

The general pattern of an early- to middle-Holocene Thermal Maximum followed by Neoglacial cooling forms a multi-millennial trend that, in most places, culminated in the 19th century. Superposed on the long-term cooling trend were many centennial-scale warmer and colder summer intervals, which are expressed to a varying extent and are interpreted with various levels of confidence in different proxy records. In northern Scandinavia, evidence for notable late Holocene cold intervals before the 16th century includes narrow tree rings (Grudd et al., 2002), lowered treeline (Eronen et al., 2002), and major glacier advances (Karlén, 1988) between 2.6 and 2.0 ka. An extended analysis of these many centennial-scale warmer and colder intervals in Russia was published by Velichko and Nechaev (2005).

5.4.9c The Medieval Climate Anomaly (MCA) Probably the most oft-cited warm interval of the late Holocene is the Medieval Climate Anomaly (MCA), earlier referred to as the Medieval Warm Period (MWP). The anomaly was recognized on the basis of several lines of evidence in Western Europe, but the term is commonly applied to other regions to refer to any of the relatively warm intervals of various magnitudes and at various times between about 950 and 1200 AD (Lamb, 1977) (Figure 5.35). In the Arctic, evidence for climate variability, such as relative warmth, during this interval is based on glacier extents, marine sediments, **speleothems**, ice cores, borehole temperatures, tree rings, and archaeology. The most consistent records of an Arctic Medieval Climate Anomaly come from the North Atlantic sector of the Arctic. The summit of Greenland (Dahl-Jensen et al., 1998), western Greenland (Crowley and Lowery, 2000), Swedish Lapland (Grudd et al., 2002), northern Siberia (Naurzbaev et al., 2002), and Arctic Canada (Anderson et al., 2008) were all relatively warm around 1000 AD. During Medieval time, Inuit populations moved out of Alaska into the eastern Canadian Arctic and hunted whale from skin boats in regions perennially ice-covered in the 20th century (McGhee, 2004).

FIGURE 5.35 NEAR HERE

The evidence for Medieval warmth throughout the rest of the Arctic is less clear. However, some indications of Medieval warmth include the general retreat of glaciers in southeastern Alaska (Reyes et al., 2006; Wiles et al., 2008) and the wider tree rings in some high-latitude tree-ring records from Asia and North America (D’Arrigo et al., 2006). However D’Arrigo et al. (2006) emphasized the uncertainties involved in estimating Medieval Climate Anomaly warmth relative to that of the 20th century, owing in part to the sparse geographic distribution of proxy data as well as to the less coherent variability of tree growth temperature estimates for this anomaly. Hughes and Diaz (1994) argued that the Arctic as a whole was not anomalously warm throughout Medieval time (also see Bradley et al., 2003b, and National Research Council, 2006). Warmth during the Medieval interval is generally ascribed to lack of explosive volcanoes that produce particles that block the sun and perhaps to greater brightness of the sun (Crowley, 2000; Goosse et al., 2005; also see Jansen et al., 2007). Warming around the North Atlantic and adjacent regions may have been linked to changes in oceanic circulation as well (Broecker, 2001).

5.4.9d Climate of the past millennium and the Little Ice Age

Given the importance of understanding climate in the most recent past and the richness of the available evidence, intensive scientific effort has resulted in numerous temperature reconstructions for the past millennium (Jones, et al., 1998; Mann et al., 1998; Briffa et al., 2001; Esper et al., 2002; Crowley et al., 2003; Mann and Jones, 2003; Moberg et al., 2005; National Research Council, 2006; Jansen et al., 2007), and especially the last 500 years (Bradley and Jones, 1992; Overpeck et al., 1997). Most of these reconstructions are based on annually resolved proxy records, primarily from tree rings, and they attempt to extract a record of air-temperature change over large regions or entire hemispheres. Data from Greenland ice cores and a few annually laminated lake sediment records are typically included in these compilations, but few other records of quantitative temperature changes spanning the last millennium are available from the Arctic. In general, the temperature records are broadly similar: they show modest summer warmth during Medieval times, a variable, but cooling climate from about 1250 to 1850

AD, followed by warming as shown by both paleoclimate proxies and the instrumental record. Less is known about changes in precipitation, which is spatially and temporally more variable than temperature.

The trend toward colder summers after about 1250 AD coincides with the onset of the Little Ice Age (LIA), which persisted until about 1850 AD, although the timing and magnitude of specific cold intervals were different in different places. Proxy climate records, both glacial and non-glacial from around the Arctic and for the Northern Hemisphere as a whole, show that the coldest interval of the Holocene was sustained sometime between about 1500 and 1900 AD (Bradley et al., 2003a). Recent evidence from the Canadian Arctic indicates that, following their recession in Medieval times, glaciers and ice sheets began to expand again between 1250 and 1300 AD. Expansion was further amplified about 1450 AD (Anderson et al., 2008).

Glacier mass balances throughout most of the Northern Hemisphere during the Holocene are closely correlated with summer temperature (Koerner, 2005), and the widespread evidence of glacier re-advances across the Arctic during the Little Ice Age is consistent with estimates of summer cooling that are based on tree rings. The climate history of the Little Ice Age has been extensively studied in natural and historical archives, and it is well documented in Europe and North America (Grove, 1988). Historical evidence from the Arctic is relatively sparse, but it generally agrees with historical records from northwest Europe (Grove, 1988). Icelandic written records indicate that the duration and extent of sea ice in the Nordic Seas were high during the Little Ice Age (Ogilvie and Jónsson, 2001).

The average temperature of the Northern Hemisphere during the Little Ice Age was less than 1°C lower than in the late 20th century (Bradley and Jones, 1992; Hughes and Diaz, 1994; Crowley and Lowery, 2000), but regional temperature anomalies varied. Little Ice Age cooling appears to have been stronger in the Atlantic sector of the Arctic than in the Pacific (Kaufman et al., 2004), perhaps because ocean circulation promoted the development of sea ice in the North Atlantic, which further amplified Little Ice Age cooling there (Broecker, 2001; Miller et al., 2005).

The Little Ice Age also shows evidence of multi-decadal climatic variability, such as widespread warming during the middle through late 18th century (e.g., Cronin et al., 2003). Although the initiation of the Little Ice Age and the structure of climate fluctuations during this multi-centennial interval vary around the Arctic, most records show warming beginning in the late 19th century (Overpeck et al., 1997). The end of the Little Ice Age was apparently more uniform both spatially and temporally than its initiation (Overpeck et al., 1997).

The climate change that led to the Little Ice Age is manifested in proxy records other than those that reflect temperature. For example, it was associated with a positive shift in transport of dust and other chemicals to the summit of Greenland (O’Brien et al., 1995), perhaps related to deepening of the Icelandic low-pressure system (Meeker and Mayewski, 2002). According to modeling studies, the negative phase [see http://www.ldeo.columbia.edu/res/pi/NAO/] of the North Atlantic Oscillation could have been amplified during the Little Ice Age (Shindell et al., 2001) whereas, in the North Pacific, the Aleutian low was significantly weakened during the Little Ice Age (Fisher et al., 2004; Anderson et al., 2005).

Seasonal cooling into the Little Ice Age resulted from the orbital changes as described above, together with increased explosive volcanism and probably also decreased solar luminosity as recorded by sunspot numbers as far back as 1600 AD (Renssen et al., 2005; Ammann et al., 2007; Jansen et al., 2007).

5.4.10 Placing 20th century warming in the Arctic in a millennial perspective

Much scientific effort has been devoted to learning how 20th-century and 21st-century warmth compares with warmth during earlier times (e.g., National Research Council, 2006; Jansen et al., 2007). Owing to the orbital changes affecting midsummer sunshine (a drop in June insolation of about 1 W/m^2 at 75°N. and 2 W/m^2 at 90°N. during the last 1000 years; Berger and Loutre, 1991), additional forcing was needed in the 20th century to give the same summertime temperatures as achieved in the Medieval Warm Period.

After it evaluated globally or even hemispherically averaged temperatures, the National Research Council (2006) found that “Presently available proxy evidence indicates that temperatures at many, but not all, individual locations were higher during the past 25 years than during any period of comparable length since A.D. 900” (p. 3). Greater uncertainties for hemispheric or global reconstructions were identified in assessing older comparisons. As reviewed next, some similar results are available for the Arctic.

Thin, cold ice caps in the eastern Canadian Arctic preserve intact—but frozen—vegetation beneath them that was killed by the expanding ice. As these ice caps melt, they expose this dead vegetation, which can be dated by radiocarbon with a precision of a few decades. A recent compilation of more than 50 radiocarbon dates on dead vegetation emerging from beneath thin ice caps on northern Baffin Island shows that some ice caps formed more than 1600 years ago and persisted through Medieval times before melting early in the 21st century (Anderson et al., 2008).

Records of the melting from ice caps offer another view by which 20th century warmth can be placed in a millennial perspective. The most detailed record comes from the Agassiz Ice Cap in the Canadian High Arctic, for which the percentage of summer melting of each season’s snowfall is reconstructed for the past 10 k.y. (Fisher and Koerner, 2003). The percent of melt follows the general trend of decreasing summer insolation from orbital changes, but some brief departures are substantial. Of particular note is the significant increase in melt percentage during the past century; current percentages are greater than any other melt intensity since at least 1700 years ago, and melting is greater than any in sustained interval since 4–5 ka.

As reviewed by Smol and Douglas (2007b), changes in lake sediments record climatic and other changes in the lakes. Extensive changes especially in the post-1850 interval are most easily interpreted in terms of warming above the Medieval warmth on Ellesmere Island and probably in other regions, although other explanations cannot be excluded (also see Douglas et al., 1994). D’Arrigo et al. (2006) show tree-ring evidence from a few North American and Eurasian records that imply that summers were cooler in the Medieval Warm Period than in the late 20th century, although the statistical confidence is weak. Tree-ring and treeline studies in western Siberia (Esper and Schweingruber, 2004) and Alaska (Jacoby and D’Arrigo, 1995) suggest that warming since 1970 is has been optimal for tree growth and follows a circumpolar trend.

Hantemirov and Shiyatov (2002) records from the Russian Yamal Penisula, well north of the Arctic Circle, show that summer temperatures of recent decades are the most favorable for tree growth within the past 4 millennia.

Whole-Arctic reconstructions are not yet available to allow confident comparison of late 20th century warmth with Medieval temperatures, nor has the work been done to correct for the orbital influence and thus to allow accurate comparison of the remaining forcings.

5.5 Summary

5.5.1 Major features of Arctic Climate in the past 65 Ma

Section 5.4 summarized some of the extensive evidence for changes in Arctic temperatures, and to a lesser extent in Arctic precipitation, during the last 65 m.y. To some degree it also discussed “attribution”—the best scientific understanding of the causes of the climate changes. In this subsection, a brief synopsis is provided; for citations, the reader is referred to the extensive discussion just above.

At the start of the Cenozoic, 65 Ma, the Arctic was much warmer year around than it was recently; forests grew on all land regions and no perennial sea ice or Greenland Ice Sheet existed. Gradual but bumpy cooling has dominated most of the last 65 million years, and falling atmospheric CO_2 concentration apparently is the most important contributor to the cooling—although possible changing continental positions and their effect on atmospheric or oceanic circulation may also contribute. One especially prominent “bump,” the Paleocene-Eocene Thermal Maximum about 55 Ma, warmed the

Arctic Ocean more than 5°C and the Arctic landmass about 8°C, probably in a few centuries to a millennium or so, followed by cooling for about 100 ka. Warming from release of much CO_2 (possibly initially as sea-floor methane that was then oxidized to CO_2) is the most likely explanation. In the middle Pliocene (about 3 Ma) a modest warming was sufficient to allow deciduous trees on Arctic land that at present supports only High Arctic polar-desert vegetation; whether this warming originated from changes to circulation, CO_2, or some other cause remains unclear.

About 2.7 Ma, the cooling reached the threshold beyond which extensive continental ice sheets developed in the North American and Eurasian Arctic, and it marked the onset of the Quaternary Ice Age. Initially, the growth and shrinkage of the ice ages were directly controlled by changes in northern sunshine caused by features of Earth's orbit (the 41-k.y. cycle of sunshine that is tied to the obliquity (tilt) of Earth's axis is especially prominent). More recently, a 100-k.y. cycle has become more prominent, perhaps because the ice sheets became large enough that their behavior became important. Short, warm interglacials (usually lasting about 10,000 years, although the one about 440,000 years ago lasted longer) have alternated with longer glacial intervals. Recent work suggests that, in the absence of human influence, the current interglacial would continue for a few tens of thousands of years before the start of a new ice age (Berger and Loutre, 2002). Although driven by the orbital cycles, the large temperature differences between glacials and interglacials, and the globally synchronous response, reflect the effects of strong positive feedbacks, such as changes in atmospheric CO_2 and other greenhouse gases and in the areal extent of reflective snow and ice.

Interactions among the various orbital cycles have caused small differences between successive interglacials. More summer sunshine was received in the Arctic during the interglacial of about 130–120 ka than has been received in the current interglacial. Thus, summer temperatures in many places were about 4°–6°C warmer than recently, and these higher temperatures reduced ice on Greenland (Chapter 7, Greenland Ice Sheet), raised sea level, and melted widespread small glaciers and ice caps.

The seasonal cooling into and warming out of the most recent glacial were punctuated by numerous abrupt climate changes, and conditions persisted for millennia between jumps that were complete in years to decades. These events were very pronounced around the North Atlantic, but they had a much smaller effect on temperature elsewhere in the Arctic. Temperature changes extended to equatorial regions and caused a seesaw response in the far south (i.e., mean annual warming in the south when the north cooled). Large changes in extent of sea ice in the North Atlantic were probably responsible, linked to changes in regional to global patterns of ocean circulation; freshening of the North Atlantic favored expansion of sea-ice.

These abrupt temperature changes also were a feature of the current interglacial, the Holocene, but they ended as the Laurentide Ice Sheet on Canada melted away. Arctic temperatures in the Holocene broadly responded to orbital changes, and temperatures warmed during the middle Holocene when there was more summer sunshine. Warming generally led to northward migration of vegetation and to shrinkage of ice on land and sea. Smaller oscillations in climate during the Holocene, including the so-called Medieval Warm Period and the Little Ice Age, were linked to variations in the sun-blocking effect of particles from explosive volcanoes and perhaps to small variations in solar output, or in ocean circulation, or other factors. The warming from the Little Ice Age began for largely natural reasons, but it appears to have been accelerated by human contributions and especially by increasing CO_2 concentrations in the atmosphere (Jansen, 2007).

5.5.2. Arctic Amplification

The scientific understanding of climate processes shows that Arctic climate operates by use of many strong positive feedbacks (Serreze and Francis, 2006; Serreze et al., 2007a). As outlined in section 5.2, these feedbacks especially depend on the interactions of snow and ice with sunlight, the ocean, and the land surface (including its vegetation). For example, higher temperature tends to remove reflective ice and snow, more solar heat is then absorbed, and absorption of that heat promotes further warming (ice-albedo feedback). Also, higher temperature tends to remove sea ice that insulates the cold wintertime air from the warmer ocean beneath, further warming the air (ice-insolation feedback). Furthermore, higher temperature tends to allow dark shrubs to replace low-growing tundra that is easily covered by snow, intensifying the ice-albedo feedback. Similarly strong negative feedbacks are not known to stabilize Arctic climate, so physical understanding indicates that climate changes should be amplified in the Arctic as compared with lower latitude sites. This expectation is confirmed by the available data, as shown in Figure 5.36.

FIGURE 5.36 NEAR HERE

As we consider Arctic amplification, we must account for forcing. For the three younger time intervals shown in Figure 5.36, the Holocene Thermal Maximum (about 6 ka), the Last Glacial Maximum (LGM, about 20 ka), and marine isotope stage 5e, also known as the last interglacial (LIG, about 130–125 ka), the climate changes were primarily forced by Milankovitch features of Earth's orbit. The anomalies of incoming solar radiation (insolation) averaged throughout the whole planet for a year are very small for all times considered, and the orbital changes serve primarily to shift sunlight around on the planet. However, during these intervals the insolation forcing was relatively uniform throughout the Northern Hemisphere, and insolation anomalies north of 60°N. typically were only 10–20% greater than the anomalies for corresponding times averaged throughout the Northern Hemisphere. For example, at the peak of the last interglacial (130–125 ka), the Arctic (60°–90°N.) summer (May-June-July) insolation anomaly was 12.7% above present, while the Northern Hemisphere anomaly was 11.4% above present (Berger and Loutre, 1991).

To assess the geographic distribution of climate response, we compare Arctic and Northern Hemisphere summer temperature anomalies for the three younger time periods because of the similar forcing in the Arctic and Northern Hemisphere. During the Pliocene (and during earlier warm times discussed below but not plotted in the figure), warmth persisted much longer than the cycle time of insolation changes resulting from Earth's orbital irregularities (about 20 ka and about 40 ka). Consequently, we compare global temperature anomalies with Arctic anomalies.

A difficulty is that for some of those younger times, global and Arctic estimates of temperature anomalies are available but hemispheric estimates are not. (The global estimates clearly include hemispheric data, but those data have not been summarized in anomaly maps or hemispheric anomaly estimates that were published in the refereed scientific literature.) To obtain hemispheric estimates here, we note (as described in more detail below) that climate models driven by the known forcings show considerable fidelity in reproducing the global anomalies shown by the data for the relevant times, and that hemispheric anomalies can be assessed within these models. The hemispheric anomalies so produced are consistent with our understanding of the data, and so they are used here.

The Palaeoclimate Modelling Intercomparison Project (PMIP2; Harrison et al., 2002, and see http://pmip2.lsce.ipsl.fr/) coordinates an international effort to compare paleoclimate simulations produced by a range of climate models, and to compare these climate model simulations with data-based paleoclimate reconstructions for a middle Holocene warm time (6 ka) and for the last glacial maximum (LGM; 21 ka). A comparison of simulations for 6 and 21 ka by the project is reported by Braconnot et al. (2007).

As part of this Palaeoclimate Modelling Intercomparison Project effort, Harrison et al. (1998) compared global (mostly Northern Hemisphere) vegetation patterns simulated by using the output of 10 different climate model simulations for 6 ka. The model simulations closely agreed with the vegetation reconstructed from paleoclimate records. Similar comparisons on a regional basis for the Northern Hemisphere north of 55°N. (Kaplan et al., 2003), the Arctic (CAPE Project Members, 2001), Europe (Brewer et al., 2007), and North America (Bartlein et al., 1998) also showed close matches between paleoclimate data and models for the early Holocene. Comparison of models and data for the Last Glacial Maximum (Bartlein et al., 1998; Kaplan et al., 2003), and Last Interglaciation (CAPE Last Interglacial Project Members, 2006; Otto-Bliesner et al., 2006) reached similar conclusions. (Also see Pollard and Thompson, 1997; Farrera et al., 1999; Pinot et al., 1999; Kageyama et al., 2001.) Paleoclimate data corresponded closely with model simulations of the Holocene Thermal Maximum, Last Interglaciation warmth, and Last Glacial Maximum cold. This agreement provides confidence that we can compare climate-model simulations of past times with paleoclimate-based reconstructions of summer temperatures for the Arctic in order to evaluate the magnitude of Arctic amplification. (Figure 5.34 shows such a comparison.) Clearly, however, additional data and additional analyses of existing as well as new data would improve confidence in the results and perhaps reduce the error bars.

The forcing of the warmth of the middle Pliocene remains unclear. Orbital oscillations have continued throughout Earth history, but the Pliocene warmth persisted long enough to cross many orbital oscillations, which thus cannot have been responsible for the warmth.

The data indicate that Arctic temperature anomalies were much larger than global ones (Figure 5.34). The regression line through the four data points has a slope of 3.6 ± 0.6, suggesting that the change in Arctic summer temperatures tends to be 3 to 4 times as large as the global change.

This trend of larger Arctic anomalies was already well established during the greater warmth of the early Cenozoic peak warming and of the Cretaceous before that. Somewhat greater uncertainty is attached to these more ancient times in which continents were differently configured, so these data are not plotted in Figure 5.34; even so, the leading result is fully consistent with the regression. Barron et al. (1995) estimated global-average temperatures about 6°C warmer in the Cretaceous than recently. As reviewed by Alley (2003) (also see Bice et al., 2006), subsequent work suggests upward revision of tropical sea-surface temperatures by as much as a few degrees. The Cretaceous peak warmth seems to have been somewhat higher than early Cenozoic values, or perhaps similar (Zachos et al., 2001). In the Arctic, as discussed in section 5.4.1, the early Cenozoic (late Paleocene) temperature records probably mostly recorded summertime conditions of about 18°C in the ocean and about 17°C on land, followed during the short-lived Paleocene-Eocene Thermal Maximum by warming to about 23°C in the summer ocean and 25°C on land (Moran et al., 2006; Sluijs et al.; 2006; 2008; Weijers et al., 2007). No evidence of wintertime ice exists, and temperatures may have remained higher than during the mid-Pliocene. Recently, the oceanic site has remained ice covered; it is near or below freezing during the summer and much colder in winter. Hence, changes in the Arctic were much larger than the globally averaged change.

We have not included quantitative estimates in Figure 5.34 for the pre-Pliocene warm times, but a 3-fold Arctic amplification is consistent with the data within the broad uncertainties. The Cretaceous and early-Cenozoic warmth seems to have been forced by increased greenhouse-gas concentration, as discussed above, so the Arctic amplification seems to be independent of the forcing. This conclusion is expectable; many of the strong Arctic feedbacks serve to amplify temperature change without regard to causation—warmer summer temperatures melt reflective snow and ice, regardless of whether the warmth came from changing solar output, orbital configuration, greenhouse-gas concentrations, or other causes. Global warmth and an ice-free Arctic during the early

Eocene occurred without albedo feedbacks at the same time that the tropics experienced sustained warmth (Pearson et al., 2007).

Targeted studies designed to quantitatively assess Arctic amplification of climate change remain relatively rare, and they could be clarified. The available data, as assessed here, point to 3-fold to 4-fold Arctic amplification, such that, in response to the same forcing, Arctic temperature changes are 3 to 4 times as large as hemispheric-average changes, which are dominated by changes in the much larger lower latitude regions.

5.5.3 Implications for the future

Paleoclimatology shows that climate has changed greatly in the Arctic with time, and that the changes typically have been much larger in the Arctic than in lower latitudes. Strong feedbacks have promoted these Arctic changes, such as the ice-albedo feedback in which summer cooling expands reflective snow and ice that in turn amplify the cooling, or warming causes melting that amplifies the warming. Changes in sea-ice coverage of the Arctic Ocean have also been critical—open water cannot fall below the freezing point, but air above ice-covered water can become very cold in the dark Arctic winter. Thus, sustained changes in sea-ice coverage may cause perhaps the largest temperature changes observed on the planet (see, e.g., Denton et al., 2005).

These feedbacks have served to amplify climate changes with various causes, including those forced primarily by greenhouse-gas changes, consistent with physical understanding of the nature of the feedbacks. By simple analogy, and taken together with physical understanding, this knowledge indicates that climate changes will continue to be amplified in the Arctic. In turn, this knowledge indicates that continuing greenhouse-gas forcing of global climate or other human influences will change climate more in the Arctic than in lower latitude regions.

Chapter 5 Figure Captions

Figure 5.1 Median extent of sea ice in September, 2007, compared with averaged intervals during recent decades. Red curve, 1953–2000; orange curve, 1979–2000; green curve, September 2005. Inset: Sea ice extent time series plotted in square kilometers, shown from 1953–2007 in the graph below (Stroeve et al., 2008). The reduction in Arctic Ocean summer sea ice in 2007 was greater than that predicted by most recent climate models.

Figure 5.2 Projected surface-temperature changes for the last decade of the 21st century (2090–2099) relative to the period 1980–1999. The map shows the IPCC multi-Atmosphere-Ocean coupled Global Climate Model [average projection for the A1B (balanced emphasis on all energy resources) scenario. The most significant substantial warming is projected for the Arctic (IPCC, 2007; that report's Figure SPM6).

Figure 5.3 Global mean observed near-surface air temperatures for January 2003, derived from Atmospheric Infrared Sounder (AIRS) data. Contrast between equatorial and Arctic temperatures is greatest during the Northern Hemisphere winter. The transfer of heat from the tropics to the polar regions is a primary feature of Earth's climate system. Color scale is in Kelvin degrees such that 0°C=273.15 Kelvin. (Source: http://www-airs.jpl.nasa.gov/graphics/features/airs_surface_temp1_full.jpg) .

Figure 5.4 Albedo values in the Arctic

a) Advanced Very High Resolution Radiometery (AVHRR) -derived Arctic albedo values in June,1982–2004. The multi-year average shows the strong contrast between snow- and ice-covered areas (green through red) and open water or land (blue). (Image courtesy of X. Wang, University of Wisconsin–Madison, CIMSS/NOAA)

b) Albedo feedbacks. Albedo is the fraction of incident sunlight that is reflected. Snow, ice, and glaciers have high albedo. Dark objects such as the open ocean, which absorbs some 93% of the sun's energy, have low albedo (about 0.06), absorbing some 93% of the sun's energy. Bare ice has an albedo of 0.5; however, sea ice covered with snow has an albedo of nearly 90% (*Source:* *http://nsidc.org/seaice/processes/albedo.html).*

Figure 5.5 Changes in vegetation cover throughout the Arctic can influence albedo, as can altering the onset of snow melt in spring. A) Progression of the melt season in northern Alaska, May 2001 (top) and May 2002 (bottom), demonstrates how areas with exposed shrubs show earlier snow melt. B) Dark branches against reflective snow alter albedo (Sturm et al., 2005; Photograph courtesy of Matt Sturm).

Figure 5.6 Warming trend in Arctic permafrost (permanently frozen ground), 1970–present. Local effects can modify this trend. A) Sits in Alaska: WD, West Dock; DH, Deadhorse; FB, Franklin Bluffs; HV, Happy Valley; LG, Livengood; GK, Gulkana; BL, Birch Lake; OM, Old Man. B) Sites in northwest Canada: WG, Wrigley; NW, Norman Wells; NA, Northern Alberta; FS, Fort Simpson. C) Sites in European Russia: VT, Vorkuta; RG, Rogovoi; KT, Karataikha; MB, Mys Bolvansky. D) Northwest Siberia:

UR, Urengoi; ND, Nadym. E) Sites in Yakutia: TK, Tiksi; YK,Yakutsk. F) Sites in central Asia: KZ, Kazakhstan; MG, Mongolia (Brown and Romanovsky, 2008).

Figure 5.7 Inflows and outflows of water in the Arctic Ocean. Red lines, components and paths of the surface and Atlantic Water layer in the Arctic; black arrows, pathways of Pacific water inflow from 50–200 m depth; blue arrows, surface-water circulation; green, major river inflow; red arrows, movements of density-driven Atlantic water and intermediate water masses into the Arctic (AMAP, 1998).

Figure 5.8 Upper three panels: Correlation of global sea-level curve (Lambeck et al., 2002), Northern Hemisphere summer insolation (Berger and Loutre, 1991), and the Greenland Ice Sheet (GISP2) $\delta^{18}O$ record (Grootes et al., 1993), ages all given in calendar years. Bottom panel: temporal changes in the percentages of the main taxa of trees and shrubs, herbs and spores at Elikchan 4 Lake in the Magadan region of Chukotka, Russia. Lake core x-axis is depth, not time (Brigham-Grette et al., 2004). Habitat was reconstructed on the basis of modern climate range of collective species found in fossil pollen assemblages. The reconstruction can be used to estimate past temperatures or the seasonality of a particular site. The GISP2 record: Base of core roughly 60 ka (Lozhkin and Anderson, 1996). H1 above arrow, timing of Heinrich event event 1 (and so on); number 1 above curve, Dansgaard-Oscheger event (and so on). During approximately 27 ka to nearly 55 ka, vegetation, especially treeline, recovered for short intervals to nearly Holocene conditions at the same time that the isotopic record in Greenland suggests repeated warm warm-cold cycles of change. kyr BP, thousands of years before the present.

Figure. 5.9 Annual tree rings composed of seasonal early and late wood are clear in this a 64-year year-old *Larix siberica* from western Siberia (Esper and Schweingruber, 2004). Initial growth was restricted; narrow rings average 0.035 mm/year, punctuated by one thicker ring (one single arrow). Later (two arrows), tree-ring width abruptly at least doubled for more than three years. Ring widths increased to 0.2 mm/year (Photograph courtesy of Jan Esper, Swiss Federal Research Institute).

Figure 5.10 Typical tree ring samples. a) Increment cores taken from trees with a small small-bore hollow drill. They can be easily stored and transported in plastic soda straws for analysis in the laboratory. b) Alternatively, cross sections or disks can be sanded for study. A cross section of *Larix decidua* root shows differing wood thickness within single rings, caused by exposure. (Photographs courtesy of Jan Esper and Holger Gärtner, Swiss Federal Research Institute, respectively).

Figure 5.11 14 Microscopic marine plankton known as (foraminiferaifers (see inset) grow a shell of calcium carbonate ($CaCO_3$) in or near isotopic equilibrium with ambient sea water. The oxygen isotope ratio measured in these shells can be used to determine the temperature of the surrounding waters. (The oxygen-isotope ratio is expressed in $\delta^{18}O$ parts per million (ppm) = $10^3[(R_{sample}/R_{standard}) - 1]$, where R_x = $(^{18}O)/(^{16}O)$ is the ratio of isotopic composition of a sample compared to that of an established standard, such as ocean water) However, factors other than temperature can influence the ratio of ^{18}O to ^{16}O. Warmer seasonal temperatures, glacial meltwater, and river runoff with depleted values all will produce a more negative (lighter) ∂^{18}O [should the Greek letter be δ ?] ratio. On the other hand, cooler temperatures or higher salinity waters will drive the ratio up, making it heavier, or more positive. The growth of large continental ice sheets selectively removes the lighter isotope (^{16}O), leaving the ocean enriched in the heavier isotope (^{18}O).

Figure 5.12 Lake El'gygytgyn in the Arctic Far East of Russia. Open and closed lake systems in the Arctic differ hydrologically according to the balance between inflow, outflow, and the ratio of precipitation to evaporation. These parameters are the dominant influence on lake stable stable-isotopic chemistry and on the depositional character of the sediments and organic matter. Lake El'gygytgyn is annually open and flows to the Bering Sea during July and August, but the outlet closes by early September as lake level drops and storms move beach gravels that choke the outlet. (Photograph by J. Brigham-Grette).

Figure 5.13 Locations of Arctic and sub-Arctic lakes (blue) and ice cores (green) whose oxygen isotope records have been used to reconstruct Holocene paleoclimate. (Map adapted from the Atlas of Canada, © 2002. Her Majesty the Queen in Right of Canada, Natural Resources Canada. / Sa Majesté la Reine du chef du Canada, Ressources naturelles Canada.)

Figure 5.14 a) One-meter section of Greenland Ice Core Project-2 core from 1837 m depth showing annual layers. (Photograph courtesy of Eric Cravens, Assistant Curator, U.S. National Ice Core Laboratory). b) Field site of Summit Station on top of the Greenland Ice sheet (Photograph by Michael Morrison, GISP2 SMO, University of New Hampshire; NOAA Paleoslide Set)

Figure 5.15 Relation between isotopic composition of precipitation and temperature in the parts of the world where ice sheets exist**.** Sources of data as follows: International Atomic Energy Agency (IAEA) network (Fricke and O'Neil, 1999; calculated as the means of summer and winter data of their Table 1 for all sites with complete data. Open squares, poleward of 60° latitude (but with no inland ice-sheet sites); open circles, 45°–60° latitude; filled circles, equatorward of 45° latitude. x, data from Greenland (Johnsen et al., 1989); +, data from Antarctica (Dahe et al., 1994). About 71% of Earth's surface area is equatorward of 45°, where dependence of δ^{18}O on temperature is weak to nonexistent. Only 16% of Earth's surface falls in the 45°–60° band, and only 13% is poleward of 60°. The linear array is clearly dominated by data from the ice sheets.

Figure 5.16 Paleotemperature estimates of site and source waters from on Greenland: GRIP and NorthGrip, Masson-Delmotte et al., 2005). GRIP (left) and NorthGRIP (right) site (top) and source (bottom) temperatures derived from GRIP and NorthGRIP δ^{18}O and deuterium excess corrected for seawater δ^{18}O (until 6000 BP). Shaded lines in gray behind the black line provide an estimate of uncertainties due to the tuning of the isotopic model and the analytical precision. Solid line (in part above zigzag line), GRIP temperature derived from the borehole-temperature profile (Dahl-Jensen et al., 1998).

Figure 5.17 Biomarker alkenone. U_{37}^{K} versus measured water temperature for ocean-water surface mixed layer (0–30 m) samples. A) Atlantic region: Empirical 3rd-order polynomial regression for samples collected in warmer-than-4°C waters is U_{37}^{K} = 1.004 10 4T3 + 5.744 10 3T2 6.207 10 2T + 0.407 (r2 = 0.98, n = 413) (Outlier data from the southwest Atlantic margin and northeast Atlantic upwelling regime is excluded.). B) Pacific, Indian, and Southern Ocean regions: The empirical linear regression of Pacific samples is U_{37}^{K} = 0.0391T 0.1364 (r2 = 0.97, n = 131). Pacific regression does not include the Indian and Southern Ocean data. C) Global data: The empirical 3rd order polynomial regression, excluding anomalous southwest Atlantic margin data, is U_{37}^{K} = 5.256 10 5T3 + 2.884 10 3T2 8.4933 10 3T + 9.898 (r2 = 0.97, n = 588). +, sample excluded from regressions. (Conte et al, 2006).

Figure 5.18 Diatom assemblages reflect a variety of environmental conditions in Arctic lake systems. Transitions, especially rapid change from one assemblage to another, can reflect large changes in conditions such as light, nutrient availability, or temperature, for example. Biogenic silica, chiefly the silica skeletal framework constructed by diatoms, is commonly measured in lake sediments and used as an index of past changes in aquatic primary productivity.

Figure 5.19 Changing ice and snow conditions on an Arctic lake during relatively (a) cold, (b) moderate, and (c) warm conditions. During colder years, a permanent raft of ice may persist throughout the short summer, precluding the development of large populations of phytoplankton, and restricting much of the primary production to a shallow, open open-water moat. Many other physical, chemical and biological changes occur in lakes that are either directly or indirectly affected by snow and ice cover (see Table 1; Douglas and Smol, 1999). Modified from Smol (1988).

Figure 5.20 A–D) Lake ice melts as it continues to warm. D) Eventually, in deeper lakes (as opposed to ponds), thermal layers may stratify or be prolonged during the summer months, further altering the limnological characteristics of the lake. Modified from Douglas (2007).

Figure 5.21 The form and distribution of wind-blown silt (loess), wind-blown sand (dunes), and other deposits of wind-blown sediment in Alaska, have been used to infer both Holocene and last-glacial past wind directions. (Compiled from many sources by Muhs and Budahn, 2006.).

Figure 5.22 Unnamed, hydrologically closed lake in the Yukon Flats Wildlife Refuge, Alaska. Concentric rings of vegetation developed progressively inward as water level fell, owing to a negative change in the lake's overall water balance. Historic Landsat imagery and air photographs indicate that these shorelines formed during within the last 40 years or so. (Photograph by Lesleigh Anderson.)

Figure 5.23 Recovered sections and palynological and geochemical results across the Paleocene-Eocene Thermal Maximum about 55 Ma; IODP Hole 302-4A (87° 52.00' N.; 136° 10.64' E.; 1288 m water depth, in the central Arctic Ocean basin). Mean annual surface-water temperatures (as indicated in the TEX_{86}' column) are estimated to have reached 23°C, similar to water in the tropics today. (Error bars for Core 31X show the uncertainty of its stratigraphic position. Orange bars, indicate intervals affected by drilling disturbance.) Stable carbon isotopes are expressed relative to the PeeDee Belemnite standard. Dinocysts tolerant of low salinity comprise *Senegalinium* spp., *Cerodinium* spp., and *Polysphaeridium* spp., whereas *Membranosphaera* spp., *Spiniferites ramosus* complex, and *Areoligera-Glaphyrocysta* cpx. represent typical marine species. Arrows and *A. aug* (second column) indicate the first and last occurrences of dinocyst *Apectodinium augustum*—a diagnostic indicator of Paleocene-Eocene Thermal Maximum warm conditions. (Sluijs et al., 2006).

Figure 5.24 Atmospheric CO_2 and continental glaciation 400 Ma to present. Vertical blue bars, timing and palaeolatitudinal extent of ice sheets (after Crowley, 1998). Plotted CO_2 records represent five-point running averages from each of four major proxies (see Royer, 2006 for details of compilation). Also plotted are the plausible ranges of CO_2 derived from the geochemical carbon cycle model GEOCARB III (Berner and Kothavala, 2001). All data adjusted to the Gradstein et al. (2004) time scale. Continental ice sheets grow extensively when CO_2 is low. (after Jansen, 2007, that report's Figure 6.1)

Figure 5.25 The average isotopic composition ($\delta^{18}O$) of bottom-dwelling foraminiferaifers from in a globally distributed set of 57 sediment cores that record the last 5.3 Ma (modified from Lisiecki and Raymo, 2005). The $\delta^{18}O$ is controlled primarily by global ice volume and deep-ocean temperature, with less ice or warmer temperatures (or both) upward in the core. The influence of Milankovitch frequencies of Earth's orbital variation are present throughout, but glaciation increased about 2.7 Ma ago concurrently with establishment of a strong 41 ka variability linked to Earth's obliquity (changes in tilt of Earth's spin axis), and the additional increase in glaciation about 1.2–0.7 Ma parallels a shift to stronger 100 ka variability. Dashed lines are used because the changes seem to have been gradual. The general trend toward higher $\delta^{18}O$ that runs through this series reflects the long-term drift toward a colder Earth that began in the early Cenozoic (see Figure 4.8).

Figure 5.26 a) Greenland without ice for the last time? Dark green, boreal forest; light green, deciduous forest; brown, tundra and alpine heaths; white, ice caps. The north-south temperature gradient is constructed from a comparison between North Greenland and northwest European temperatures, using standard lapse rate; distribution of precipitation assumed to retain the Holocene pattern. Topographical base, from model by Letreguilly et al. (1991) of Greenland's sub-ice topography after isostatic recovery. b) Upper part of the Kap København Formation, North Greenland. The sand was deposited in an estuary about 2.4 Ma; it contains abundant well-preserved leaves, seeds, twigs, and insect remains. (Figure and Photograph of by S.V. Funder.).

Figure 5.27 The largely marine Gubik Formation, North Slope of Alaska, contains three superposed lower units that record relative sea level as high +30-+ to +40 m. Pollen in these deposits suggests that borderland vegetation at each of these times was less forested; boreal forests or spruce-birch woodlands at 2.7 Ma gave way to larch and spruce forests at about 2.6 Ma and to open tundra by about 2.4 Ma (see photographs by Robert Nelson, Colby College, who analyzed the pollen; oldest at top). Isotopic reference time series of Lisecki and Raymo (2005) suggests best as assignments for these sea level events (Brigham and Carter, 1992).

Figure 5.28 Glacial cycles of the past 800 ka derived from marine-sediment and ice cores (McManus, 2004). The history of deep-ocean temperatures and global ice volume inferred from $\delta^{18}O$ measured in bottom-dwelling foraminifera shells preserved in Atlantic Ocean sediments. Air temperatures over Antarctica inferred from the ratio of deuterium to hydrogen in ice from central Antarctica (EPICA, 2004). Marine isotope stage 11 (MIS 11) is an interglacial whose orbital parameters were similar to those of the Holocene, yet it lasted about twice as long as most interglacials. Note the smaller magnitude and less-pronounced interglacial warmth of the glacial cycles that preceded MIS 11. Interglaciations older than MIS 11 were less warm than subsequent integlaciations.

Figure. 5.29 Polar projection showing regional maximum LIG last interglacial summer temperature anomalies relative to present summer temperatures; derived from paleotemperature proxies (see tables Tables 1 and 2, in from CAPE Last Interglacial Project Members, 2006). Circles, terrestrial; squares, marine sites.

Figure 5.30 Winter sea-ice limit during MIS 5e and at present. Fossiliferous paleoshorelines and marine sediments were used by Brigham-Grette and Hopkins (1995) to evaluate the seasonality of coastal sea ice on both sides of the Bering Strait during the Last Last Interglaciation. Winter sea limit is estimated to have been north of the narrowest section of the strait, 800 km north of modern limits. Pollen data derived from Last Interglacial lake sediments suggest that tundra was nearly eliminated from the Russian coast at this time (Lozhkin and Anderson, 1995). In Chukokta during the warm interglaciation, additional open water favored some taxa tolerant of deeper winter snows. (Map of William Manley, http://instaar.colorado.edu/QGISL/).

Figure 5.31 The Arctic Holocene Thermal Maximum. Items compared, top to bottom: seasonal insolation patterns at 70° N. (Berger & Loutre, 1991), and reconstructed Greenland air temperature from the GISP2 drilling project (Alley 2000); age distribution of radiocarbon-dated fossil remains of various tree genera from north of present treeline (MacDonald et al., 2007),); and the frequency of Western Arctic sites that experienced Holocene Thermal Maximum conditions. (Kaufman et al. 2004).

Figure. 5.32 The timing of initiation and termination of the Holocene Thermal Maximum in the western Arctic (Kaufman et al., 2004). a) Regions reviewed in Kaufman et al., 2004. b) Initiation of the Holocene Thermal Maximum in the western Arctic.

Longitudinal distribution (left) and frequency distribution (right). c) Spatial-temporal pattern of the Holocene Thermal Maximum in the western Arctic. Upper panel, initiation; lower panel, termination. Dot colors bracket ages of the Holocene Thermal Maximum; ages contoured using the same color scheme. Gray dots, equivocal evidence for the Holocene Thermal Maximum.

Figure. 5.33 The northward extension of larch (*Larix*) treeline across the Eurasian Arctic. Treeline today compared with treeline during the Holocene Thermal Maximum and with anticipated northern forest limits (Arctic Climate Impact Assessment, 2005) due to climate warming (MacDonald et al., 2007).

Fig. 5.34 Arctic temperature reconstructions. Upper panel: Holocene summer melting on the Agassiz Ice Cap, northern Ellesmere Island, Canada. “Melt” indicates the fraction of each core section that contains evidence of melting (from Koerner and Fisher, 1990). Middle panel: Estimated summer temperature anomalies in central Swened. Black bars, elevation of ^{14}C- dated sub-fossil pine wood samples (*Pinus sylvestris* L.) in the Scandes Mountains, central Sweden, relative to temperatures at the modern pine limit in the region. Dashed line, upper limit of pine growth is indicated by the dashed line. Changes in temperature estimated by assuming a lapse rate of 6 °C km^{-1} (from Dahl and Nesje, 1996, ; based on samples collected by L. Kullman and by G. and J. Lundqvist). Lower panel: Paleotemperature reconstruction from oxygen isotopes in calcite sampled along the growth axis of a stalagmite from a cave at Mo i Rana, northern Norway.

Growth ceased around A.D. 1750 (from Lauritzen 1996; Lauritzen and Lundberg 1998; 2002). Figure from Bradley (2000).

Figure 5.35 Updated composite proxy-data reconstruction of Northern Hemisphere temperatures for most of the last 2000 years, compared with other published reconstructions. Estimated confidence limits, 95%. All series have been smoothed with a 40-year lowpass filter. The Medieval Climate Anomaly (MCA), about 950–1200 AD. The array of reconstructions demonstrate that the warming documented by instrumental data during the past few decades exceeds that of any warm interval of the past 2000 years, including that estimated for the MCA. (Figure from Mann et al. (in press). CPS, composite plus scale methodology; CRU, East Anglia Climate Research unit, a source of instrumental data; EIV, error-in-variables); HAD, Hadley Climate Center.

Figure 5.36 Paleoclimate data quantify the magnitude of Arctic amplification. Shown are paleoclimate estimates of Arctic summer temperature anomalies relative to recent, and the appropriate Northern Hemisphere or global summer temperature anomalies, together with their uncertainties, for the following: the last glacial maximum (LGM; about 20 ka), Holocene thermal maximum (HTM; about 8 ka), last interglaciation (LIG; 130–125 ka ago) and middle Pliocene (about 3.5–3.0 Ma). The trend line suggests that summer temperature changes are amplified 3 to 4 times in the Arctic**.** Explanation of data sources follows, for the different times for each time considered, beginning with the most recent.

Holocene Thermal Maximum (HTM): Arctic ΔT = 1.7 ± 0.8°C; Northern Hemisphere ΔT = 0.5 ± 0.3°C; Global ΔT = 0° ± 0.5°C.

A recent summary of summer temperature anomalies in the western Arctic (Kaufman et al., 2004) built on earlier summaries (Kerwin et al., 1999; CAPE Project Members, 2001) and is consistent with more-recent reconstructions (Kaplan and Wolfe, 2006; Flowers et al., 2007). Although the Kaufman et al. (2004) summary considered only the western half of the Arctic, the earlier summaries by Kerwin et al., (1999) and CAPE Project Members (2001) indicated that similar anomalies characterized the eastern Arctic, and all syntheses report the largest anomalies in the North Atlantic sector. Few data are available for the central Arctic Ocean; we assume that the circumpolar dataset provides an adequate reflection of air temperatures over the Arctic Ocean as well.

Climate models suggest that the average planetary anomaly was concentrated over the Northern Hemisphere. Braconnot et al. (2007) summarized the simulations from 10 different climate model contributions to the PMIP2 project that compared simulated summer temperatures at 6 ka with recent temperatures. The global average summer temperature anomaly at 6 ka was 0° ± 0.5°C, whereas the Northern Hemisphere anomaly was 0.5° ± 0.3°C. These patterns are similar to patterns in model results described by Hewitt and Mitchell (1998) and Kitoh and by Murakami (2002) for 6 ka, and a global simulation for 9 ka (Renssen et al., 2006). All simulate little difference in summer temperature outside the Arctic when those temperatures are compared to with pre-industrial temperatures.

Last Glacial Maximum (LGM): Arctic ΔT = 20° ± 5°C; global and Northern Hemisphere ΔT = –5° ± 1°C

Quantitative estimates of temperature reductions during the peak of the Last Glacial Maximum are less widespread in for the Arctic than are estimates of temperatures during warm times. Ice-core borehole temperatures, which offer the most compelling evidence (Cuffey et al., 1995; Dahl-Jensen et al., 1998), are supported by evidence from biological proxies in the North Pacific sector (Elias et al., 1996a), where no ice cores are available that extend back to the Last Glacial Maximum. Because of the limited datasets for temperature reduction in the Arctic during the Last Glacial Maximum, we incorporate a large uncertainty. The global-average temperature decrease during peak glaciations, based on paleoclimate proxy data, was 5°–6°C, and little difference existed between the Northern and Southern Hemispheres (Farrera et al., 1999; Braconnot et al., 2007; Braconnot et al., 2007). A similar temperature anomaly is derived from climate-model simulations (Otto-Bliesner et al., 2007).

Last Interglaciation (LIG): Arctic $\Delta T = 5° \pm 1°C$; global and Northern Hemisphere $\Delta T = 1° \pm 1°C$)

A recent summary of all available quantitative reconstructions of summer-temperature anomalies for in the Arctic during peak Last Interglaciation warmth shows a spatial pattern similar to that shown by Holocene Thermal Maximum reconstructions. The largest anomalies are in the North Atlantic sector and the smallest anomalies are in the North Pacific sector, but those small anomalies are substantially larger (5° ± 1°C) than they were during the Holocene Thermal Maximum (CAPE Last Interglacial Project Members, 2006). A similar pattern of Last Interglaciation summer-temperature anomalies is apparent in climate model simulations (Otto-Bliesner et al., 2006). Global and Northern Hemisphere summer-temperature anomalies are derived from summaries in

CLIMAP Project Members (1984), Crowley (1990), Montoya et al. (2000), and Bauch and Erlenkeuser (2003).

Middle Pliocene: Arctic $\Delta T = 12° \pm 3°C$; global $\Delta T = 4° \pm 2°C$)

Widespread forests throughout the Arctic in the middle Pliocene offer a glimpse of a notably warm time in the Arctic, which had essentially modern continental configurations and connections between the Arctic Ocean and the global ocean. Reconstructed Arctic temperature anomalies are available from several sites that show much warmth and no summer sea ice in the Arctic Ocean basin. These sites include the Canadian Arctic Archipelago (Dowsett et al., 1994; Elias and Matthews, 2002; Ballantyne et al., 2006), Iceland (Buchardt and Símonarson, 2003), and the North Pacific (Heusser and Morley, 1996). A global summary of mid-Pliocene biomes by Salzmann et al. (2008) concluded that Arctic mean-annual-temperature anomalies were in excess of 10°C; some sites indicate temperature anomalies of as much as 15°C. Estimates of global sea-surface temperature anomalies are from Dowsett (2007).

Global reconstructions of mid-Pliocene temperature anomalies from proxy data and general circulation models show modest warming (average, $4° \pm 1°C$) across low to middle latitudes (Dowsett et al., 1999; Raymo et al., 1996; Sloan et al., 1996, Budyko et al., 1985; Haywood and Valdes, 2004; Jiang et al., 2005; Haywood and Valdes, 2006; Salzmann et al., 2008).

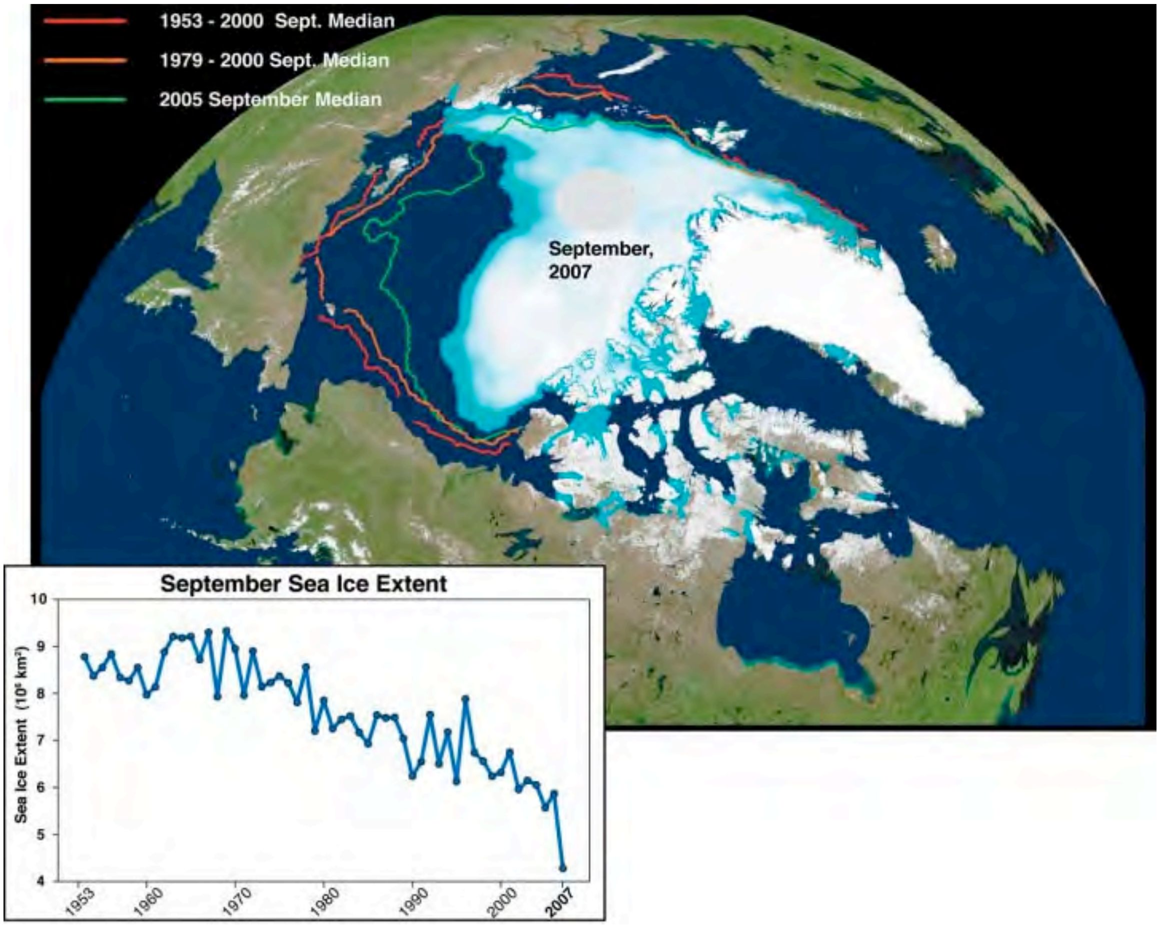

Figure 5.1 Median extent of sea ice in September, 2007, compared with averaged intervals during recent decades. Red curve, 1953–2000; orange curve, 1979–2000; green curve, September 2005. Inset: Sea ice extent time series plotted in square kilometers, shown from 1953–2007 in the graph below (Stroeve et al., 2008). The reduction in Arctic Ocean summer sea ice in 2007 was greater than that predicted by most recent climate models.

Geographical pattern of surface warming

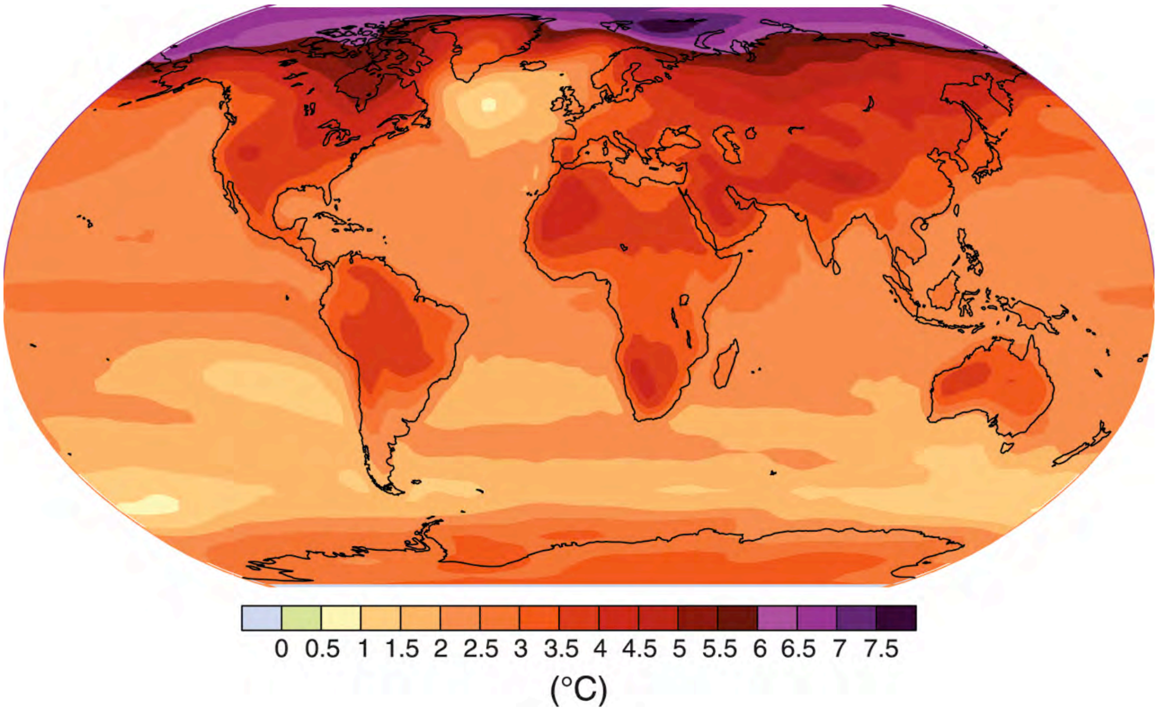

Figure 5.2 Projected surface temperature changes for the last decade of the 21st century (2090-2099) relative to the period 1980-1999. The map shows the IPCC multi- multi-Atmosphere-Ocean coupled Global Climate Model average projection for the A1B (balanced emphasis on all energy resources) scenario. The most significant warming is projected to occur in the Arctic. (IPCC, 2007; Figure SPM6)

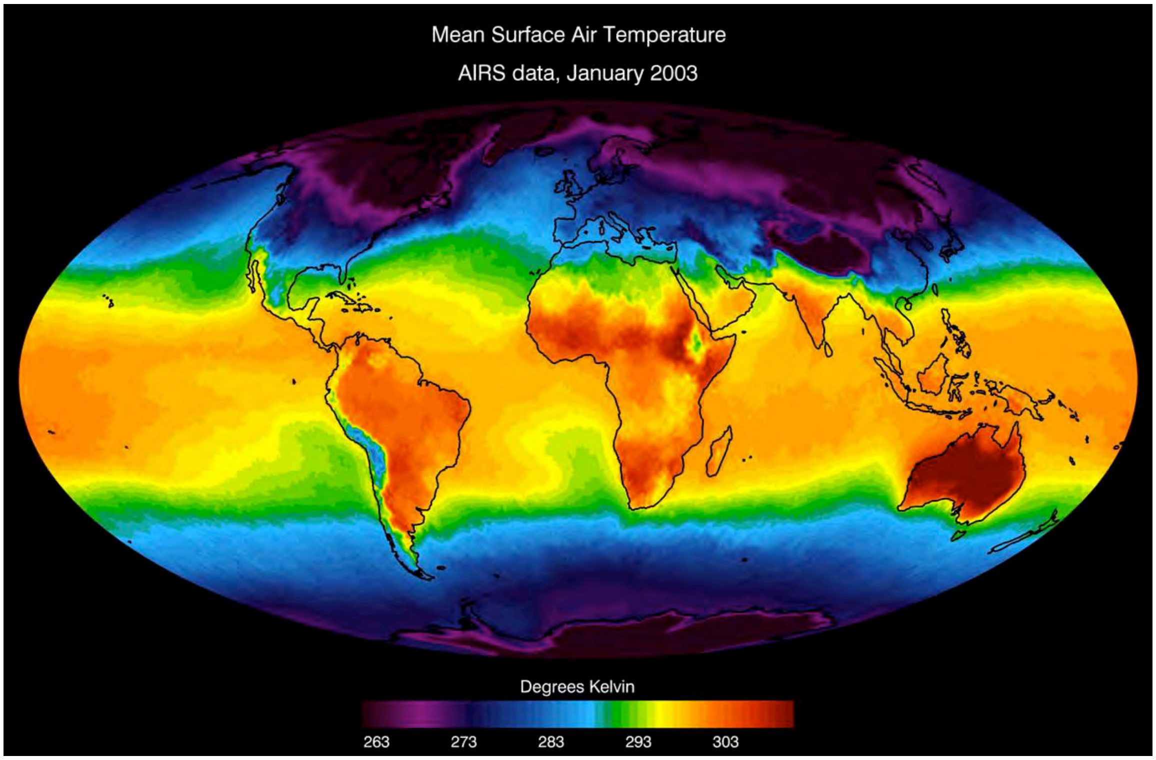

Figure 5.3 Global mean observed near-surface air temperatures for the month of January, 2003 derived from the Atmospheric Infrared Sounder (AIRS) data. Contrast between equatorial and Arctic temperatures is greatest during the northern hemisphere winter. The transfer of heat from the tropics to the polar regions is a primary feature of the Earth's climate system (Color scale is in Kelvin degrees such that 0°C=273.15 Kelvin.)
(Source: http://www-airs.jpl.nasa.gov/graphics/features/airs_surface_temp1_full.jpg)

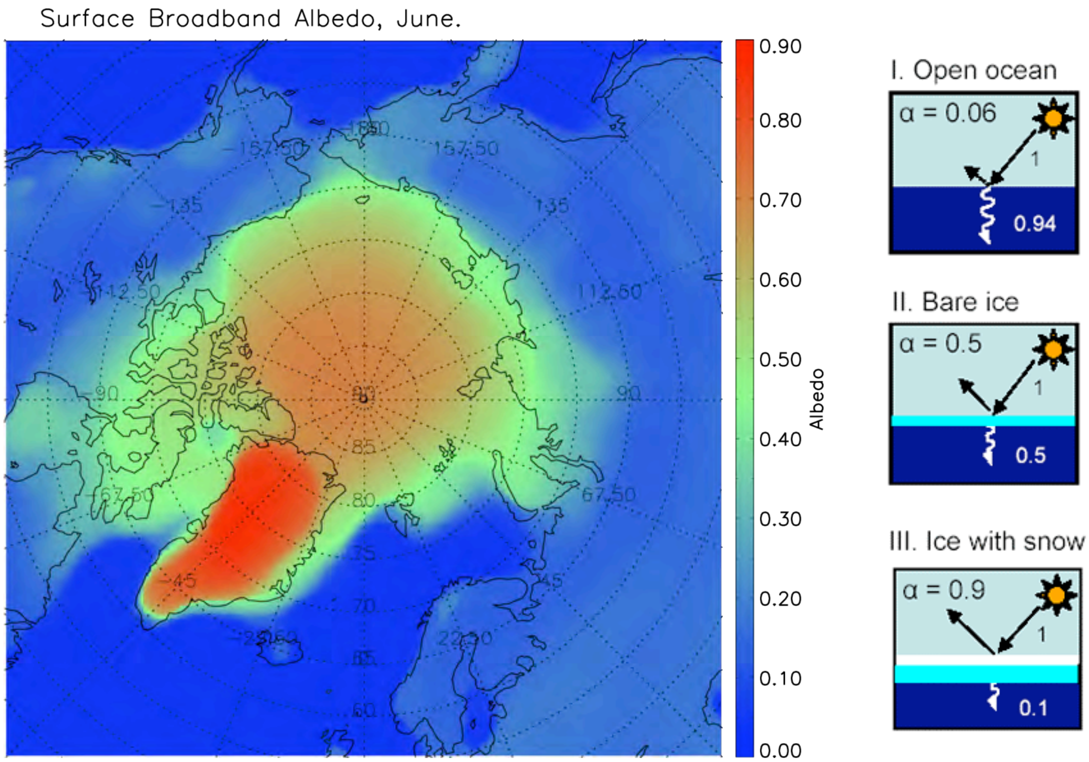

a **b**

Figure 5.4 Albedo values in the Arctic
5a. Advanced Very High Resolution Radiometery (AVHRR)-derived Arctic albedo values in June, 1982-2004 multi-year average, showing the strong contrast between snow and ice covered areas (green through red) and open water or land (blue). (Image courtesy of X. Wang, University of Wisconsin-Madison, CIMSS/NOAA)
5b. Albedo feedbacks. Albedo is the fraction of incident sunlight that is reflected. Snow, ice, and glaciers have high albedo. Dark objects such as the open ocean, which absorbs some 93% of the sun's energy, have low albedo (about 0.06), absorbing some 93% of the sun's energy. Bare ice has an albedo of 0.5; however, sea ice covered with snow has an albedo of nearly 90% (*Source:* [*http://nsidc.org/seaice/processes/albedo.html*](http://nsidc.org/seaice/processes/albedo.html)).

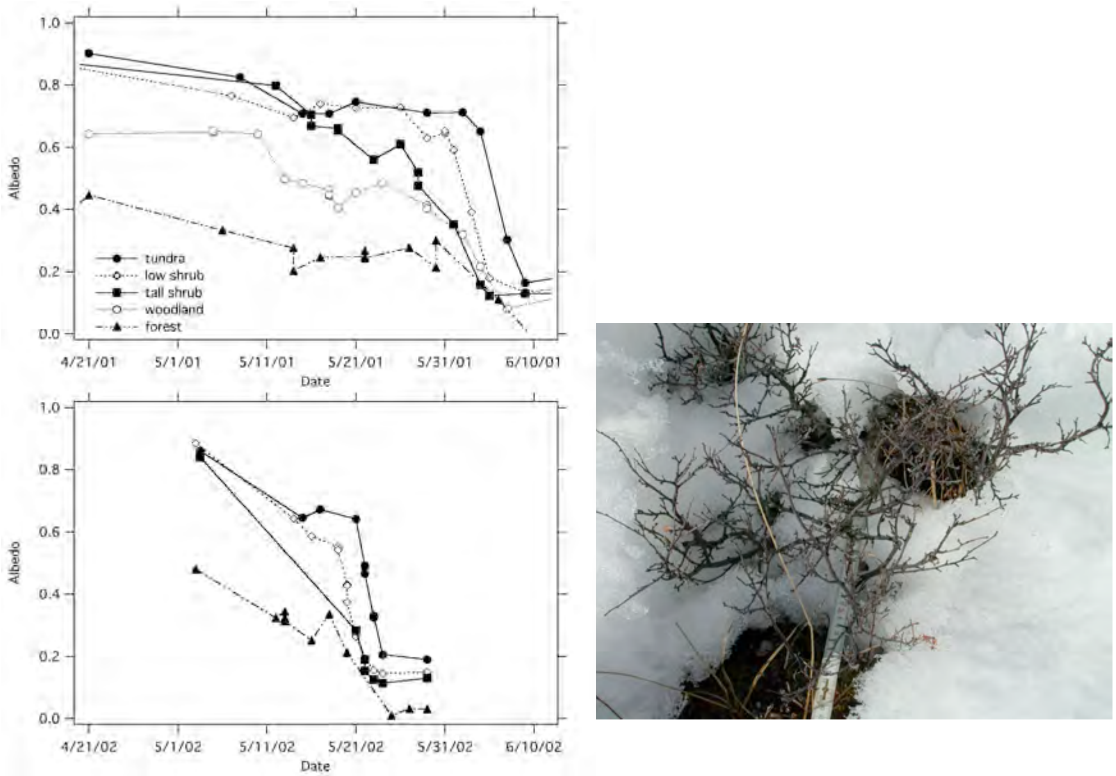

a b

Figure 5.5 Changes in vegetation cover throughout the Arctic can influence albedo, as can altering the onset of snow melt in spring. a) Progression of the melt season in northern Alaska, May 2001 (top) and May 2002 (bottom), demonstrates how areas with exposed shrubs show earlier snow melt. b) Dark branches against reflective snow alter albedo (Sturm et al., 2005; Photograph courtesy of Matt Sturm).

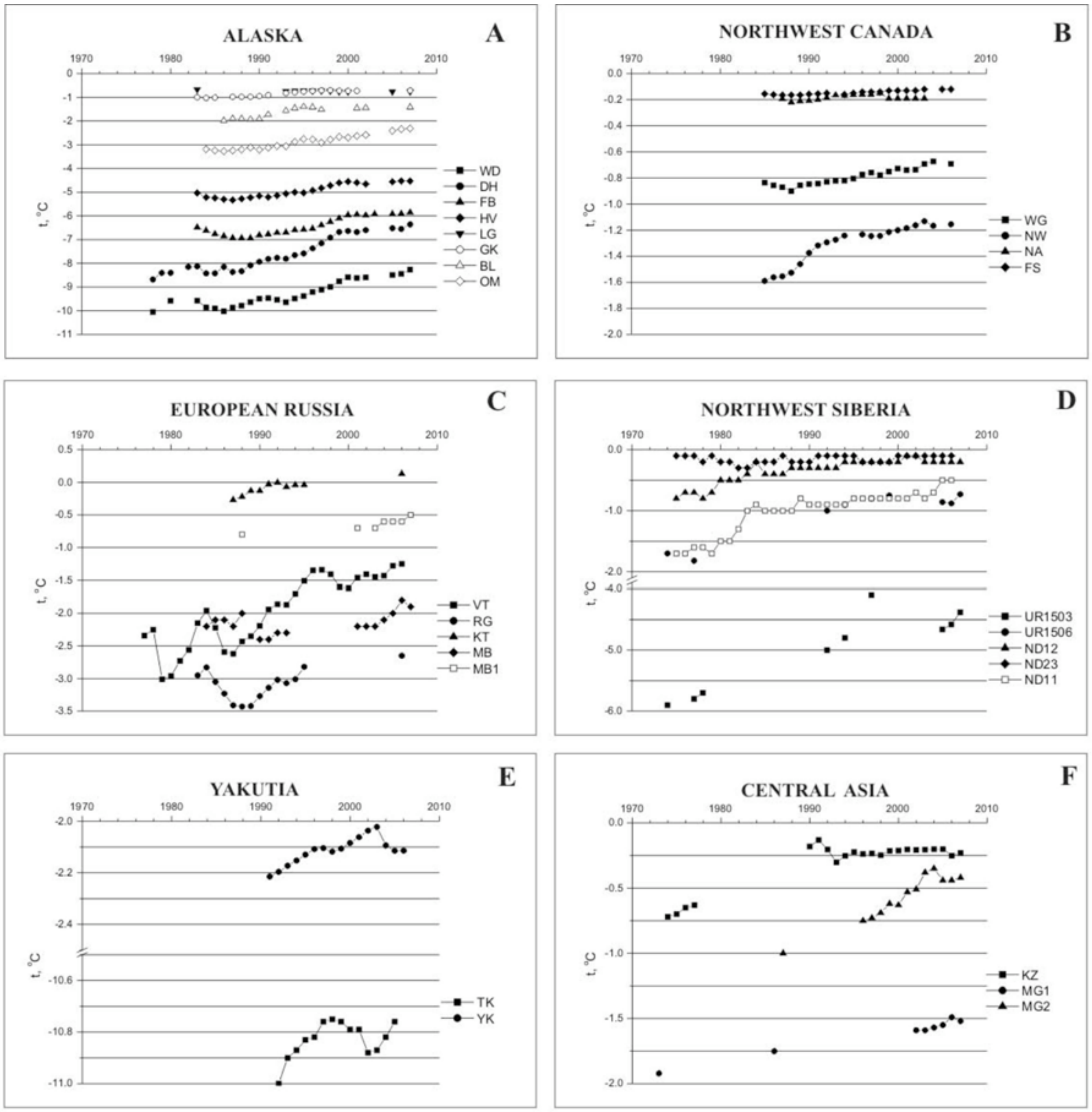

Figure 5.6 Warming trend in Arctic permafrost (permanently frozen ground), 1970–present. Local effects can modify this trend. A) Sites in Alaska: WD, West Dock; DH, Deadhorse; FB, Franklin Bluffs; HV, Happy Valley; LG, Livengood; GK, Gulkana; BL, Birch Lake; OM, Old Man. B) Sites in northwest Canada: WG, Wrigley; NW, Norman Wells; NA, Northern Alberta; FS, Fort Simpson. C) Sites in European Russia: VT, Vorkuta; RG, Rogovoi; KT, Karataikha; MB, Mys Bolvansky. D) Northwest Siberia: UR,

Urengoi; ND, Nadym. E) Sites in Yakutia: TK, Tiksi; YK,Yakutsk. F) Sites in central Asia: KZ, Kazakhstan; MG, Mongolia (Brown and Romanovsky, 2008).

Figure 5.7 Inflows and outflows of water in the Arctic Ocean. Red lines, components and paths of the surface and Atlantic Water layer in the Arctic; black arrows, pathways of Pacific water inflow from 50–200 m depth; blue arrows, surface-water circulation; green, major river inflow; red arrows, movements of density-driven Atlantic water and intermediate water masses into the Arctic (AMAP, 1998).

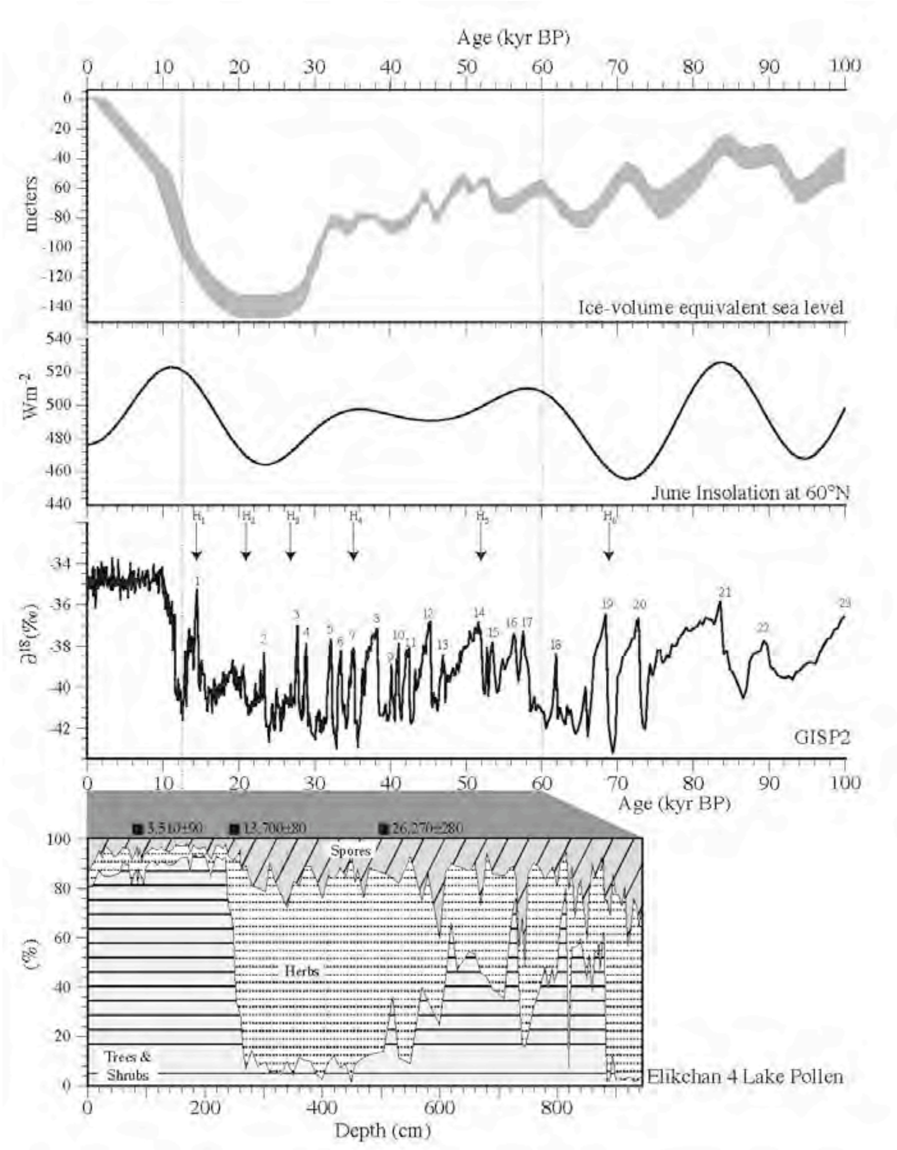

Figure 5.8 Upper three panels: Correlation of global sea-level curve (Lambeck et al., 2002), Northern Hemisphere summer insolation (Berger and Loutre, 1991), and the Greenland Ice Sheet (GISP2) $\delta^{18}O$ record (Grootes et al., 1993), ages all given in calendar years. Bottom panel: temporal changes in the percentages of the main taxa of trees and shrubs, herbs and spores at Elikchan 4 Lake in the Magadan region of Chukotka, Russia. Lake core x-axis is depth, not time (Brigham-Grette et al., 2004). Habitat was reconstructed on the basis of modern climate range of collective species found in fossil pollen assemblages. The reconstruction can be used to estimate past

temperatures or the seasonality of a particular site. The GISP2 record: Base of core roughly 60 ka (Lozhkin and Anderson, 1996). H1 above arrow, timing of Heinrich event event 1 (and so on); number 1 above curve, Dansgaard-Oscheger event (and so on). During approximately 27 ka to nearly 55 ka, vegetation, especially treeline, recovered for short intervals to nearly Holocene conditions at the same time that the isotopic record in Greenland suggests repeated warm warm-cold cycles of change. kyr BP, thousands of years before the present.

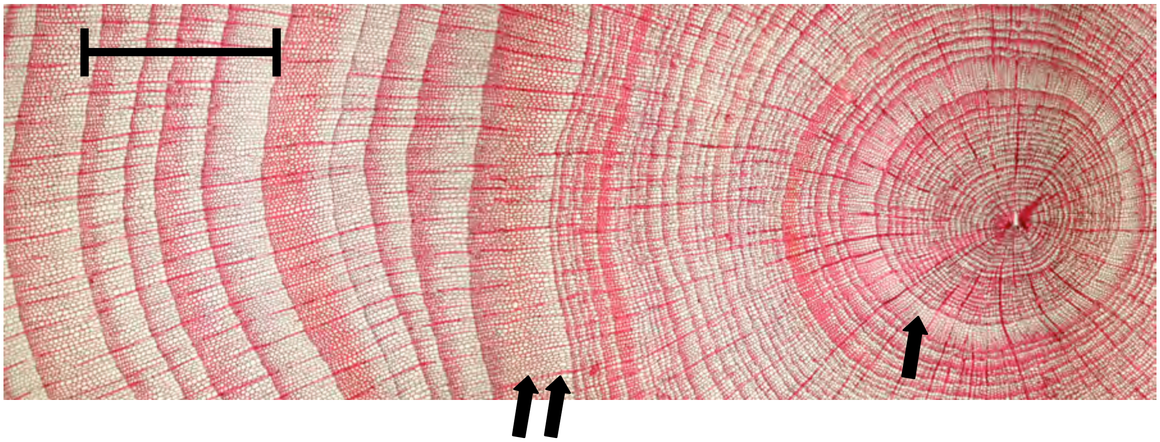

Figure 5.9 Annual tree rings composed of seasonal early and late wood are clear in this a 64-year year-old *Larix siberica* from western Siberia (Esper and Schweingruber, 2004). Initial growth was restricted; narrow rings average 0.035 mm/year, punctuated by one thicker ring (one single arrow). Later (two arrows), tree-ring width abruptly at least doubled for more than three years. Ring widths increased to 0.2 mm/year (Photograph courtesy of Jan Esper, Swiss Federal Research Institute).

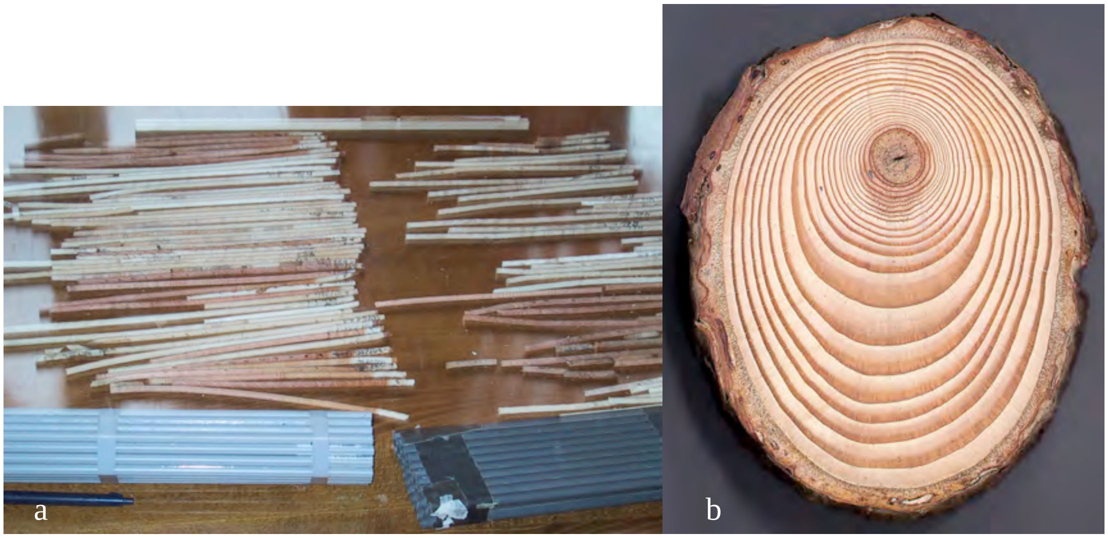

Figure 5.10 Typical tree ring samples. a) Increment cores taken from trees with a small small-bore hollow drill. They can be easily stored and transported in plastic soda straws for analysis in the laboratory. b) Alternatively, cross sections or disks can be sanded for study. A cross section of *Larix decidua* root shows differing wood thickness within single rings, caused by exposure. (Photographs courtesy of Jan Esper and Holger Gärtner, Swiss Federal Research Institute, respectively).

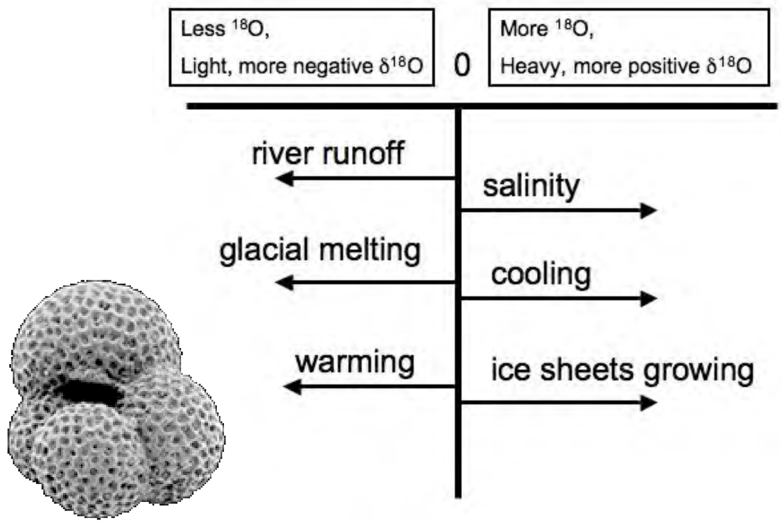

Figure 5.11 14 Microscopic marine plankton known as (foraminiferaifers (see inset) grow a shell of calcium carbonate ($CaCO_3$) in or near isotopic equilibrium with ambient sea water. The oxygen isotope ratio measured in these shells can be used to determine the temperature of the surrounding waters. (The oxygen-isotope ratio is expressed in $\delta^{18}O$ parts per million (ppm) = $10^3[(R_{sample}/R_{standard}) -1]$, where $R_x = (^{18}O)/(^{16}O)$ is the ratio of isotopic composition of a sample compared to that of an established standard, such as ocean water) However, factors other than temperature can influence the ratio of ^{18}O to ^{16}O. Warmer seasonal temperatures, glacial meltwater, and river runoff with depleted values all will produce a more negative (lighter) $\partial^{18}O$ [should the Greek letter be δ ?] ratio. On the other hand, cooler temperatures or higher salinity waters will drive the ratio up, making it heavier, or more positive. The growth of large continental ice sheets selectively removes the lighter isotope (^{16}O), leaving the ocean enriched in the heavier isotope (^{18}O).

Figure 5.12 Lake El'gygytgyn in the Arctic Far East of Russia. Open and closed lake systems in the Arctic differ hydrologically according to the balance between inflow, outflow, and the ratio of precipitation to evaporation. These parameters are the dominant influence on lake stable stable-isotopic chemistry and on the depositional character of the sediments and organic matter. Lake El'gygytgyn is annually open and flows to the Bering Sea during July and August, but the outlet closes by early September as lake level drops and storms move beach gravels that choke the outlet. (Photograph by J. Brigham-Grette).

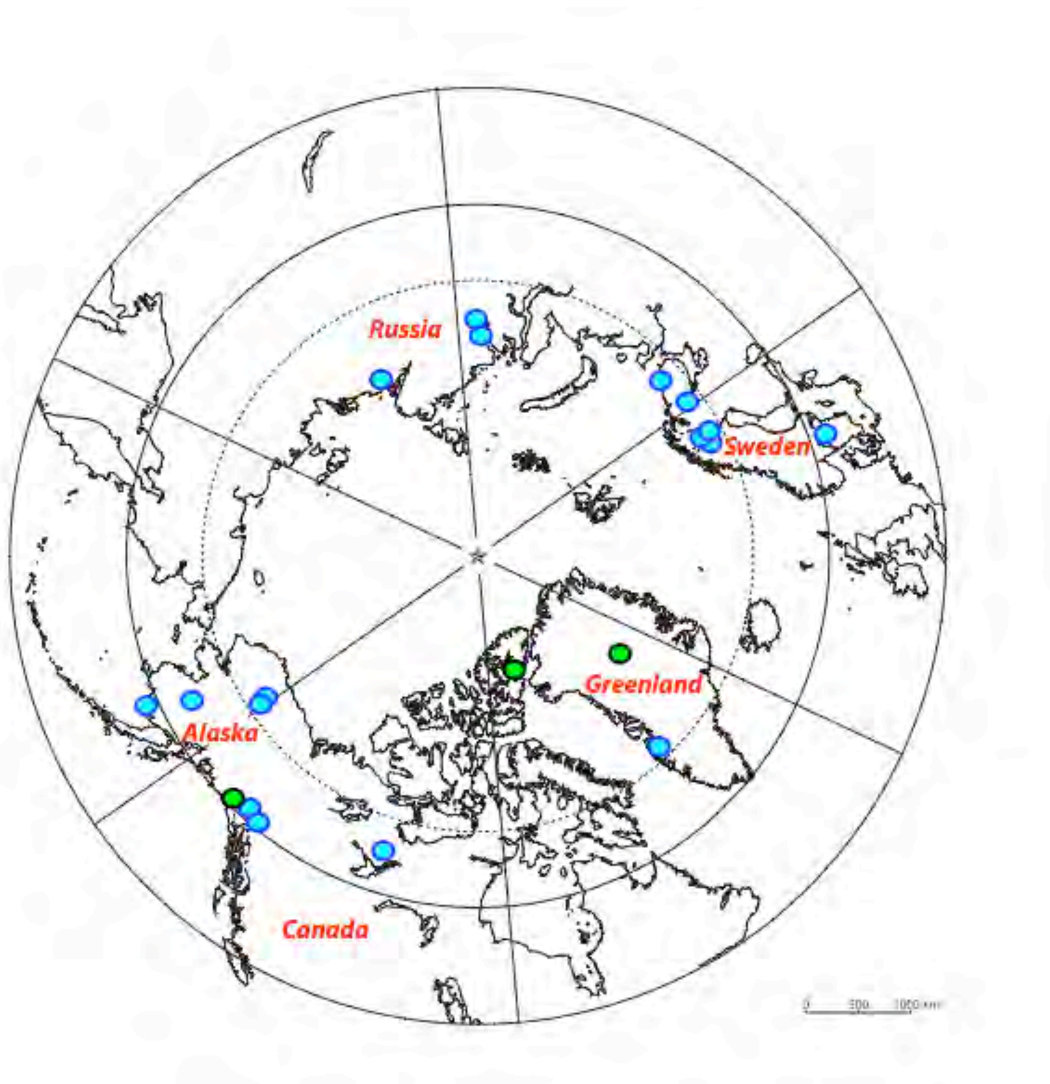

Figure 5.13 Locations of Arctic and sub-Arctic lakes (blue) and ice cores (green) whose oxygen isotope records have been used to reconstruct Holocene paleoclimate. (Map adapted from the Atlas of Canada, © 2002. Her Majesty the Queen in Right of Canada, Natural Resources Canada. / Sa Majesté la Reine du chef du Canada, Ressources naturelles Canada.)

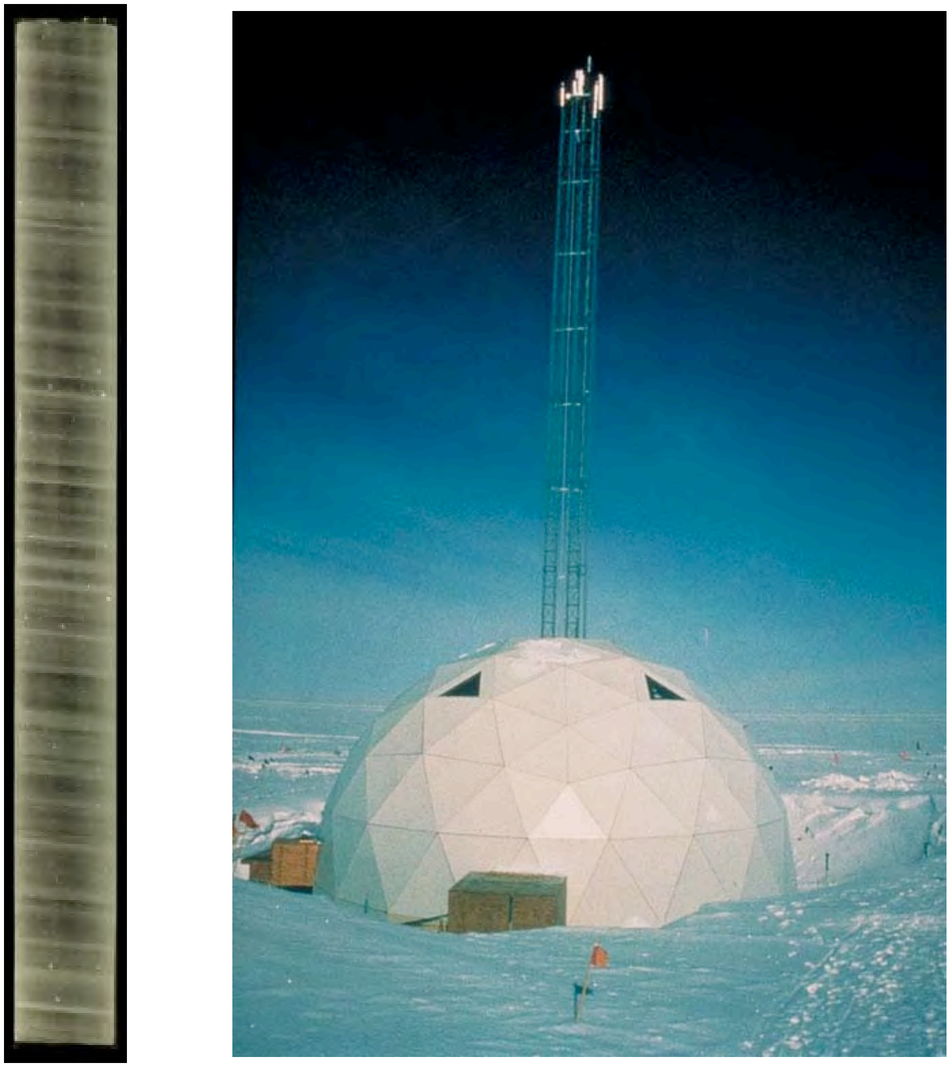

a b

Figure 5.14 a) One-meter section of Greenland Ice Core Project-2 core from 1837 m depth showing annual layers. (Photograph courtesy of Eric Cravens, Assistant Curator, U.S. National Ice Core Laboratory). b) Field site of Summit Station on top of the Greenland Ice sheet (Photograph by Michael Morrison, GISP2 SMO, University of New Hampshire; NOAA Paleoslide Set)

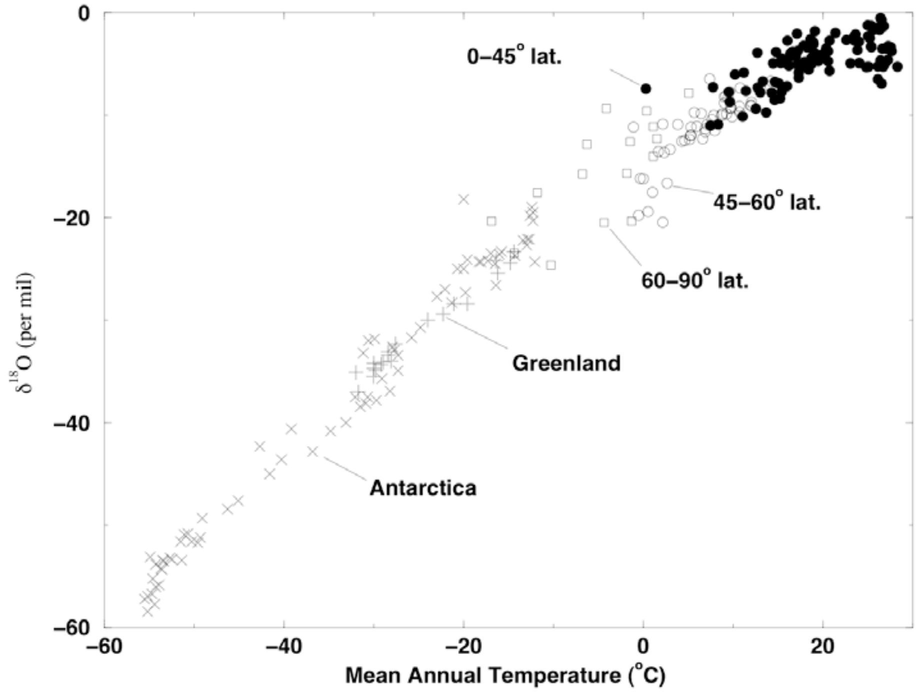

Figure 5.15 Relation between isotopic composition of precipitation and temperature in the parts of the world where ice sheets exist**.** Sources of data as follows: International Atomic Energy Agency (IAEA) network (Fricke and O'Neil, 1999; calculated as the means of summer and winter data of their Table 1 for all sites with complete data. Open squares, poleward of 60° latitude (but with no inland ice-sheet sites); open circles, 45°–60° latitude; filled circles, equatorward of 45° latitude. x, data from Greenland (Johnsen et al., 1989); +, data from Antarctica (Dahe et al., 1994). About 71% of Earth's surface area is equatorward of 45°, where dependence of $\delta^{18}O$ on temperature is weak to nonexistent. Only 16% of Earth's surface falls in the 45°–60° band, and only 13% is poleward of 60°. The linear array is clearly dominated by data from the ice sheets. (Source: Alley and Cuffey, 2001)

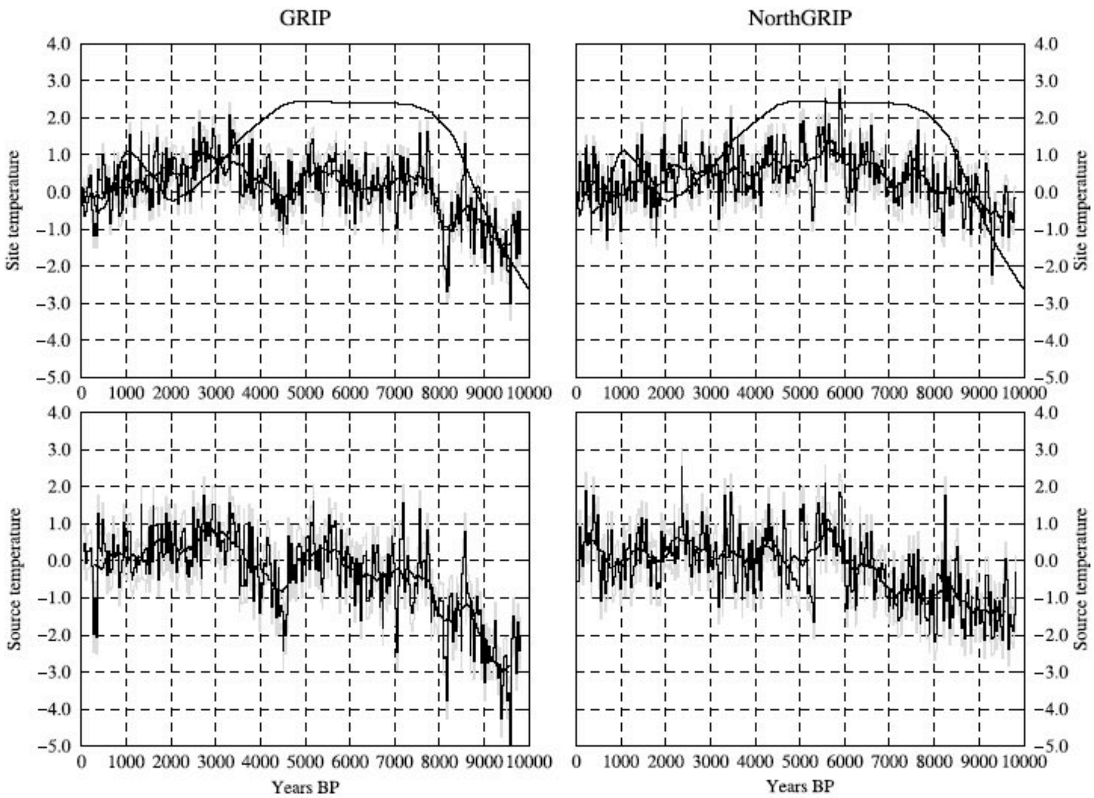

Figure 5.16 Paleotemperature estimates of site and source waters from on Greenland: GRIP and NorthGrip, Masson-Delmotte et al., 2005). GRIP (left) and NorthGRIP (right) site (top) and source (bottom) temperatures derived from GRIP and NorthGRIP $\delta^{18}O$ and deuterium excess corrected for seawater $\delta^{18}O$ (until 6000 BP). Shaded lines in gray behind the black line provide an estimate of uncertainties due to the tuning of the isotopic model and the analytical precision. Solid line (in part above zigzag line), GRIP temperature derived from the borehole-temperature profile (Dahl-Jensen et al., 1998).

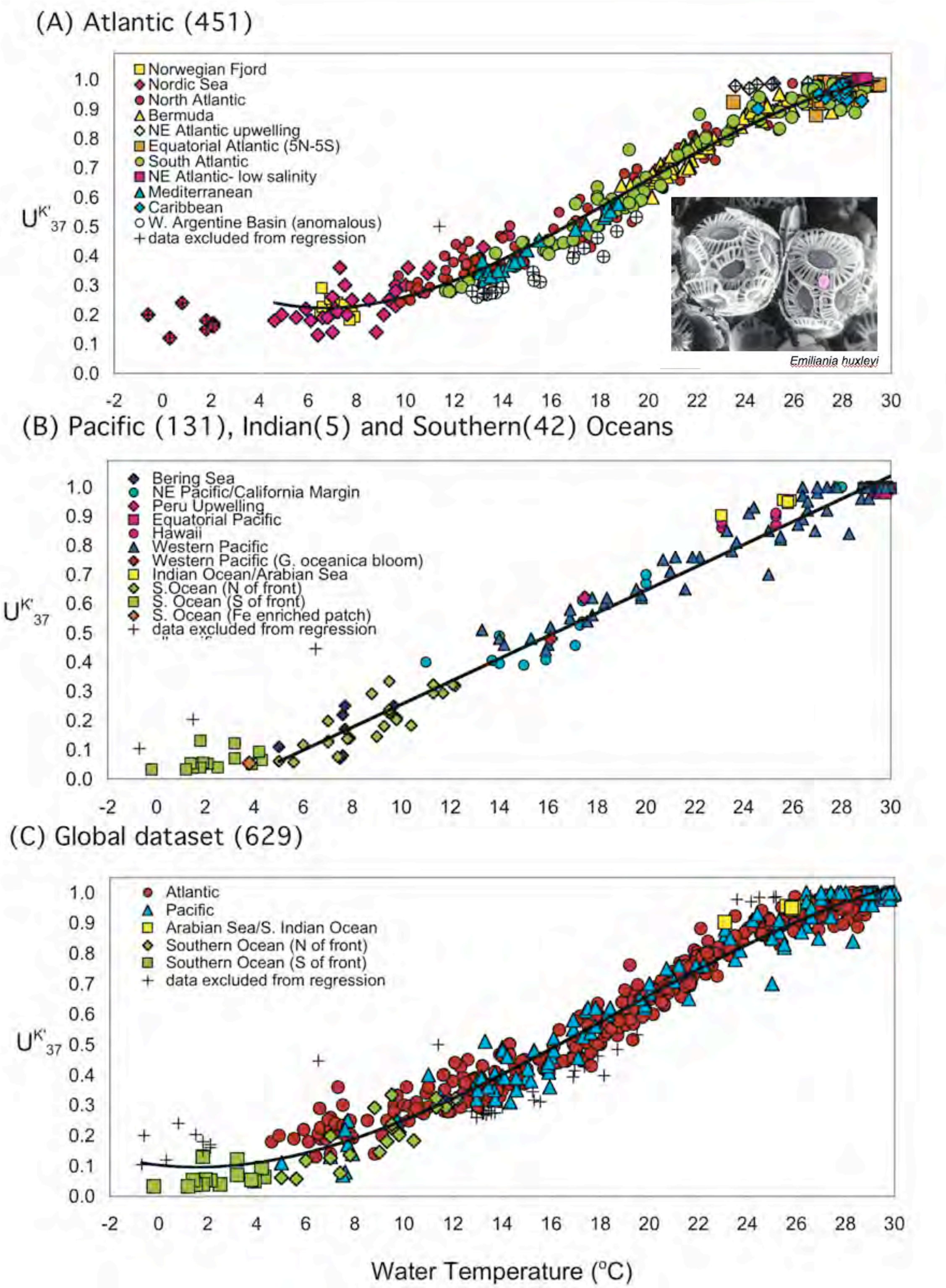

Figure 5.17 Biomarker alkenone. U_{37}^{K} versus measured water temperature for ocean-water surface mixed layer (0–30 m) samples. A) Atlantic region: Empirical 3rd-order

polynomial regression for samples collected in warmer-than-4°C waters is U_{37}^{K} = 1.004   10 4T3 + 5.744   10 3T2   6.207   10 2T + 0.407 (r2 = 0.98, n = 413) (Outlier data from the southwest Atlantic margin and northeast Atlantic upwelling regime is excluded.). B) Pacific, Indian, and Southern Ocean regions: The empirical linear regression of Pacific samples is U_{37}^{K} = 0.0391T   0.1364 (r2 = 0.97, n = 131). Pacific regression does not include the Indian and Southern Ocean data. C) Global data: The empirical 3rd order polynomial regression, excluding anomalous southwest Atlantic margin data, is U_{37}^{K} = 5.256   10 5T3 + 2.884   10 3T2   8.4933   10 3T + 9.898 (r2 = 0.97, n = 588). +, sample excluded from regressions. (Conte et al, 2006).

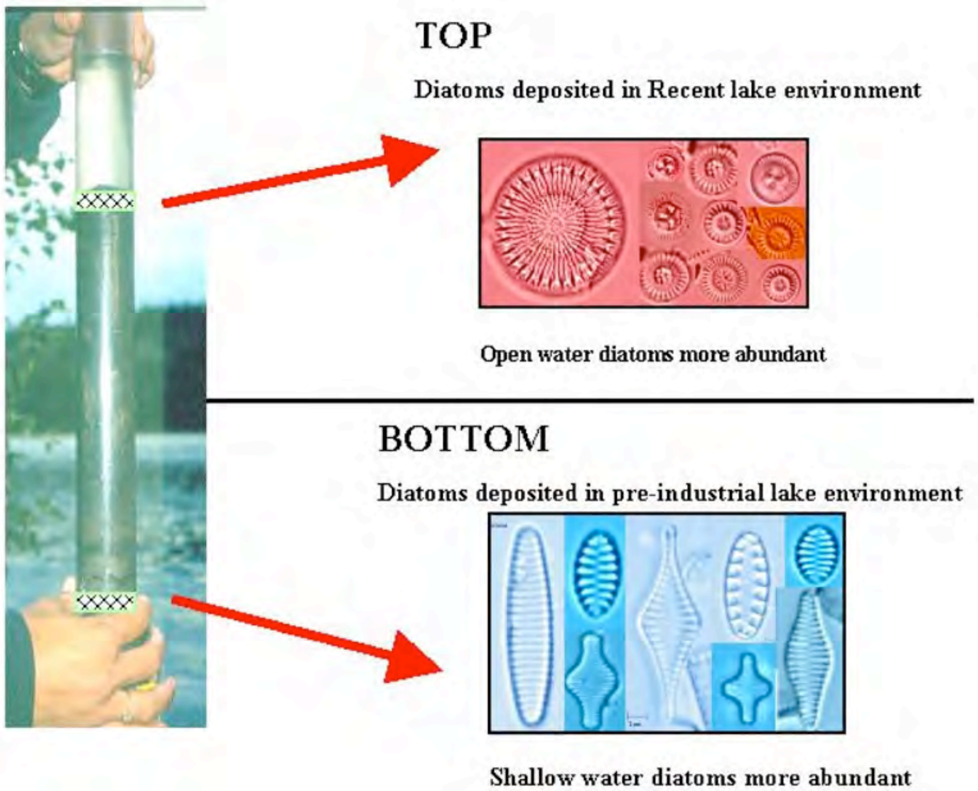

Figure 5.18 Diatom assemblages reflect a variety of environmental conditions in Arctic lake systems. Transitions, especially rapid change from one assemblage to another, can reflect large changes in conditions such as light, nutrient availability, or temperature, for example. Biogenic silica, chiefly the silica skeletal framework constructed by diatoms, is commonly measured in lake sediments and used as an index of past changes in aquatic primary productivity.

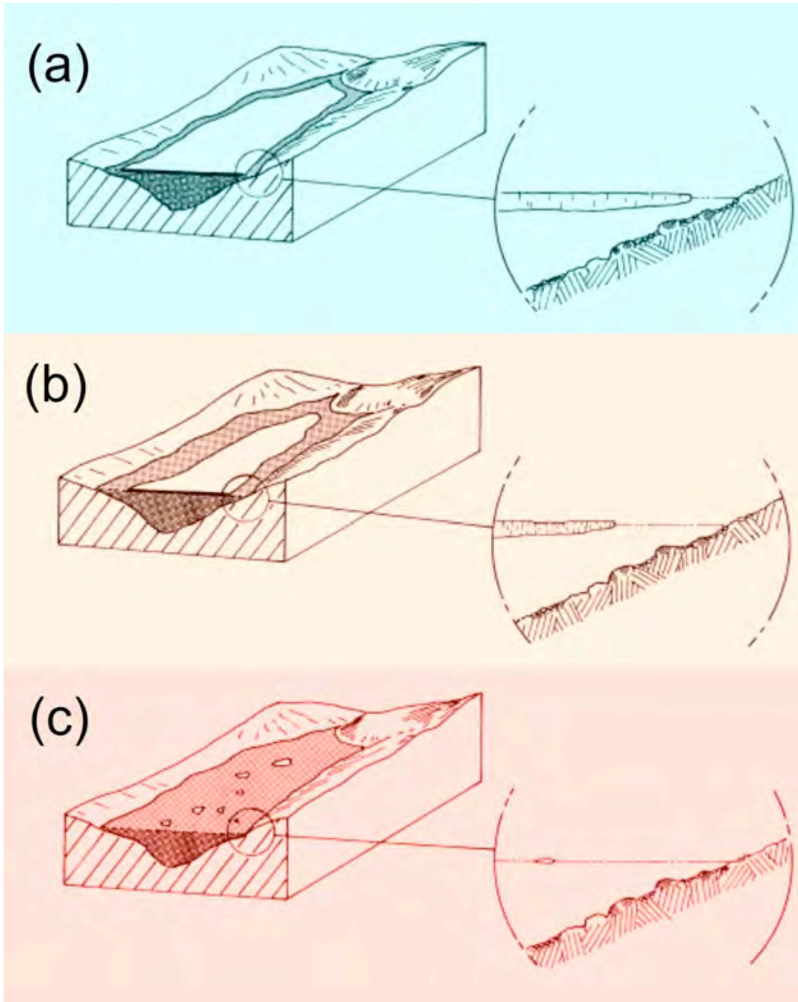

Figure 5.19 Changing ice and snow conditions on an Arctic lake during relatively (a) cold, (b) moderate, and (c) warm conditions. During colder years, a permanent raft of ice may persist throughout the short summer, precluding the development of large populations of phytoplankton, and restricting much of the primary production to a shallow, open open-water moat. Many other physical, chemical and biological changes occur in lakes that are either directly or indirectly affected by snow and ice cover (see Table 1; Douglas and Smol, 1999). Modified from Smol (1988).

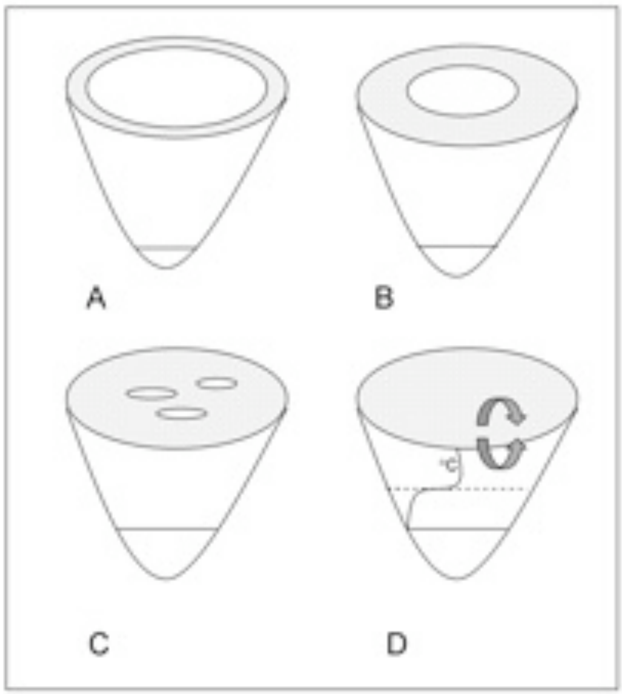

Figure 5.20 Lake ice melts as it continues to warm (A – D). Eventually, in deeper lakes (vs ponds) thermal stratification may also occur (or be prolonged) during the summer months (D), further altering the limnological characteristics of the lake. Modified from Douglas (2007).

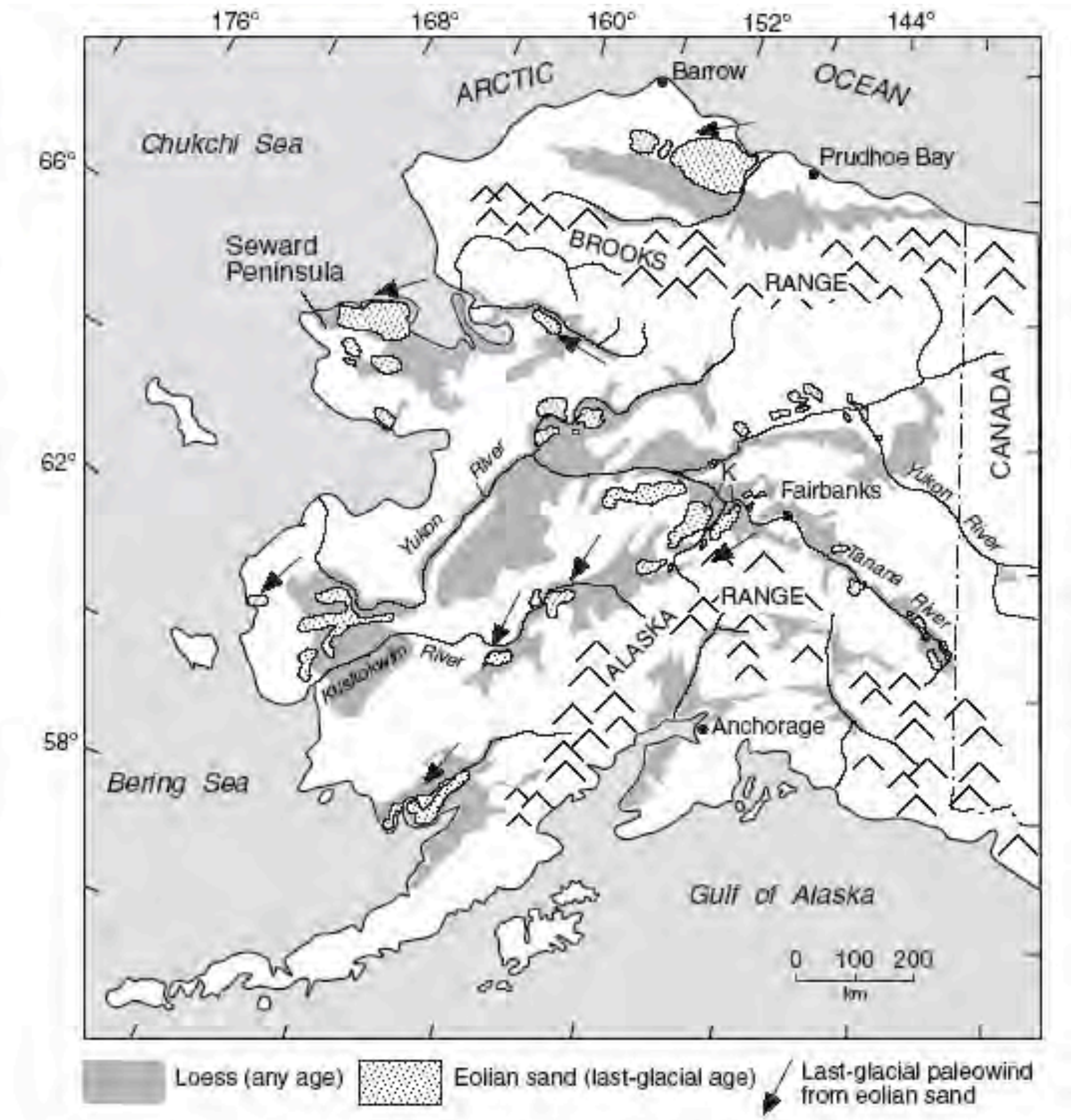

Figure 5.21 The form and distribution of wind-blown silt (loess), wind-blown sand (dunes), and other deposits of wind-blown sediment in Alaska, have been use to infer both Holocene and last-glacial past wind directions. (Compiled from multiple sources by Muhs and Budahn, 2006).

Figure 5.22 Unnamed, hydrologically closed lake in the Yukon Flats Wildlife Refuge, Alaska. Concentric rings of vegetation developed progressively inward as water level fell, owing to a negative change in the lake's overall water balance. Historic Landsat imagery and air photographs indicate that these shorelines formed during within the last 40 years or so. (Photograph by Lesleigh Anderson.)

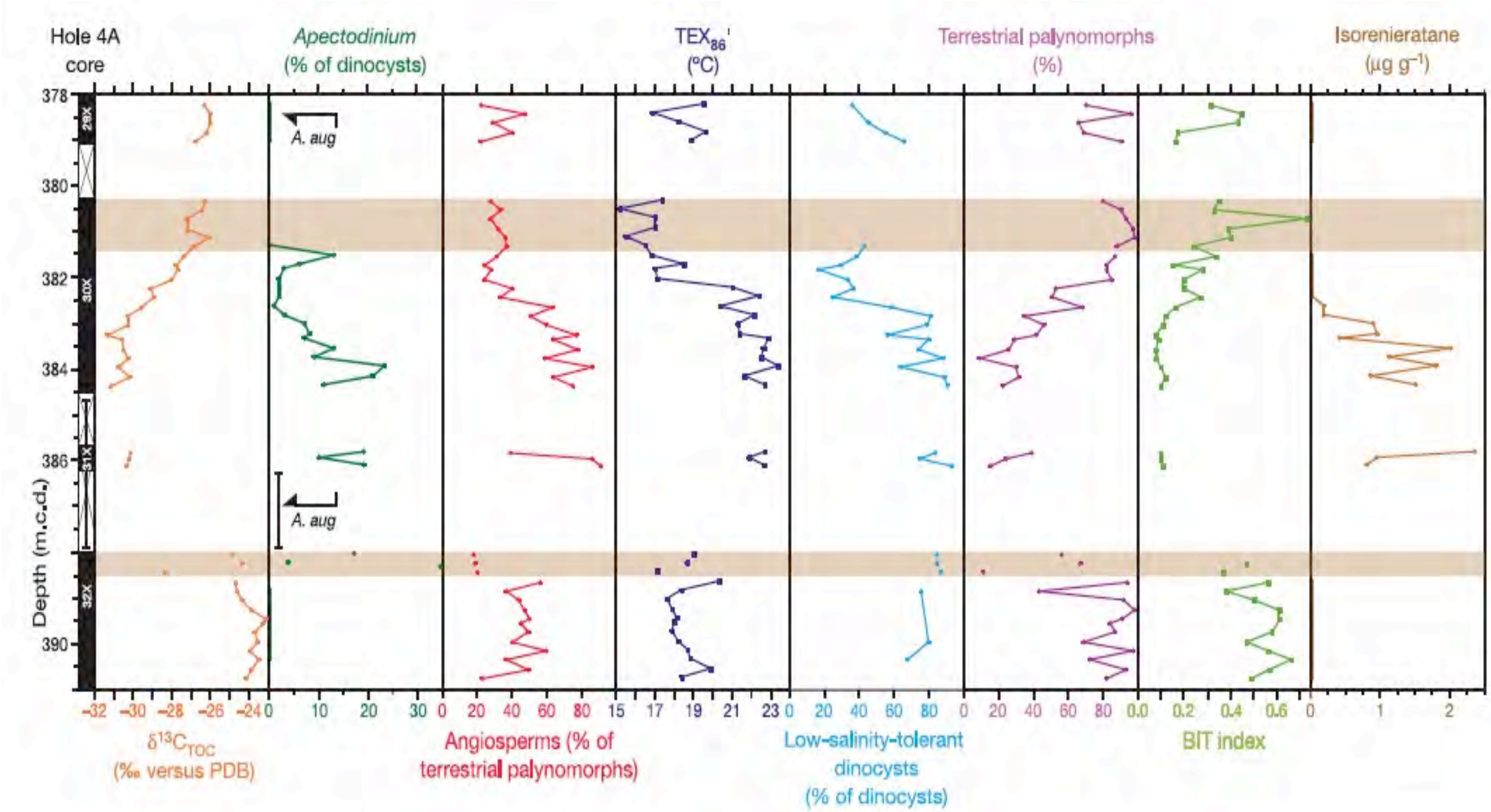

Figure 5.23 Recovered sections and palynological and geochemical results across the Paleocene-Eocene Thermal Maximum about 55 Ma; IODP Hole 302-4A (87° 52.00' N.; 136° 10.64' E.; 1288 m water depth, in the central Arctic Ocean basin). Mean annual surface-water temperatures (as indicated in the TEX_{86}' column) are estimated to have reached 23°C, similar to water in the tropics today.

(Error bars for Core 31X show the uncertainty of its stratigraphic position. Orange bars, indicate intervals affected by drilling disturbance.) Stable carbon isotopes are expressed relative to the PeeDee Belemnite standard. Dinocysts tolerant of low salinity comprise *Senegalinium* spp., *Cerodinium* spp., and *Polysphaeridium* spp., whereas *Membranosphaera* spp., *Spiniferites ramosus* complex, and *Areoligera-Glaphyrocysta* cpx. represent typical marine species. Arrows and *A. aug* (second column) indicate the first and last occurrences of dinocyst *Apectodinium augustum*—a diagnostic indicator of Paleocene-Eocene Thermal Maximum warm conditions. (Sluijs et al., 2006).

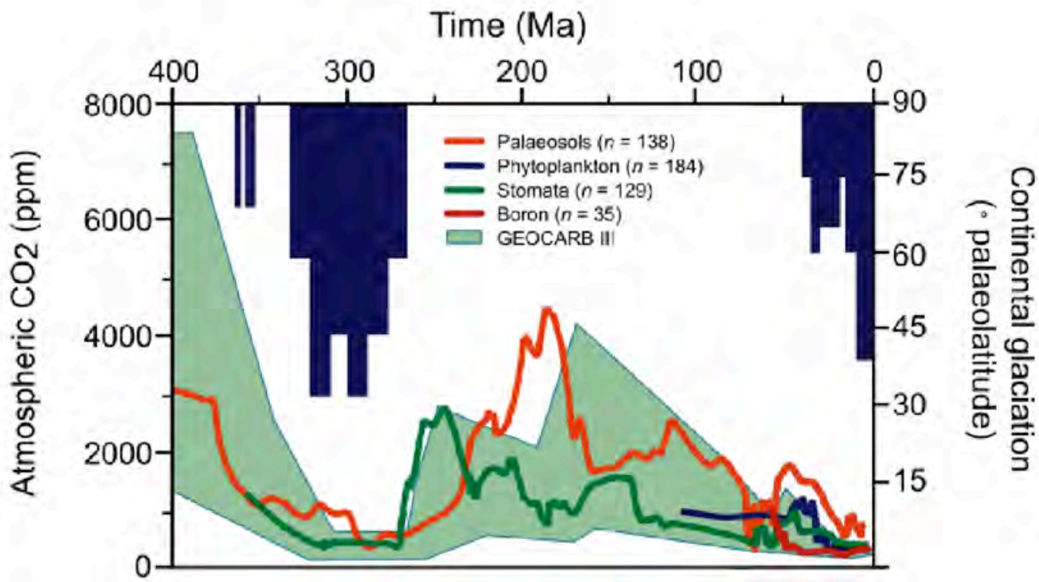

Figure 5.24 Atmospheric CO_2 and continental glaciation 400 Ma to present. Vertical blue bars, timing and palaeolatitudinal extent of ice sheets (after Crowley, 1998). Plotted CO_2 records represent five-point running averages from each of four major proxies (see Royer, 2006 for details of compilation). Also plotted are the plausible ranges of CO_2 derived from the geochemical carbon cycle model GEOCARB III (Berner and Kothavala, 2001). All data adjusted to the Gradstein et al. (2004) time scale. Continental ice sheets grow extensively when CO_2 is low. (after Jansen, 2007, that report's Figure 6.1)

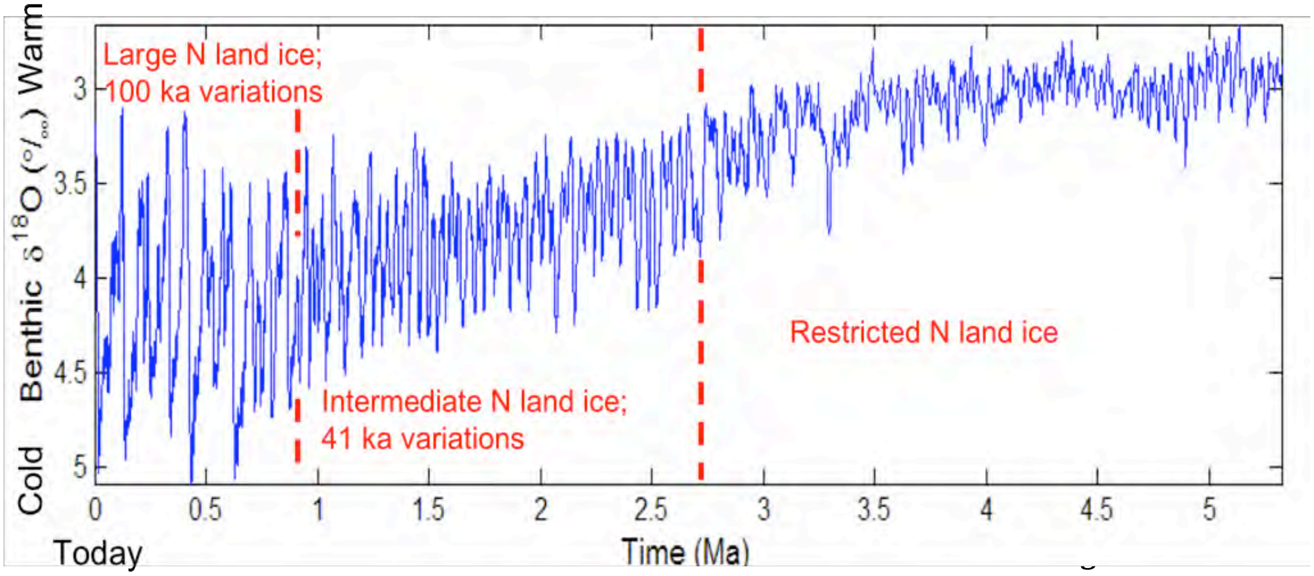

Figure 5.25 The average isotopic composition ($\delta^{18}O$) of bottom-dwelling foraminiferaifers from in a globally distributed set of 57 sediment cores that record the last 5.3 Ma (modified from Lisiecki and Raymo, 2005). The $\delta^{18}O$ is controlled primarily by global ice volume and deep-ocean temperature, with less ice or warmer temperatures (or both) upward in the core. The influence of Milankovitch frequencies of Earth's orbital variation are present throughout, but glaciation increased about 2.7 Ma ago concurrently with establishment of a strong 41 ka variability linked to Earth's obliquity (changes in tilt of Earth's spin axis), and the additional increase in glaciation about 1.2–0.7 Ma parallels a shift to stronger 100 ka variability. Dashed lines are used because the changes seem to have been gradual. The general trend toward higher $\delta^{18}O$ that runs through this series reflects the long-term drift toward a colder Earth that began in the early Cenozoic (see Figure 4.8).

a

b

Figure 5.26 a) Greenland without ice for the last time? Dark green, boreal forest; light green, deciduous forest; brown, tundra and alpine heaths; white, ice caps. The north-south temperature gradient is constructed from a comparison between North Greenland and

northwest European temperatures, using standard lapse rate; distribution of precipitation assumed to retain the Holocene pattern. Topographical base, from model by Letreguilly et al. (1991) of Greenland’s sub-ice topography after isostatic recovery. b) Upper part of the Kap København Formation, North Greenland. The sand was deposited in an estuary about 2.4 Ma; it contains abundant well-preserved leaves, seeds, twigs, and insect remains. (Figure and Photograph of by S.V. Funder.).

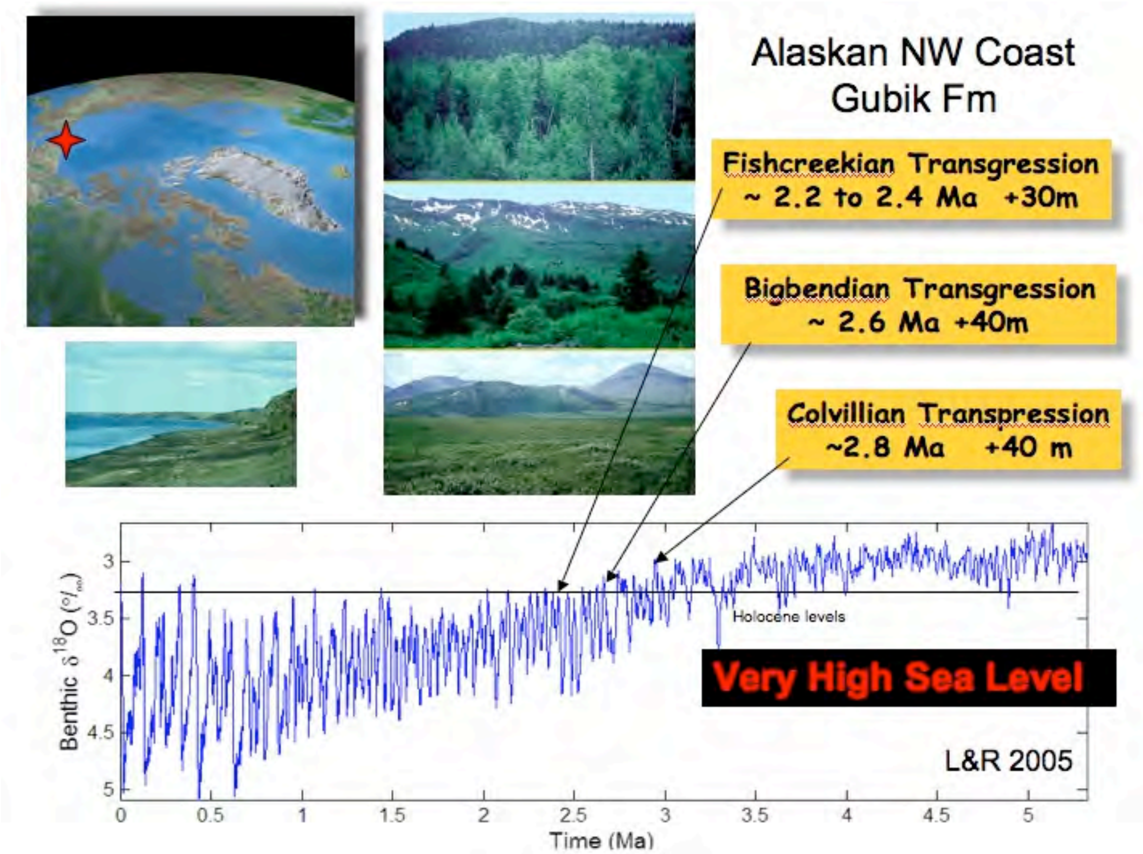

Figure 5.27 The largely marine Gubik Formation, North Slope of Alaska, contains three superposed lower units that record relative sea level as high +30-+ to +40 m. Pollen in these deposits suggests that borderland vegetation at each of these times was less forested; boreal forests or spruce-birch woodlands at 2.7 Ma gave way to larch and spruce forests at about 2.6 Ma and to open tundra by about 2.4 Ma (see photographs by Robert Nelson, Colby College, who analyzed the pollen; oldest at top). Isotopic reference time series of Lisecki and Raymo (2005) suggests best as assignments for these sea level events (Brigham and Carter, 1992).

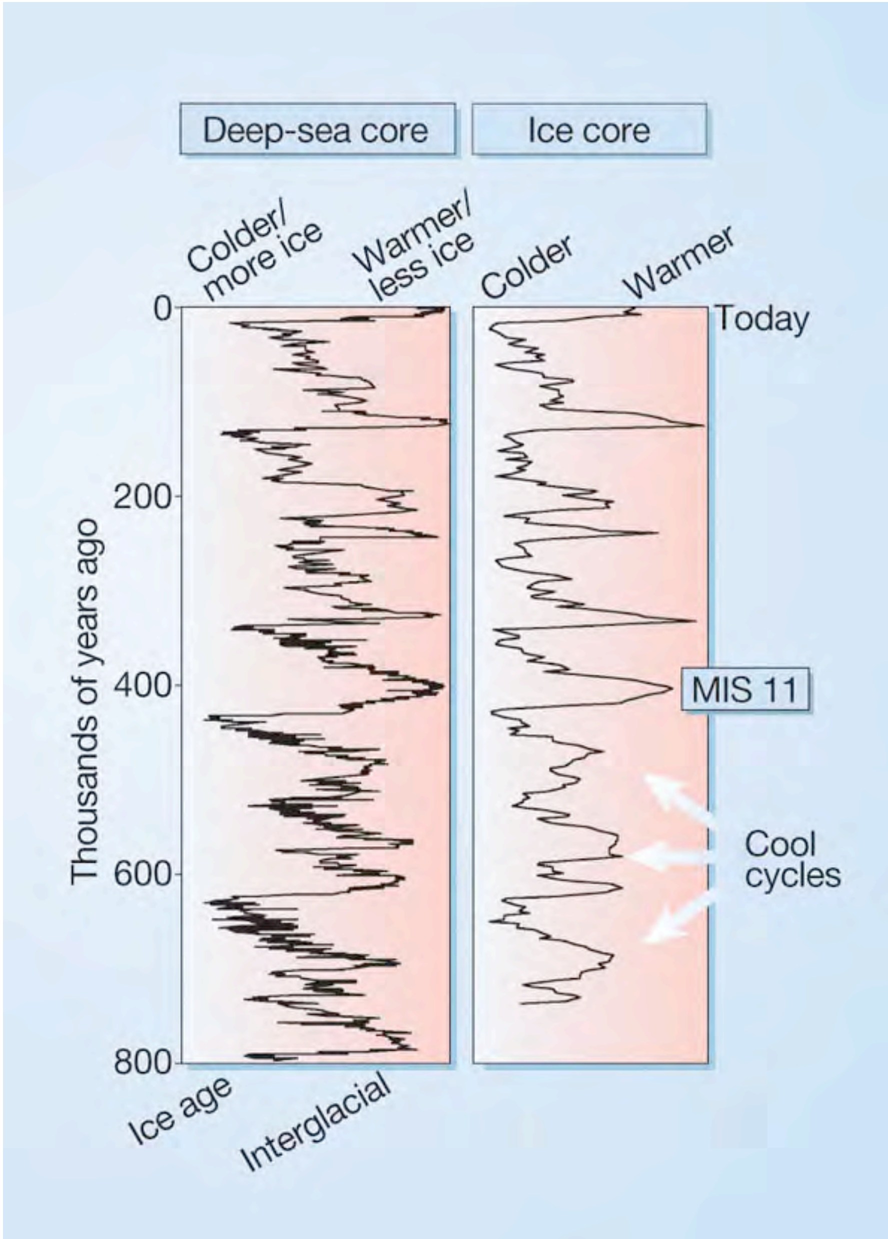

Figure 5.28 Glacial cycles of the past 800 ka derived from marine-sediment and ice cores (McManus, 2004). The history of deep-ocean temperatures and global ice volume inferred from $\delta^{18}O$ measured in bottom-dwelling foraminifera shells preserved in Atlantic Ocean sediments. Air temperatures over Antarctica inferred from the ratio of deuterium to hydrogen in ice from central Antarctica (EPICA, 2004). Marine isotope stage 11 (MIS 11) is an interglacial whose orbital parameters were similar to those of the Holocene, yet it lasted about twice as long as most interglacials. Note the smaller magnitude and less-pronounced interglacial warmth of the glacial cycles that preceded MIS 11.

Interglaciations older than MIS 11 were less warm than subsequent integlaciations.

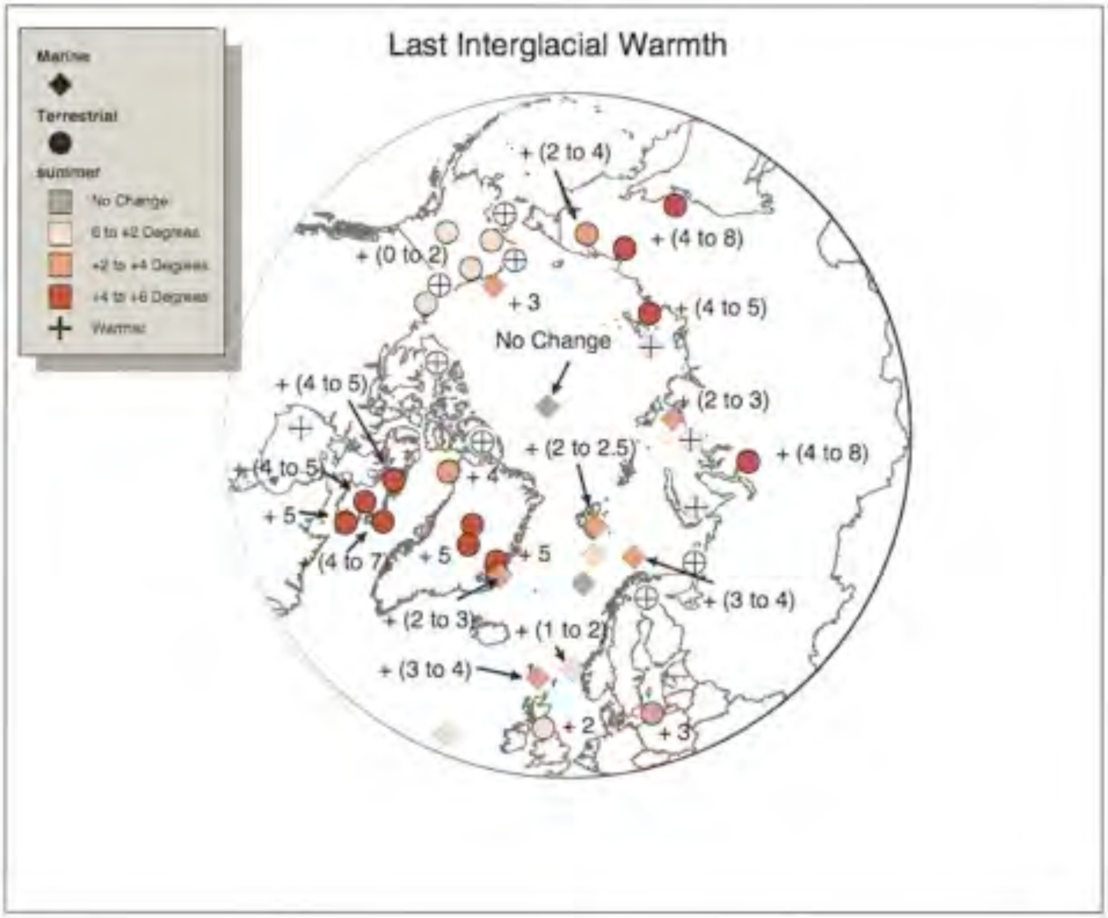

Figure 5.29 Polar projection showing regional maximum LIG last interglacial summer temperature anomalies relative to present summer temperatures; derived from paleotemperature proxies (see tables Tables 1 and 2, in from CAPE Last Interglacial Project Members, 2006). Circles, terrestrial; squares, marine sites.

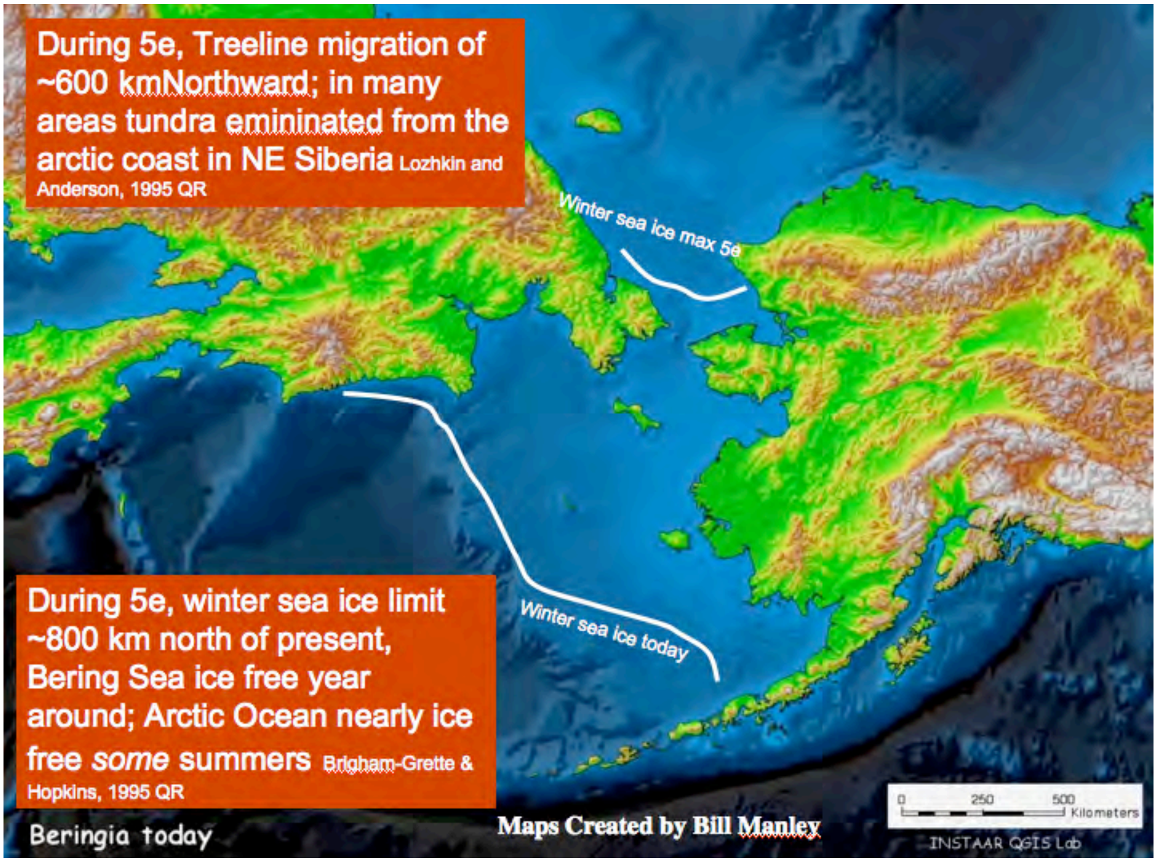

Figure 5.30 Winter sea-ice limit during MIS 5e and at present. Fossiliferous paleoshorelines and marine sediments were used by Brigham-Grette and Hopkins (1995) to evaluate the seasonality of coastal sea ice on both sides of the Bering Strait during the Last Last Interglaciation. Winter sea limit is estimated to have been north of the narrowest section of the strait, 800 km north of modern limits. Pollen data derived from Last Interglacial lake sediments suggest that tundra was nearly eliminated from the Russian coast at this time (Lozhkin and Anderson, 1995). In Chukokta during the warm interglaciation, additional open water favored some taxa tolerant of deeper winter snows. (Map of William Manley, http://instaar.colorado.edu/QGISL/).

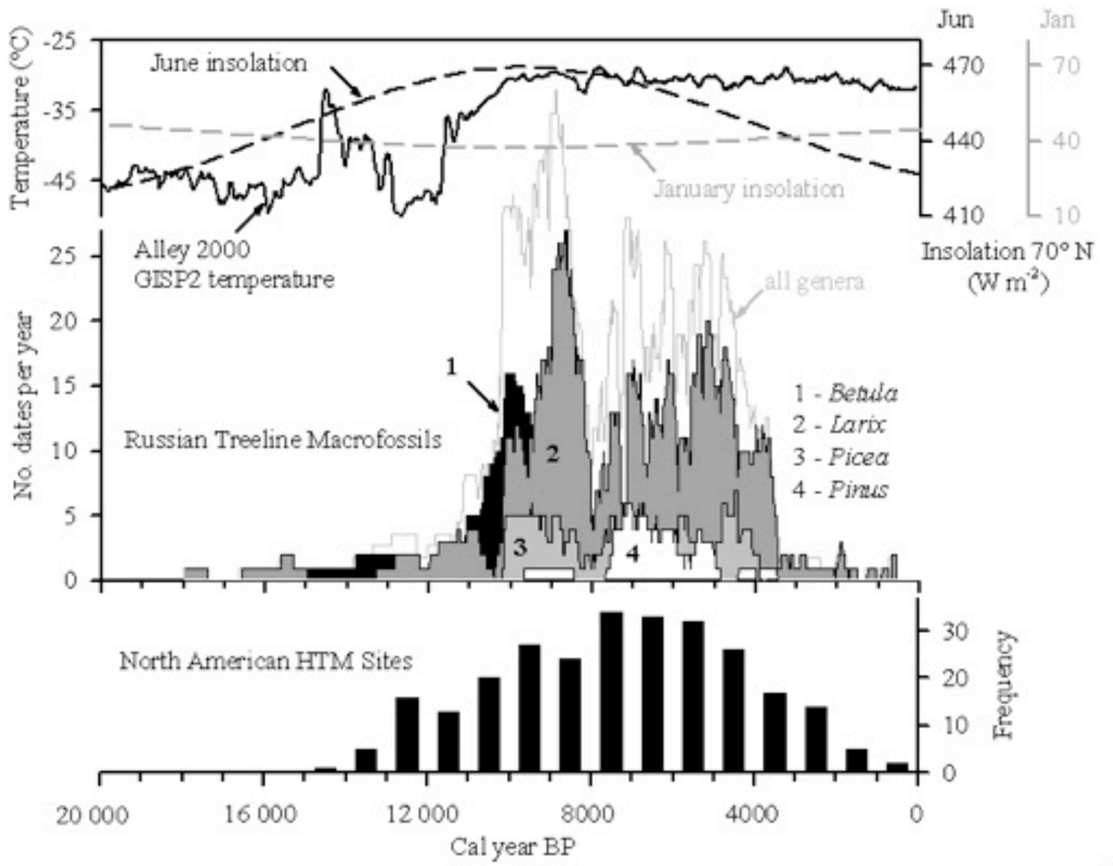

Figure 5.31 The Arctic Holocene Thermal Maximum. Items compared, top to bottom: seasonal insolation patterns at 70° N. (Berger & Loutre, 1991), and reconstructed Greenland air temperature from the GISP2 drilling project (Alley 2000); age distribution of radiocarbon-dated fossil remains of various tree genera from north of present treeline (MacDonald et al., 2007),); and the frequency of Western Arctic sites that experienced Holocene Thermal Maximum conditions. (Kaufman et al. 2004).

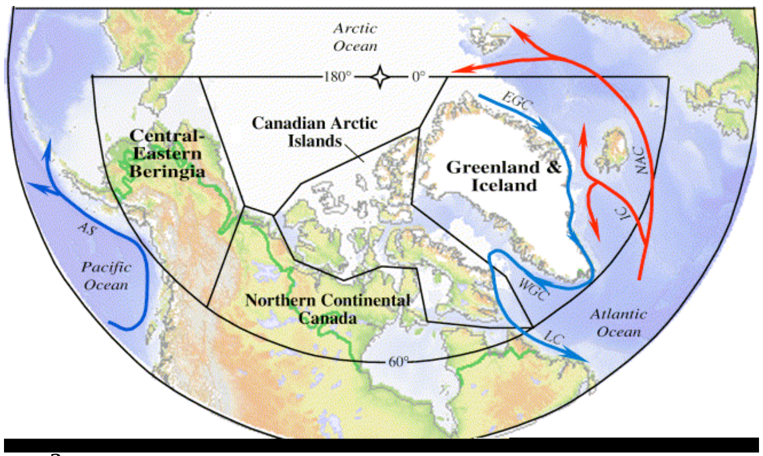

Arctic Ocean
180°
0°
Central-Eastern Beringia
Canadian Arctic Islands
Greenland & Iceland
Northern Continental Canada
Pacific Ocean
Atlantic Ocean
60°
AS
EGC
NAC
IC
WGC
LC

a

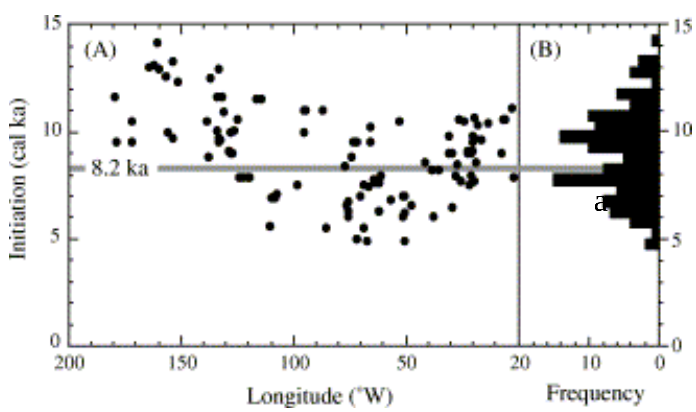

(A)
(B)
8.2 ka
Initiation (cal ka)
Longitude (°W)
Frequency
15
10
5
0
200
150
100
50
20
10
0

b

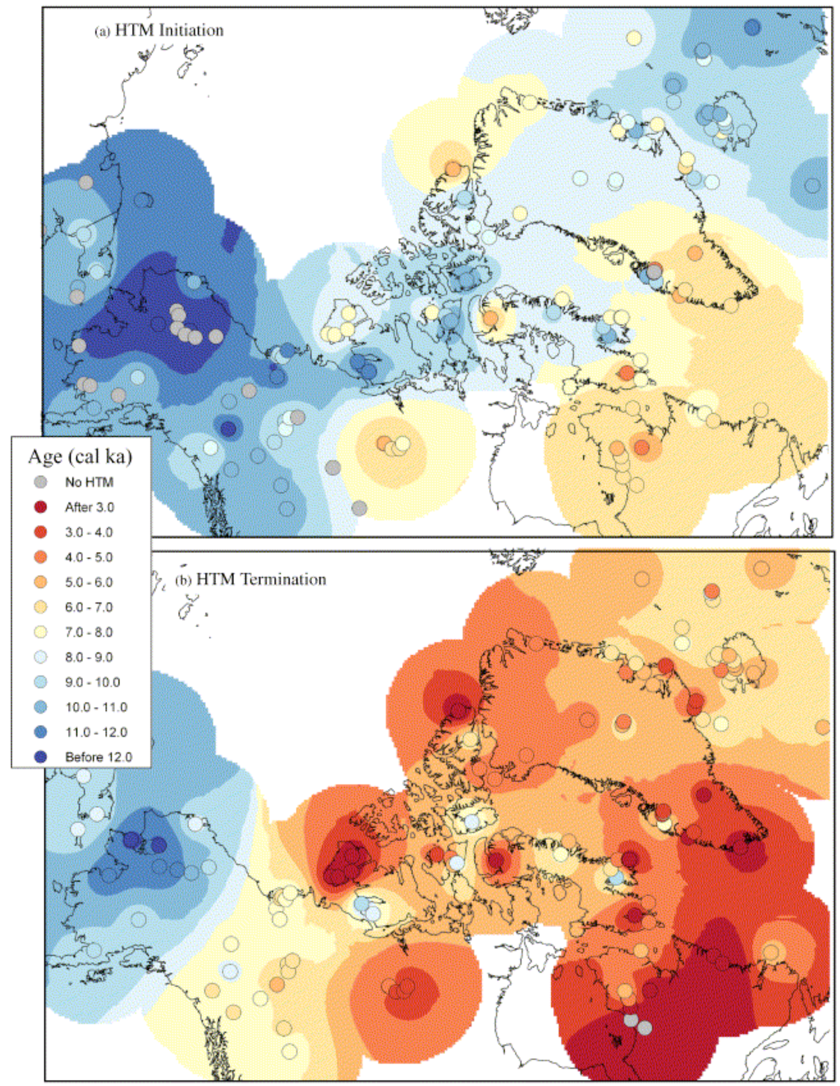

(a) HTM Initiation
(b) HTM Termination
Age (cal ka)
No HTM
After 3.0
3.0 - 4.0
4.0 - 5.0
5.0 - 6.0
6.0 - 7.0
7.0 - 8.0
8.0 - 9.0
9.0 - 10.0
10.0 - 11.0
11.0 - 12.0
Before 12.0

c

Figure. 5.32 The timing of initiation and termination of the Holocene Thermal Maximum in the western Arctic (Kaufman et al., 2004). a) Regions reviewed in Kaufman et al., 2004. b) Initiation of the Holocene Thermal Maximum in the western Arctic. Longitudinal distribution (left) and frequency distribution (right). c) Spatial-temporal pattern of the Holocene Thermal Maximum in the western Arctic. Upper panel, initiation; lower panel, termination. Dot colors bracket ages of the Holocene Thermal Maximum; ages contoured using the same color scheme. Gray dots, equivocal evidence for the Holocene Thermal Maximum.

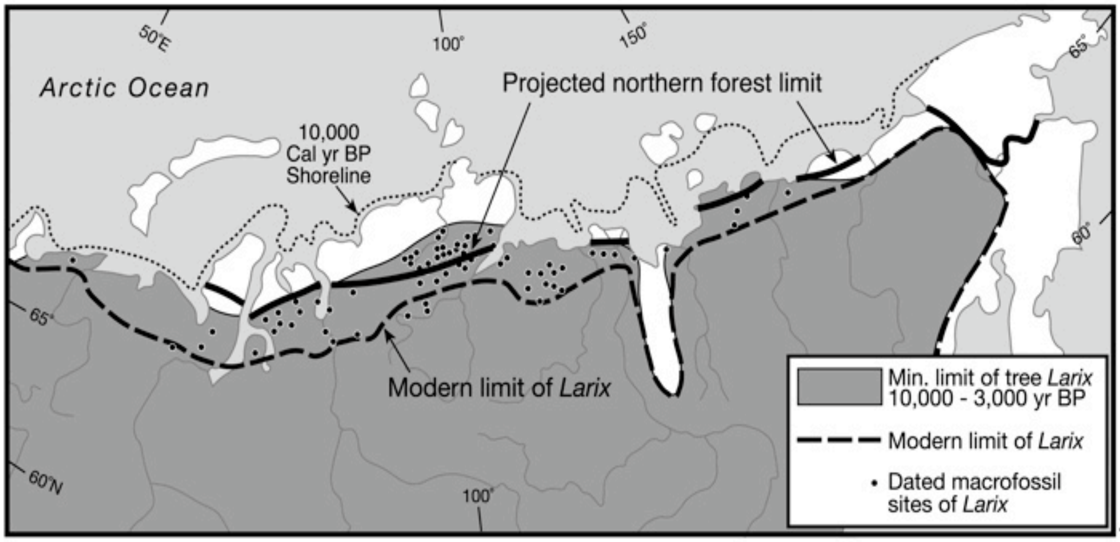

Figure. 5.33 The northward extension of larch (*Larix*) treeline across the Eurasian Arctic. Treeline today compared with treeline during the Holocene Thermal Maximum and with anticipated northern forest limits (Arctic Climate Impact Assessment, 2005) due to climate warming (MacDonald et al., 2007).

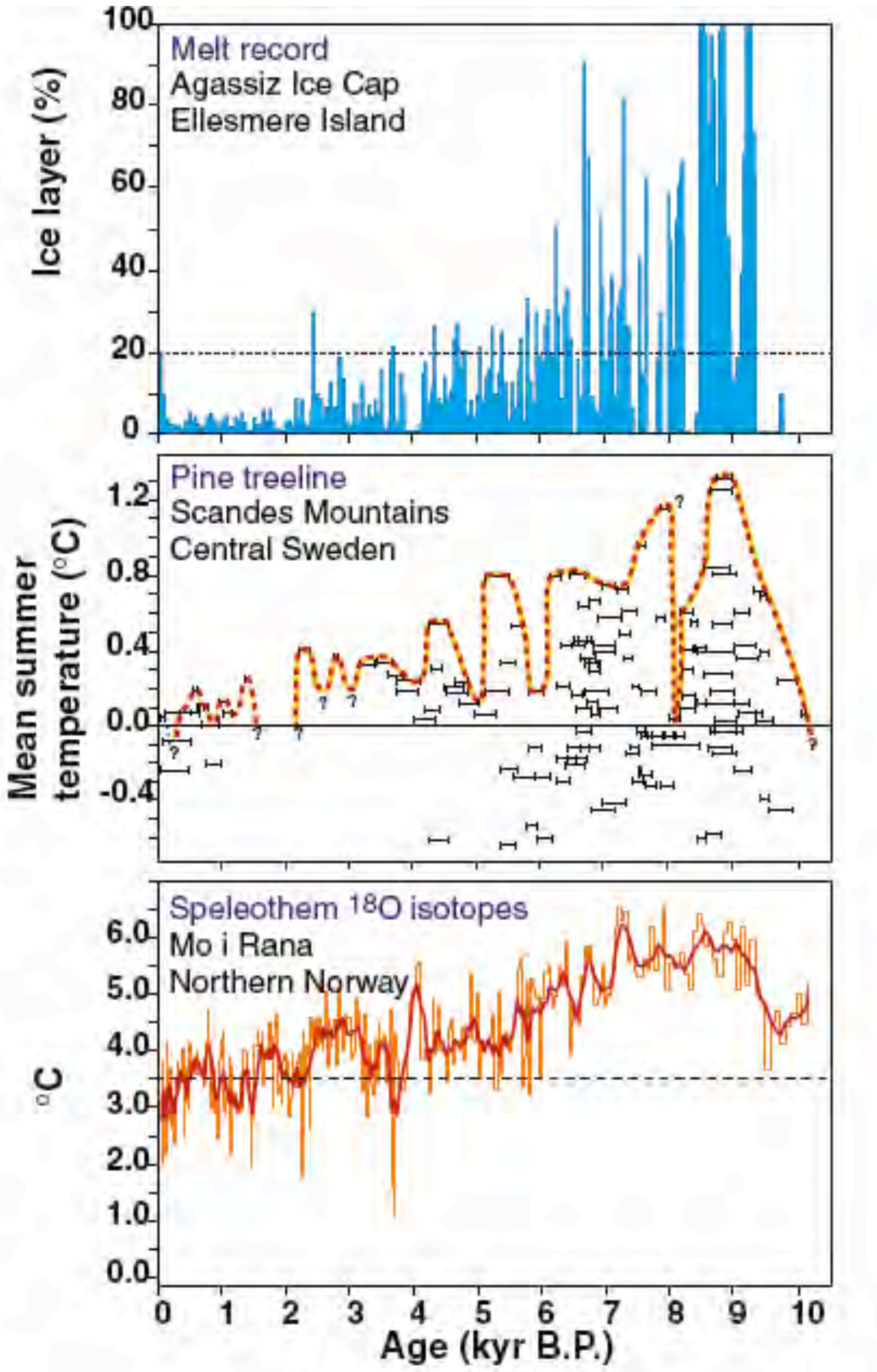

Fig. 5.34 Arctic temperature reconstructions. Upper panel: Holocene summer melting on the Agassiz Ice Cap, northern Ellesmere Island, Canada. "Melt" indicates the fraction of each core section that contains evidence of melting (from Koerner and Fisher, 1990). Middle panel:

Estimated summer temperature anomalies in central Swened. Black bars, elevation of ^{14}C- dated sub-fossil pine wood samples (*Pinus sylvestris* L.) in the Scandes Mountains, central Sweden, relative to temperatures at the modern pine limit in the region. Dashed line, upper limit of pine growth is indicated by the dashed line. Changes in temperature estimated by assuming a lapse rate of 6 °C km^{-1} (from Dahl and Nesje, 1996, ; based on samples collected by L. Kullman and by G. and J. Lundqvist). Lower panel: Paleotemperature reconstruction from oxygen isotopes in calcite sampled along the growth axis of a stalagmite from a cave at Mo i Rana, northern Norway. Growth ceased around A.D. 1750 (from Lauritzen 1996; Lauritzen and Lundberg 1998; 2002). Figure from Bradley (2000).

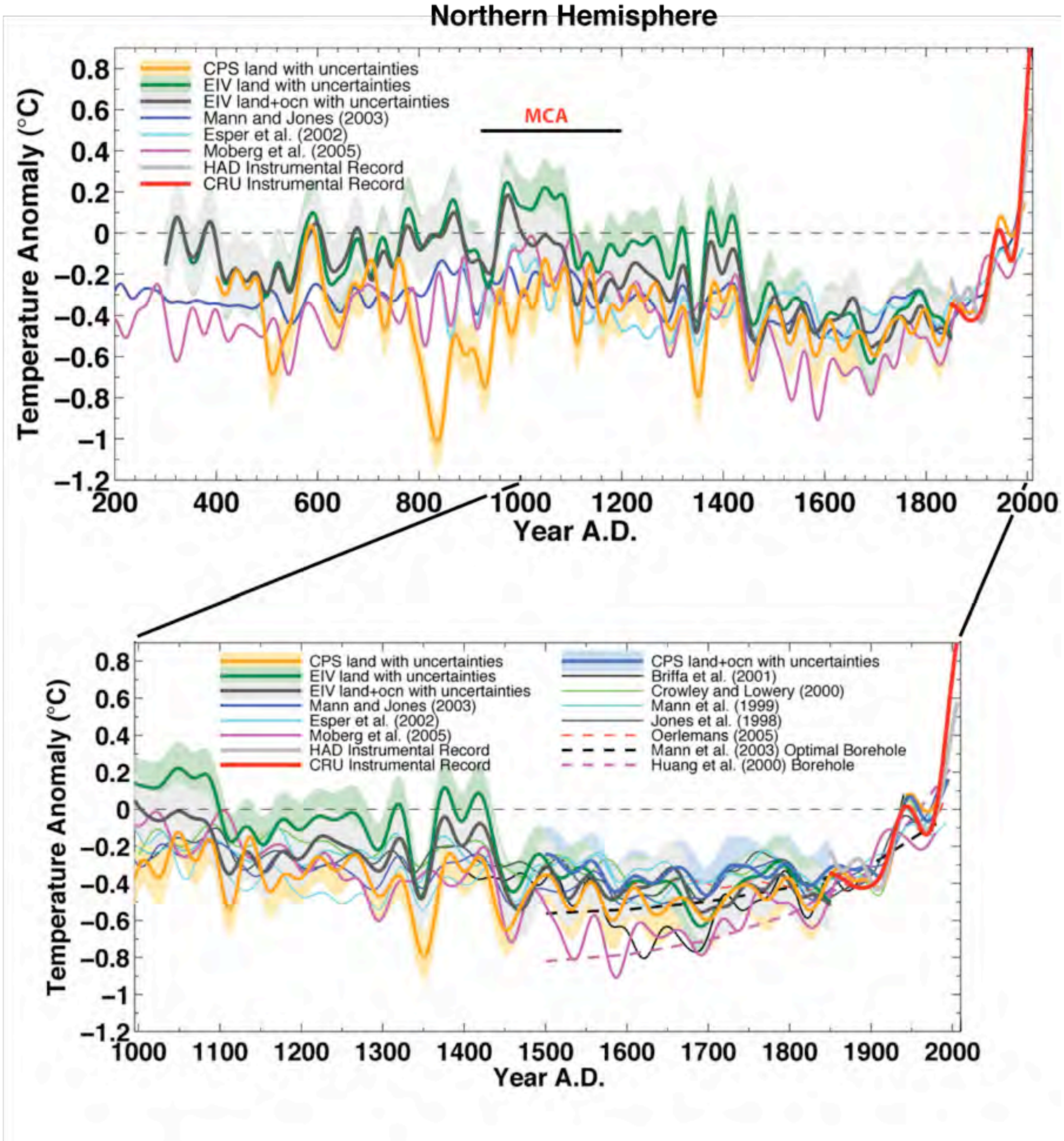

Figure 5.35. Updated composite proxy-data reconstruction of Northern Hemisphere temperatures for most of the last 2000 years, compared with other published reconstructions. Estimated confidence limits, 95%. All series have been smoothed with a 40-year lowpass filter. The Medieval Climate Anomaly (MCA), about 950–1200 AD. The array of reconstructions demonstrate that the warming documented by instrumental data during the past few decades exceeds that of any warm interval of the past 2000 years, including that estimated for the MCA.

(Figure from Mann et al. (in press). CPS, composite plus scale methodology; CRU, East Anglia Climate Research unit, a source of instrumental data; EIV, error-in-variables); HAD, Hadley Climate Center.

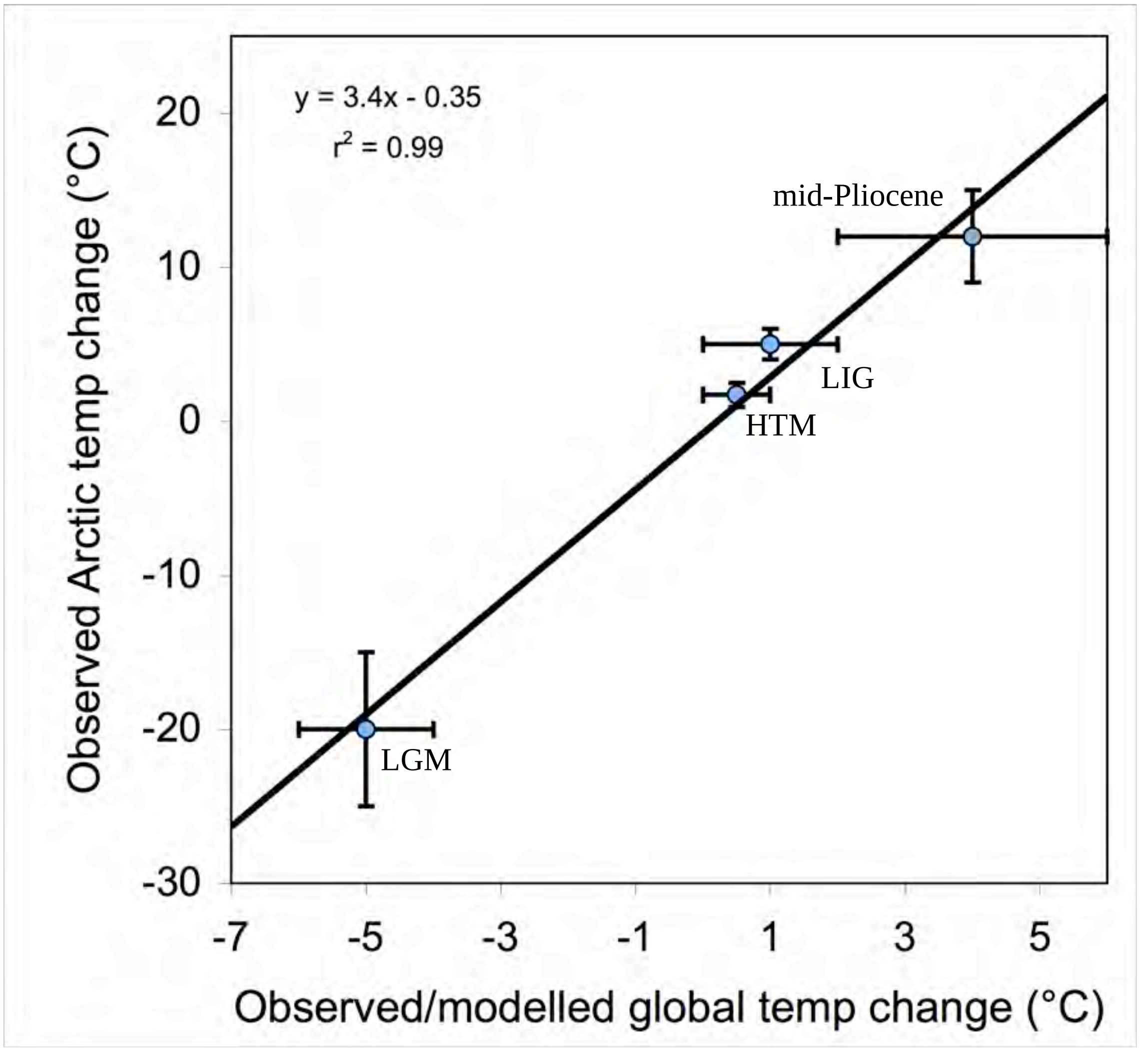

Figure 5.36 Paleoclimate data quantify the magnitude of Arctic amplification. Shown are paleoclimate estimates of Arctic summer temperature anomalies relative to recent, and the appropriate Northern Hemisphere or global summer temperature anomalies, together with their uncertainties, for the following: the last glacial maximum (LGM; about 20 ka), Holocene thermal maximum (HTM; about 8 ka), last interglaciation (LIG; 130–125 ka ago) and middle Pliocene (about 3.5–3.0 Ma). The trend line suggests that summer temperature changes are amplified 3 to 4 times in the Arctic**.** Explanation of data sources follows, for the different times for each time considered, beginning with the most recent.

Holocene Thermal Maximum (HTM): Arctic $\Delta T = 1.7 \pm 0.8°C$; Northern Hemisphere $\Delta T = 0.5 \pm 0.3°C$; Global $\Delta T = 0° \pm 0.5°C$.

A recent summary of summer temperature anomalies in the western Arctic (Kaufman et al., 2004) built on earlier summaries (Kerwin et al., 1999; CAPE Project Members, 2001) and is consistent with more-recent reconstructions (Kaplan and Wolfe, 2006; Flowers et al., 2007). Although the Kaufman et al. (2004) summary considered only the western half of the Arctic, the earlier summaries by Kerwin et al., (1999) and CAPE Project Members (2001) indicated that similar anomalies characterized the eastern Arctic, and all syntheses report the largest anomalies in the North Atlantic sector. Few data are available for the central Arctic Ocean; we assume that the circumpolar dataset provides an adequate reflection of air temperatures over the Arctic Ocean as well.

Climate models suggest that the average planetary anomaly was concentrated over the Northern Hemisphere. Braconnot et al. (2007) summarized the simulations from 10 different climate model contributions to the PMIP2 project that compared simulated summer temperatures at 6 ka with recent temperatures. The global average summer temperature anomaly at 6 ka was $0° \pm 0.5°C$, whereas the Northern Hemisphere anomaly was $0.5° \pm 0.3°C$. These patterns are similar to patterns in model results described by Hewitt and Mitchell (1998) and Kitoh and by Murakami (2002) for 6 ka, and a global simulation for 9 ka (Renssen et al., 2006). All simulate little difference in summer temperature outside the Arctic when those temperatures are compared to with pre-industrial temperatures.

Last Glacial Maximum (LGM): Arctic $\Delta T = 20° \pm 5°C$; global and Northern Hemisphere $\Delta T = –5° \pm 1°C$

Quantitative estimates of temperature reductions during the peak of the Last Glacial Maximum are less widespread in for the Arctic than are estimates of temperatures during warm times. Ice-core borehole temperatures, which offer the most compelling evidence (Cuffey et al., 1995; Dahl-Jensen et al., 1998), are supported by evidence from biological proxies in the North Pacific sector (Elias et al., 1996a), where no ice cores are available that extend back to the Last Glacial Maximum. Because of the limited datasets for temperature reduction in the Arctic during the Last Glacial Maximum, we incorporate a large uncertainty. The global-average temperature decrease during peak glaciations, based on paleoclimate proxy data, was 5°–6°C, and little difference existed between the Northern and Southern Hemispheres (Farrera et al., 1999; Braconnot et al., 2007; Braconnot et al., 2007). A similar temperature anomaly is derived from climate-model simulations (Otto-Bliesner et al., 2007).

Last Interglaciation (LIG): Arctic $\Delta T = 5° \pm 1°C$; global and Northern Hemisphere $\Delta T = 1° \pm 1°C$)

A recent summary of all available quantitative reconstructions of summer-temperature anomalies for in the Arctic during peak Last Interglaciation warmth shows a spatial pattern similar to that shown by Holocene Thermal Maximum reconstructions. The largest anomalies are in the North Atlantic sector and the smallest anomalies are in the North Pacific sector, but those small anomalies are substantially larger (5° ± 1°C) than they were during the Holocene Thermal Maximum (CAPE Last Interglacial Project Members, 2006). A similar pattern of Last Interglaciation summer-temperature anomalies is apparent in climate model simulations (Otto-Bliesner et al., 2006). Global and Northern Hemisphere summer-temperature anomalies are derived from summaries in CLIMAP Project Members (1984), Crowley (1990), Montoya et al. (2000), and Bauch and Erlenkeuser (2003).

Middle Pliocene: Arctic ΔT = 12° ± 3°C; global ΔT = 4° ± 2°C)

Widespread forests throughout the Arctic in the middle Pliocene offer a glimpse of a notably warm time in the Arctic, which had essentially modern continental configurations and connections between the Arctic Ocean and the global ocean. Reconstructed Arctic temperature anomalies are available from several sites that show much warmth and no summer sea ice in the Arctic Ocean basin. These sites include the Canadian Arctic Archipelago (Dowsett et al., 1994; Elias and Matthews, 2002; Ballantyne et al., 2006), Iceland (Buchardt and Símonarson, 2003), and the North Pacific (Heusser and Morley, 1996). A global summary of mid-Pliocene biomes by Salzmann et al. (2008) concluded that Arctic mean-annual-temperature anomalies were in excess of 10°C; some sites indicate temperature anomalies of as much as 15°C. Estimates of global sea-surface temperature anomalies are from Dowsett (2007).

Global reconstructions of mid-Pliocene temperature anomalies from proxy data and general circulation models show modest warming (average, 4° ± 1°C) across low to middle latitudes (Dowsett et al., 1999; Raymo et al., 1996; Sloan et al., 1996, Budyko et al., 1985; Haywood and Valdes, 2004; Jiang et al., 2005; Haywood and Valdes, 2006; Salzmann et al., 2008).

Chapter 5 References

Abbott, M.B., B.P. Finney, M.E. Edwards, and K.R. Kelts, 2000: Lake-level reconstructions and paleohydrology of Birch Lake, central Alaska, based on seismic reflection profiles and core transects. *Quaternary Research*, **53**, 154-166.

Adkins, J.F., E.A. Boyle, L.D. Keigwin, E. Cortijio, 1997: Variability of the North Atlantic thermohalinecirculation during the last interglacial period. *Nature*, **390**, 154-156.

Ager, T.A. and L.B. Brubaker, 1985: Quaternary palynology and vegetation history of Alaska. In: *Pollen Records of Late-Quaternary North American Sediments*, [Bryant, V.M., Jr. and R.G. Holloway, (eds.)]. American Association of Stratigraphic Palynologists, Dallas, pp. 353-384.

Aksu, A.E., 1985: Planktonic foraminiferal and oxygen isotope stratigraphy of CESAR cores 102 and 103—Preliminary results. In: *Initial geological report on CESAR—The Canadian Expedition to Study the Alpha Ridge, Arctic Ocean* [Jackson, H.R., P.J. Mudie, and S.M. Blasco (eds.)]. Geological Survey of Canada Paper 84-22, pp. 115-124.

Alfimov, A.V., D.I. Berman, and A.V. Sher, 2003: Tundra-steppe insect assemblages and the reconstruction of the Late Pleistocene climate in the lower reaches of the Kolyma River. *Zoologicheskiy Zhurnal*, **82**, 281-300 (In Russian).

Alley, R.B., 1991: Deforming-bed origin for southern Laurentide till sheets*? Journal of Glaciology*, **37(125),** 67-76.

Alley, R.B., 2003: Paleoclimatic insights into future climate challenges. *Philosophical Transactions of the Royal Society of London, Series A*, **361(1810)**, 1831-1849.

Alley, R.B., 2007: Wally was right: Predictive ability of the North Atlantic “conveyor belt” hypothesis for abrupt climate change. *Annual Review of Earth and Planetary Sciences*, **35,** 241-272.

Alley, R.B. and S. Anandakrishnan, 1995: Variations in melt-layer frequency in the GISP2 ice core: implications for Holocene summer temperatures in central Greenland. *Annals of Glaciology*, **21**, 64-70.

Alley, R.B. and A.M. Ágústsdóttir, 2005: The 8k event: Cause and consequences of a major Holocene abrupt climate change. *Quaternary Science Reviews*, **24**, 1123 -1149.

Alley, R.B., E.J. Brook and S. Anandakrishnan, 2002: A northern lead in the orbital band: North-south phasing of ice-age events. *Quaternary Science Reviews,* **21(1-3),** 431-441.

Alley, R.B. and K.M. Cuffey, 2001: Oxygen- and hydrogen-isotopic ratios of water in precipitation: Beyond paleothermometry. In: *Stable Isotope Geochemistry*, [Valley, J.W. and D. Cole (eds.)]. Mineralogical Society of America Reviews in Mineralogy and Geochemistry, **43**, , p. 527-553

Alley, R.B., D.A. Meese, C.A. Shuman, A.J. Gow, K.C. Taylor, P.M. Grootes, J.W.C. White, M. Ram, E.D. Waddington, P.A. Mayewski, and G.A. Zielinski, 1993: Abrupt increase in snow accumulation at the end of the Younger Dryas event. *Nature*, **362**, 527-529.

Alley, R.B., C.A. Shuman, D.A. Meese, A.J. Gow, K.C. Taylor, K.M. Cuffey, J.J. Fitzpatrick, P.M. Grootes, G.A. Zielinski, M. Ram, G. Spinelli, and B. Elder, 1997: Visual-stratigraphic dating of the GISP2 ice core—Basis, reproducibility, and application. *Journal of Geophysical Research*, **102**, 26,367-26,381.

Ammann, C.M., F.Joos, D.S. Schimel, B.L. Otto-Bliesner, and .R.A. Tomas, 2007: Solar influence on climate during the past millennium—Results from transient simulations with the NCAR Climate System Model. *Proceedings of the National Academy of Sciences*, *U.S.A.*, www.pnas.org/cgi//doi/10.1073/pnas.0605064103

Andersen, K.K., A. Svensson, S. Johnsen, S.O. Rasmussen, M. Bigler, R. Rothlisberger, U. Ruth, M.L. Siggaard-Andersen, J.P. Steffensen, D. Dahl-Jensen, B.M. Vinther, and H.B. Clausen, 2006: The Greenland Ice Core Chronology 2005, 15–42 kyr. Part I—Constructing the time scale. *Quaternary Science Reviews*, **25**, 3246-3257.

Anderson, N.J. and M.J. Leng, 2004: Increased aridity during the early Holocene in West Greenland inferred from stable isotopes in laminated-lake sediments. *Quaternary Science Reviews*, **23**, 841-849.

Anderson, L., M.B. Abbott, and B.P. Finney, 2001: Holocene climate inferred from oxygen isotope ratios in lake sediments, central Brooks Range, Alaska. *Quaternary Research*, **55**, 313-321.

Anderson, L., M.B. Abbott, B.P. Finney, and S.J. Burns, 2005: Regional atmospheric circulation change in the North Pacific during the Holocene inferred from lacustrine carbonate oxygen isotopes, Yukon Territory, Canada. *Quaternary Research*, **64**, 1-35.

Anderson, P.M. and A.V. Lozhkin, 2001: The stage 3 interstadial complex (Karginskii/middle Wisconsinan interval) of Beringia: variations in paleoenvironments and implications for paleoclimatic interpretations. *Quaternary Science Reviews*, **20,** 93-125.

Anderson, P.M., P.J. Bartlein, L.B. Brubaker, K. Gajewski, and J.C. Ritchie, 1989: Modern analogues of late Quaternary pollen spectra from the western interior of North America. *Journal of Biogeography*, **16**, 573-596.

Anderson, P.M., P.J. Bartlein, L.B. Brubaker, K. Gajewski, and J.C. Ritchie, 1991: Vegetation-pollen-climate relationships for the arcto-boreal region of North America and Greenland. *Journal of Biogeography*, **18,** 565-582.

Anderson, R.K., G.H. Miller, J.P. Briner, N.A. Lifton, and S.B. DeVogel, 2008: A millennial perspective on Arctic warming from 14C in quartz and plants emerging from beneath ice caps. *Geophyical Research Letters*, **35**, L01502, doi:10.1029/2007GL032057.

Andreev, A.A., D.M. Peteet, P.E. Tarasov, F.A. Romanenko, L.V. Filimonova, and L.D. Sulerzhitsky, 2001: Late pleistocene interstadial environment on Faddeyevskiy Island, East-Siberian Sea, Russia. *Arctic, Antarctic, and Alpine Research,* **33**, 28-35.

Andrews, J.T., L.M. Smith, R. Preston, T. Cooper, and A.E. Jennings, 1997: Spatial and temporal patterns of iceberg rafting (IRD) along the East Greenland margin, ca. 68 N, over the last 14 cal ka. *Journal of Quaternary Science*, **12**, 1-13.

Archer, D., 2007: Methane hydrate stability and anthropogenic climate change. *Biogeosciences*, **4**,521-544

Arctic Climate Impact Assessment (ACIA), 2004: *Impacts of a Warming Arctic—Arctic Climate Impact Assessment*. Cambridge University Press, Cambridge, U.K., 1042 pp.

Arctic Monitoring and Assessment Programme (AMAP), 1998: *AMAP Assessment Report Arctic Pollution Issues.* AMAP, Oslo, Norway, 871 pp.

Astakhov, V.I., 1995: The mode of degradation of Pleistocene permafrost in West Siberia. *Quaternary International*, **28**, 119-121.

Backman, J., M. Jakobsson, R. Løvlie, L. Polyak, and L.A. Febo, 2004: Is the central Arctic Ocean a sediment starved basin? *Quaternary Science Reviews*, **23**, 1435-1454.

Backman, J., K. Moran, D.B. McInroy, L.A. Mayer, and the Expedition 302 scientists, 2006: *Proceedings of IODP, 302*. Edinburgh (Integrated Ocean Drilling Program Management International, Inc.). doi:10.2204/iodp.proc.302.2006.

Balco, G., C.W. Rovey, and O.H. Stone, 2005a: The First Glacial Maximum in North America. *Science*, **307**, 222.

Balco, G., O.H. Stone, and C..Jennings, 2005b: Dating Plio-Pleistocene glacial sediments using the cosmic-ray-produced radionuclides ^{10}Be and ^{26}Al. *American Journal of Science*, **305,** 1-41.

Ballantyne, A.P., N.L. Rybczynski, P.A. Baker, C.R. Harington, and D. White, 2006: Pliocene Arctic temperature constraints from the growth rings and isotopic composition of fossil larch. *Palaeogeography, Palaeoclimatology, Palaeoecology*, **242**, 188-200

Barber, V.A. and B.P. Finney, 2000: Lake Quaternary paleoclimatic reconstructions for interior Alaska based on paleolake-level data and hydrologic models. *Journal of Paleolimnology*, **24**, 29-41.

Bard, E., 2002: Climate shocks—Abrupt changes over millennial time scales. *Physics Today*, **December**, 32-38.

Barley, E.M., I.R. Walker, and J. Kurek, L.C. Cwynar, R.W. Mathewes, K. Gajeweski, and B.P. Finney, 2006: A northwest North American training set—Distribution of freshwater midges in relation to air temperature and lake depth. *Journal of Paleolimnology*, **36**, 295-314.

Barnekow, L. and P. Sandgren, 2001: Palaeoclimate and tree-line changes during the Holocene based on pollen and plant macrofossil records from six lakes at different altitudes in northern Sweden. *Review of Palaeobotany and Palynology*, **117**, 109-118.

Barron, E.J., P.J. Fawcett, D. Pollard, and S. Thompson, 1993: Model simulations of cretaceous climates - the role of geography and carbon-dioxide. *Philosophical Transactions of the Royal Society of London Series B-Biological Sciences*, **341(1297),** 307-315.

Barron, E.J., P.J. Fawcett, W.H. Peterson, D. Pollard, and S.L. Thompson, 1995: A "simulation" of mid-Cretaceous climate. *Paleoceanography*, **8,** 785-798.

Barry, R.G., M.C. Serreze, J.A. Maslanik,and R.H. Preller, 1993: The arctic sea-ice climate system — observations and modeling. *Reviews of Geophysics,* **31(4)**, 397-422.

Bartlein, P.J., K.H. Anderson, P.M. Anderson, M.E. Edwards, C.J. Mock, R.S. Thompson, R.S. Webb, T. Webb, III, and C. Whitlock, 1998: Paleoclimate simulations for North America over the past 21,000 years: features of the simulated climate and comparisons with paleoenvironmental data. *Quaternary Science Reviews*, **17**, 549–585.

Bauch, D., J. Carstens, and G. Wefer, 1997: Oxygen isotope composition of living *Neogloboquadrina pachyderma* (sin.) in the Arctic Ocean. *Earth and Planetary Science Letters*, **146**, 47-58.

Bauch, D., P. Schlosser, and R.G. Fairbanks, 1995: Freshwater balance and the sources of deep and bottom waters in the Arctic Ocean inferred from the distribution of $H_2{}^{18}O$. *Progress in Oceanography*, **35**, 53-80.

Bauch, H.A., H. Erlenkeuser, K. Fahl, R.F. Spielhagen, M.S. Weinelt, H. Andruleit, and R. Henrich, 1999: Evidence for a steeper Eemian than Holocene sea surface temperature gradient between Arctic and sub-Arctic regions. *Palaeogeography, Palaeoclimatology, Palaeoecology*, **145**, 95-117.

Bauch, H.A., H. Erlenkeuser, J.P. Helmke, and U. Struck, 2000: A paleoclimatic evaluation of marine oxygen isotope stage 11 in the high-northern Atlantic (Nordic seas). *Global and Planetary Change*, **24**, 27-39.

Bauch, H.A. and H. Erlenkeuser, 2003: Interpreting Glacial-Interglacial Changes in Ice Volume and Climate From Subarctic Deep Water Foraminiferal d18O. In: *Earth's Climate and Orbital Eccentricity: The Marine Isotope Stage 11 Question*. [Droxler, A.W., R.Z. Poore, and L.H. Burckle (eds.)]. Geophysical Monograph Series, **137. [pages??]**

Bauch, H.A. and E.S. Kandiano, 2007: Evidence for early warming and cooling in North Atlantic surface waters during the last interglacial. *Paleoceanography*, **22**, PA1201, doi:10.1029/2005PA001252.

Beget, J.E., 2001: Continuous Late Quaternary proxy climate records from loess in Beringia. Quaternary Science Reviews 20, 499-507.

Behl, R.J., and J.P. Kennett, 1996: Brief interstadial events in the Santa Barbara Basin, NE Pacific, during the past 60 kyr. *Nature,* **379,** 243-246**.**

Bennike, O., K.P. Brodersen, E. Jeppesen, and I.R. Walker, 2004: Aquatic invertebrates and high latitude paleolimnology. In: *Long-Term Environmental Change in Arctic and Antarctic Lakes* [Pienitz, R., M.S.V. Douglas, and J.P. Smol (eds.)]. Springer, Dordrecht, pp. 159-186.

Berger, A. and M.F. Loutre, 1991: Insolation values for the climate of the last million years. *Quaternary Sciences Review*, **10(4),** 297-317.

Berger, A. and M.F. Loutre, 2002: An Exceptionally long Interglacial Ahead? *Science*, **297**, 1287-1288.

Berger, A., M.F. Loutre, and J. Laskar, 1992: Stability of the Astronomical Frequencies Over the Earth's History for Paleoclimate Studies. *Science,* **255(5044)**, 560-566.

Berner, R.A., and Z. Kothavala, 2001: GEOCARB III: A revised model of atmospheric CO2 over Phanerozoic time. *American Journal of Science*, **301(2)**, 182-204.

Bice, K.L., D. Birgel, P.A. Meyers, K.A. Dahl, K.U. Hinrichs, and R.D. Norris, 2006: A multiple proxy and model study of Cretaceous upper ocean temperatures and atmospheric CO2 concentrations. *Paleoceanography*, **21(2)**, PA2002.

Bigelow, N., L.B. Brubaker, M.E. Edwards, S.P. Harrison, I.C. Prentice, P.M. Anderson, A.A. Andreev, P.J. Bartlein, T.R. Christensen, W. Cramer, J.O. Kaplan, A.V.Lozhkin, N.V. Matveyeva, D.F. Murrary, A.D. McGuire, V.Y. Razzhivin, J.C. Ritchie, B. Smith, D.A. Walker, K. Gajewski, V. Wolf, B.H. Holmqvist, Y. Igarashi, K. Kremenetskii, A. Paus, M.F.J. Pisaric, and V.S. Volkova, 2003: Climate change and Arctic ecosystems—1. Vegetation changes north of 55°N between the last glacial maximum, mid-Holocene, and present. *Journal of Geophysical Research*, **108**, doi:10.1029/2002JD002558.

Bigler, C. and R.I. Hall, 2003: Diatoms as quantitative indicators of July temperature—A validation attempt at century-scale with meteorological data from northern Sweden. *Palaeogeography, Palaeoclimatology, Palaeoecology*, **189**, 147-160.

Birks, H.H., 1991: Holocene vegetational history and climatic change in west Spitzbergen—Plant macrofossils from Skardtjorna, an arctic lake. *The Holocene,* **1**, 209–218.

Birks, H.J.B., 1998: Numerical tools in palaeolimnology—Progress, potentialities, and problems. *Journal of Paleolimnology*, **20**, 307-332.

Björk, G., J. Soöderkvist, P. Winsor, A. Nikolopoulos, and M. Steele, 2002: Return of the cold halocline layer to the Amundsen Basin of the Arctic Ocean—Implications for the sea ice mass balance. *Geophysical Research Letters*, **29(11)**, 1513, doi:10.1029/2001GL014157.

Boellstorff, J., 1987: North American Pleistocene stages reconsidered in light of probably Pliocene-Pleistocene continental glaciation. *Science,* **202(2004365)**, 305-307.

Bonan, G.B., D. Pollard, and S.L. Thompson, 1992: Effects of boreal forest vegetation on global climate. *Nature,* **359(6397)**, 716-718.

Boyd, T.J., M. Steel, R.D. Muench, and J.T. Gunn, 2002: Partial recovery of the Arctic Ocean halocline. *Geophysical Research Letters*, **29(14)**, 1657, doi:10.1029/2001GL014047

Box, J.E., D.H. Bromwich, B.A. Veenhuis, L.S. Bai, J.C. Stroeve, J.C. Rogers, K. Steffen, T. Haran, and S.H. Wang, 2006: Greenland ice sheet surface mass balance variability (1988-2004) from calibrated polar MM5 output. *Journal of Climate*, **19(12),** 2783-2800

Braconnot, P., B. Otto-Bliesner, S. Harrison, F.S. Joussaume, J.-Y. Peterchmitt, A. Abe-Ouchi, M. Crucifix, E. Driesschaert, T. Fichefet, C.D. Hewitt, M. Kageyama, A. Kitoh, A. Laine, M.-F. Loutre, O. Marti, U. Merkel, G. Ramstein, P. Valdes, S.L. Weber, Y. Yu, and Y. Zhao, 2007: Results of PMIP2 coupled simulations of the Mid-Holocene and Last Glacial Maximum – Part 1: experiments and large-scale features. *Climates of the Past*, **3**, 261– 277.

Bradley, R.S., 1990: Holocene paleoclimatology of the Queen Elizabeth Islands, Canadian high Arctic. *Quaternary Science Reviews*, **9**, 365-384.

Bradley, R.S., 1999: *Paleoclimatology: reconstructing climates of the Quaternary* (second edition), Academic Press, New York, 613 pp.

Bradley, R. S., 2000: Past global changes and their significance for the future. *Quaternary Science Reviews*, **19,** 391-402**.**

Bradley, R.S., K.R. Briffa, J. Cole, and T.J. Osborn, 2003a: The climate of the last millennium. In: *Paleoclimate, Global Change and the Future,* [Alverson, K.D., R.S. Bradley, and T.F. Pedersen (eds.)]. Springer, Berlin, pp. 105-141.

Bradley, R.S., Hughes, M.K., and Diaz, H.F., 2003b: Climate in Medieval Time. *Science*, **302**, 404-405, doi: 10.1126/science.1090372.

Bradley, R.S. and P.D. Jones (eds.), 1992: *Climate Since AD 1500*. Routlege, London. 677 pp.

Brassell, S.C., G. Eglinton, I.T. Marlowe, U. Pflaumann, and M. Sarnthein, 1986: Molecular stratigraphy—A new tool for climatic assessment. *Nature*, **320**, 129-133.

Bray, P.J., S.P.E. Blockey, G.R. Coope, L.F. Dadswell, S.A. Elias, J.J. Lowe, and A.M. Pollard, 2006: Refining mutual climatic range (MCR) quantitative estimates of paleotemperature using ubiquity analysis. *Quaternary Science Reviews,* **25(15-16)**, 1865-1876.

Brewer, S., J. Guiot, and F. Torre, 2007: Mid-Holocene climate change in Europe: a data-model comparison. *Climate of the Past,* **3,** 499-512.

Briffa, K. and E. Cook, 1990: Methods of response function analysis In: *Methods of Dendrochronology* [Cook, E.R. and L.A. Kairiukstis (eds.)], sect. 5.6.

Briffa, K.R., T.J. Osborn, F.H. Schweingruber, I.C. Harris, P.D. Jones, S.G. Shiyatov, and E.A. Vaganov, 2001: Low-frequency temperature variations from a northern tree ring density network. *Journal of Geophysical Research*, **106,** 2929-2941.

Brigham, J.K., 1985: *Marine stratigraphy and amino acid geochronology of the Gubik Formation, western Arctic Coastal Plain, Alaska*. Doctoral dissertation, University of Colorado, Boulder; U.S. Geological Survey Open-File Report 85-381, 21pp.

Brigham-Grette, J. and L.D. Carter, 1992: Pliocene marine transgressions of northern Alaska—Circumarctic correlations and paleoclimate. *Arctic*, **43(4)**, 74-89.

Brigham-Grette, J. and D.M. Hopkins, 1995: Emergent-marine record and paleoclimate of the last interglaciation along the northwest Alaskan coast. *Quaternary Research*, **43**, 154-173.

Brigham-Grette, J., A.V. Lozhkin, P.M. Anderson, and O.Y. Glushkova, 2004: Paleoenvironmental conditions in western Beringia before and during the Last Glacial Maximum. In: *Entering America: Northeast Asia and Beringia Before the Last Glacial Maximum*,.[Madsen, D.B. (ed.)]. University of Utah Press, Chapter 2, pp. 29-61.

Briner, J.P., N. Michelutti, D.R. Francis, G.H. Miller, Y. Axford, M.J. Wooller, and A.P. Wolfe, 2006: A multi-proxy lacustrine record of Holocene climate change on northeastern Baffin Island. *Quaternary Research*, **65**, 431-442.

Brinkhuis, H., S. Schouten, M.E. Collinson, A. Sluijs, J.S.S. Damsfte, G.R. Dickens, M. Huber, T.M. Cronin, J. Onodera, K. Takahashi, J.P. Bujak, R. Stein, J. van der Burgh, J.S. Eldrett, I.C. Harding, A.F. Lotter, F. Sangiorgi, H.V.V. Cittert, J.W. de Leeuw, J. Matthiessen, J. Backman, and K. Moran, (Expedition 302 Scientists), 2006: Episodic fresh surface waters in the Eocene Arctic Ocean. *Nature,* **441(7093),** 606-609.

Broecker, W.S., 2001: Was the Medieval Warm Period Global? *Science*, **291** (5508) 1497-1499, doi:10.1126/science.291.5508.1497

Broecker, W.S. and S. Hemming, 2001: Climate swings come into focus. *Nature*, **294:5550** 2308-2309.

Broecker, W.S., D.M. Peteet, D. Rind, 1985: Does the ocean-atmosphere system have more than one stable mode of operation. *Nature*, **315(6014)**, 21-26.

Brouwers, E.M., 1987: On Prerygocythereis vunnieuwenhuisei Brouwers sp.nov. In: *A stereo-atlas of ostracode shells,* [Bate, R.H., D.J. Home, J.W. Neale, and D.J. Siveter, [eds.)]. British Micropaleontological Society, London 14, Part **1**,17-20.

Brown, J. and V. Romanovsky, 2008: Report from the International Permafrost Association: State of Permafrost in the First Decade of the 21st Century. Permafrost and Periglacial Processes. *Permifrost and Periglacial Processes,* **19(2),** 255-260.

Buchardt, B. and L.A. Símonarson, 2003: Isotope palaeotemperatures from the Tjörnes beds in Iceland: evidence of Pliocene cooling. *Palaeogeography, Palaeoclimatology, Palaeoecology* ,**189,** 71-95.

Budyko, M.I., A.B. Ronov, and A.L. Yanshin, 1985: *The History of the Earth's Atmosphere*. Leningrad, Gidrometeoirdat, 209 pp. (In Russian; English translation: Springer, Berlin, 1987, 139 pp.

Calkin, P.E., 1988: Holocene glaciation of Alaska (and adjoining Yukon Territory, Canada). *Quaternary Science Reviews*, **7**, 159-184.

CAPE Project Members, 2001: Holocene paleoclimate data from the Arctic: testing models of global climate change. *Quaternary Science Reviews,* **20**, 1275-1287.

CAPE–Last Interglacial Project Members, 2006: Last Interglacial Arctic warmth confirms polar amplification of climate change. *Quaternary Science Reviews*, **25**, 1383-1400.

Carter, L.D., 1981: A Pleistocene sand sea on the Alaskan Arctic Coastal Plain. *Science*, **211(4480)**, 381-383.

Carter, L.D., J. Brigham-Grette, L. Marincovich, Jr., V.L. Pease, and U.S. Hillhouse, 1986: Late Cenozoic Arctic Ocean sea ice and terrestrial paleoclimate. *Geology*, **14**, 675-678.

Chapin, F.S. III, M. Sturm, M.C. Serreze, J.P. Mcfadden, J.R. Key, A.H. Lloyd,T.S. Rupp, A.H. Lynch, J.P. Schimel, J. Beringer, W.L. Chapman, H.E. Epstein, E.S. Euskirchen, L.D. Hinzman, G. Jia, C.L. Ping, K.D. Tape, C.D.C. Thompson, D.A. Walker, and J.M. Welker, 2005: Role of land-surface changes in Arctic summer warming. *Science*, **310**, 657-660.

Chapman, M.R., N.J. Shackleton, and J.-C. Duplessy, 2000: Sea surface temperature variability during the last glacial-interglacial cycle—Assessing the magnitude and pattern of climate change in the North Atlantic. *Palaeogeography, Palaeoclimatology, Palaeoecology*, **157**, 1-25.

Chapman, W.L. and J.E. Walsh, 2007: Simulations of Arctic temperature and pressure by global coupled models. *Journal of Climate*, **20(4),** 609-632.

Clark, P.U. and D. Pollard, 1998: Origin of the Middle Pleistocene transition by ice sheet erosion of regolith. *Paleoceanography*, **13,** 1-9.

Clark, P.U., D. Archer, D. Pollard, J.D. Blum, J.A. Rial, V. Brovkin, A.C. Mix, N.G. Pisias, and M. Roy, 2006: The middle Pleistocene transition: characteristics, mechanisms, and implications for long-term changes in atmospheric pCO_2. *Quaternary Science Reviews,* **25**, 3150-3184.

Clayden, S.L., L.C. Cwynar, G.M. MacDonald, and A.A. Velichko, 1997: Holocene pollen and stomates from a forest-tundra site on the Taimyr Peninsula, Siberia. *Arctic and Alpine Research*, **29**, 327-333.

Climate Long-Range Investigation Mapping and Prediction (**CLIMAP**) Project Members, 1981: Seasonal reconstructions of the Earth's surface at the last glacial maximum. *Geological Society of America Map and Chart Series* MC-36, p. 1-18

Climate Long-Range Investigation Mapping and Prediction (**CLIMAP**) Project Members, 1984: The last interglacial ocean. *Quaternary Research*, **21,** 123-224.

Cockford, S.J. and S.G. Frederick, 2007: Sea ice expansion in the Bering Sea during the Neoglacial—Evidence from archeozoology. *The Holocene*, **17**, 699-706.

Cohen, A.S., 2003: *Paleolimnology—The history and evolution of lake systems*. Oxford University Press, Oxford, U.K., 528 pp.

Colinvaux, P.A., 1964: The environment of the Bering Land Bridge. *Ecological Monographs,* **34**, 297-329.

Conte, M.H., M. Sicre, C. Rühlemann, J.C. Weber, S. Schulte, D. Schulz-Bull, and T. Blanz, 2006: Global temperature calibration of the alkenone unsaturation index (UK'_{37}) in surface waters and comparison with surface sediments. *Geochemistry, Geophysics, Geosystems*, **7**, Q02005, doi:10.1029/2005GC001054.

Cronin, T.M, G.S. Dwyer, T. Kamiyac, S. Schwedea, and D.A. Willarda, 2003: Medieval Warm Period, Little Ice Age and 20th century temperature variability from Chesapeake Bay. *Global and Planetary Change*, **36**, 17-29

Crowley, T.J., 1998: Significance of tectonic boundary conditions for paleoclimate simulations. In: *Tectonic Boundary Conditions for Climate Reconstructions* [Crowley, T.J., and K.C. Burke (eds.)]. Oxford University Press, New York, pp. 3-17.

Crowley, T.J., 1990: Are there any satisfactory geologic analogs for a future greenhouse warming? *Journal of Climatology*, **3**, 1282-1492.

Crowley, T.J., 2000: Causes of climate change over the past 1000 years. *Science*, **289**, 270-277.

Crowley, T.J., S.K. Baum, K.Y. Kim, G.C. Hegerl, and W.T. Hyde, 2003: Modeling ocean heat content changes during the last millennium. *Geophysical Research Letters,* **30**, 1932, doi:10.1029/2003GL017801.

Crowley, T.J. and T. Lowery, 2000: How warm was the Medieval warm period? *Ambio,* **29**, 51-54.

Cuffey, K.M. and G.D. Clow, 1997: Temperature, accumulation, and ice sheet elevation in central Greenland through the last deglacial transition. *Journal of Geophysical Research*, **102(C12)**, 26,383-26,396.

Cuffey, K.M., G.D. Clow, R.B. Alley, M. Stuiver, E.D. Waddington, and R.W. Saltus, 1995: Large Arctic temperature change at the Wisconsin-Holocene glacial transition. *Science,*

270, 455-458.

D'Arrigo, R., Wilson, R., Jacoby, G., 2006: On the long-term context for late twentieth century warming. *Journal of Geophysical Research*, **111**, D03103, doi:10.1029/2005JD006352.

Dahe, Q., J.R. Petit, J. Jouzel, and M. Stievenard, 1994: Distribution of stable isotopes in surface snow along the route of the 1990 International Trans-Antarctic Expedition. *Journal of Glaciology*, **40**, 107-118.

Dahl, S.O. and A. Nesje, 1996: A new approach to calculating Holocene winter precipitation by combining glacier equilibrium-line altitudes and pine-tree limits: a case stud from Hardangerjokulen, central southern Norway. *The Holocene*, **6(4)**, 381-398, doi:10.1177/095968369600600401

Dahl-Jensen, D., K. Mosegaard, N. Gundestrup, G.D. Clow, S.J. Johnsen, A.W. Hansen, and N. Balling, 1998: Past temperature directly from the Greenland Ice Sheet. *Science*, **282**, 268-271.

Dansgaard, W., 1964: Stable isotopes in precipitation. *Tellus*, **16**, 436-468.

Dansgaard, W., J.W.C. White, and S.J. Johnsen, 1989: The abrupt termination of the Younger Dryas climate event. *Nature*, **339(6225)**, 532-534.

Delworth, T.L., and T.R. Knutson, 2000: Simulation of early 20th century global warming. *Science*, **287(5461),** 2246-225.

de Vernal, A., C. Hillaire-Marcel, and D.A. Darby, 2005: Variability of sea ice cover in the Chukchi Sea (western Arctic Ocean) during the Holocene. *Paleoceanography*, **20**, PA4018, doi:10.1029/2005PA001157.

Denton, G.H., R.B. Alley, G.C. Comer and W.S. Broecker, 2005: The role of seasonality in abrupt climate change. *Quaternary Science Reviews*, **24(10-11)**, 1159-1182.

Digerfeldt, G., 1988: Reconstruction and regional correlation of Holocene lake-level fluctuations in Lake Bysjön, South Sweden. *Boreas*, **17**, 237-263.

Donnadieu, Y., R. Pierrehumbert, R. Jacob, and F. Fluteau, 2006: Modeling the primary control of paleogeography on Cretaceous climate. *Earth and Planetary Science Letters*, **248**, 426-437.

Douglas, M.S.V., 2007: Environmental change at high latitudes. In: *Geological and Environmental Applications of the Diatom—Pond Scum to Carbon Sink* [Starratt, S.W. (ed.)]. The Paleontological Society Papers, **13**, 169-179.

Douglas, M.S.V. and J.P. Smol, 1994: Limnology of high arctic ponds (Cape Herschel, Ellesmere Island, N.W.T.). *Archiv für Hydrobiologie*, **131**, 401-434.

Douglas, M.S.V. and J.P. Smol, 1999: Freshwater diatoms as indicators of environmental change in the High Arctic. In: *The Diatoms—Applications for the Environment and Earth Sciences*, [Stoermer, E. and J.P. Smol (eds.)]. Cambridge University Press, Cambridge, U.K., 488 pp.

Douglas, M.S.V., J.P. Smol, and W. Blake, Jr., 1994: Marked post-18th century environmental change in high Arctic ecosystems. *Science*, **266**, 416-419.

Douglas, M.S.V., J.P. Smol, R. Pienitz, and P. Hamilton, 2004: Algal indicators of environmental change in arctic and antarctic lakes and ponds. In: *Long-Term Environmental Change in Arctic and Antarctic Lakes,* [Pienitz, R., M.S.V. Douglas, and J.P. Smol (eds.)]. Springer, Dordrecht. pp. 117-157.

Dowdeswell, J.A., J.O. Hagen, H. Björnsson, A.F. Glazovsky, W.D. Harrison, P. Holmlund, J.

Jania, R.M. Koerner, B. Lefauconnier, C.S.L. Ommanney, and R.H. Thomas, 1997: The mass balance of circum-Arctic glaciers and recent climate change. *Quaternary Research*, **48**, 1-14.

Dowsett, H.J., 2007: The PRISM Palaeoclimate Reconstruction and Pliocene Sea-Surface Temperature. In: *Deep-time perspectives on climate change: marrying the signal from computer models and biological proxies*, [Williams, M., A.M. Haywood, F.J. Gregory, and D.N. Schmidt (eds.)] The Micropalaeontological Society, Special Publication, The Geological Society, London, pp. 459-480.

Dowsett, H.J. , J.A. Barron, R.Z. Poore, R.S. Thompson, T.M. Cronin, S.E. Ishman, S.E., D.A. Willard, 1999: Middle Pliocene paleoenvironmental reconstruction: PRISM2, U.S. Geological Survey Open File Report 99-535.

Dowsett, H.J., and eight others, 1994: Joint investigations of the middle Pliocene climate I—PRISM paleoenvironmental reconstructions. *Global and Planetary Change*, **9**, 169-195

Droxler, A.W. and J.W. Farrell, 2000: Marine Isotope Stage 11 (MIS11): New insights for a warm future. *Global and Planetary Change,* **24(1),** 1-5

Droxler, A.W., R.B. Alley, W.R. Howard, R.Z. Poore and L.H. Burckle. 2003: Unique and exceptionally long interglacial marine isotope stage 11: Window into Earth future climate. In: *Earth's Climate and Orbital Eccentricity: The Marine Isotope Stage 11 Question*, [Droxler, A.W., R.Z. Poore and L.H. Burckle (eds.)].Geophysical Monograph, **137**, American Geophysical Union, pp. 1-14.

Duk-Rodkin, A., R.W. Barendregt, D.G. Froese, F. Weber, R.J. Enkin, I.R. Smith, Grant D. Zazula, P. Waters, and R. Klassen, 2004: Timing and Extent of Plio-Pleistocene glaciations in North-Western Canada and East-Central Alaska. In: *Quaternary Glaciations-Extent and Chronology, Part II, North America*, [Ehlers, J. and P.L. Gibbard (eds.)]. Elsevier, New York, pp. 313-345.

Dyke, A.S. and J.M. Savelle, 2001: Holocene history of the Bering Sea bowhead whale (*Balaena mysticetus*) in its Beaufort Sea summer grounds off southwestern Victoria Island, western Canadian Arctic. *Quaternary Research*, **55**, 371-379.

Dykoski, C.A., R.L. Edwards, H. Cheng, D. Yuan, Y. Cai, M. Zhang, Y. Lin, J. Qing, Z. An, and J. Revenaugh, 2005: A high-resolution, absolute-dated Holocene and deglacial Asian monsoon record from Dongge Cave, China. *Earth and Planetary Science Letters*, **233**, 71-86.

Edwards, M.E., N.H. Bigelow, B.P. Finney, and W.R. Eisner, 2000: Records of aquatic pollen and sediment properties as indicators of late-Quaternary Alaskan lake levels. *Journal of Paleolimnology*, **24**, 55-68.

Elias, S.A., 2007: Beetle records—Late Pleistocene North America. In: *Encyclopedia of Quaternary Science* [Elias, S.A. (ed.)]. Elsevier, Amsterdam, pp. 222-236.

Elias, S.A., K. Anderson, and J.T. Andrews, 1996: Late Wisconsin climate in the northeastern United States and southeastern Canada, reconstructed from fossil

Elias, S.A., J.T. Andrews, and K.H. Anderson, 1999: New insights on the climatic constraints on the beetle fauna of coastal Alaska derived from the mutual climatic range method of paleoclimate reconstruction. *Arctic, Antarctic, and Alpine Research,* **31**, 94-98.

Elias, S.A. and J.V. Matthews, Jr., 2002: Arctic North American seasonal temperatures in the Pliocene and Early Pleistocene, based on mutual climatic range analysis of fossil beetle assemblages. *Canadian Journal of Earth Sciences*, **39**, 911-920.
beetle assemblages. *Journal of Quaternary Science*, **11**, 417-421.

Ellis, J.M., and P.E. Calkin, 1984: Chronology of Holocene glaciation, central Brooks Range, Alaska. *Geological Society of America Bulletin*, **95**, 897-912.

Epstein, S., H. Buchsbaum, H. Lowenstam, and H.C. Urey, 1953: Revised carbonate-water isotopic temperature scale. *Geological Society of America Bulletin*, **64**, 1315-1325.

Erez, J. and B. Luz, 1982: Temperature control of oxygen-isotope fractionation of cultured planktonic foraminifera. *Nature*, **297**, 220-222.

Eronen, M., P. Zetterberg, K.R. Briffa, M. Lindholm, J. Meriläinen, and M. Timonen, 2002: The supra-long Scots pine tree-ring record for Finnish Lapland: Part 1, chronology construction and initial inferences. *The Holocene*, **12(6),** 673-680.

Esper, J., E.R. Cook, and F.H. Schweingruber, 2002: Low-frequency signals in long tree-ring chronologies for reconstructing past temperature variability. *Science,* **295**, 2250-2253.

Esper, J. and F.H. Schweingruber, 2004: Large-scale treeline changes recorded in Siberia. *Geophysical Research Letters,* **31**, L06202, doi:10.1029/2003GL019178.

Fairbanks, R.G., 1989: A 17,000-year glacio-eustatic sea level record—Influence of glacial melting rates on the Younger Dryas event and deep-ocean circulation. *Nature,* **343**, 612-616.

Farrera, I., S.P. Harrison, I.C. Prentice, G. Ramstein, J. Guiot, P.J. Bartlein, R.Bonnelle, M. Bush, W. Cramer, U. von Grafenstein, K. Holmgren, H. Hooghiemstra, G. Hope, D. Jolly, S.-E. Lauritzen, Y. Ono, S. Pinot, M. Stute, and G. Yu, 1999: Tropical climates at the Last Glacial Maximum: a new synthesis of terrestrial palaeoclimate data. I. Vegetation, lake-levels and geochemistry. *Climate Dynamics,* **15**, 823-856.

Finney, B., K. Rühland, J.P. Smol, and M.-A. Fallu, 2004: Paleolimnology of the North American subarctic. In: *Long-Term Environmental Change in Arctic and Antarctic Lakes* [Pienitz, R., M.S.V. Douglas, and J.P. Smol (eds.)]. Springer, Dordrecht, pp. 269-318.

Fisher, D.A., 1979: Comparison of 100,000 years of oxygen isotope and insoluble impurity profiles from the Devon Island and Camp Century ice cores. *Quaternary Research*, **11**, 299-304.

Fisher, D.A. and R.M. Koerner, 2003: Holocene ice core climate history, a multi-variable approach. In: *Global Change in the Holocene*, [Mackay, A., R. Battarbee, J. Birks and F. Oldfield, (eds.)] Arnold, London, pp. 281-293**.**

Fisher, D.A., R.M. Koerner, J.C. Bourgeois, G. Zielinski, C. Wake, C.U. Hammer, H.B. Clausen, N. Gundestrup, S. Johnsen, K. Goto- Azuma, T. Hondoh, E. Blake, and M. Gerasimoff, 1998: Penny Ice Cap cores, Baffin Island, Canada, and the Wisconsinan Foxe Dome connection—Two states of Hudson Bay ice cover. *Science*, **279**, 692-695.

Fisher, D.A., C. Wake, K. Kreutz, K. Yalcin, E. Steig, P. Mayewski, L. Anderson, J. Aheng, S. Rupper, C. Zdanowicz, M. Demuth, M. Waskiewicz, D. Dahl-Jensen, K. Goto-Azuma, J.B. Bourgeois, R.M. Koerner, J. Sekerka, E. Osterberg, M.B. Abbott, B.P. Finney, and S.J. Burns, 2004: Stable isotope records from Mount Logan, Eclipse ice cores and nearby Jellybean Lake. Water cycle of the North Pacific over 2000 years and over five vertical kilometres—Sudden shift and tropical connections. *Geographie physique et Quaternaire*, **58**, 9033-9048.

Flowers, G.E., H. Björnsson, Á. Geirsdóttir, G.H. Miller, J.L. Black, and G.K.C. Clarke, 2008: Holocene climate conditions and glacier variation in central Iceland from physical modelling and empirical evidence. *Quaternary Science Reviews*, **27**, 797-813.

Francis, J.E., 1988: A 50-million-year-old fossil forest from Strathcona Fiord, Ellesmere Island, Arctic Canada—Evidence for a warm polar climate. *Arctic*, **41(4)**, 314-318.

Fricke, H.C. and J.R. O'Neil, 1999: The correlation between $^{18}O/^{16}O$ ratios of meteoric water and surface temperature: its use in investigating terrestrial climate change over geologic time. *Earth and Planetary Science Letters*, **170**, 181-196.

Fritts, H.C., 1976: *Tree Rings and Climate.* London Academic Press

Fronval,T. and E. Jansen, 1997: Eemian and early Weichselian (140- 60 ka) paleoceanography and paleoclimate in the Nordic seas with comparisons to Holocene conditions. *Paleoceanography*, **12**, 443-462.

Funder, S., 1989: Quaternary geology of East Greenland. In: *Quaternary Geology of Canada and Greenland*, [Fulton, R.J. (ed.)]. Geological Society of America Decade of North American Geology, vol. **K1**, pp. 756-763.

Funder, S., O. Bennike, J. Böcher, C. Israelson, K.S. Petersen, and L.A. Simonarson, 2001: Late Pliocene Greenland—The Kap Kobenhavn Formation in North Greenland. *Bulletin of the Geological Society of Denmark*, **48**, 117-134.

Funder, S., I. Demidov, and Y. Yelovicheva, 2002: Hydrography and mollusc faunas of the Baltic and the White Sea-North Sea seaway in the Eemian. *Palaeogeography, Palaeoclimatology, Palaeoecology,* **184**, 275-304.

Fyles, J.G., L. Marincovich, Jr., J.V. Mathews, Jr., and R. Barendregt, 1991: Unique mollusc find in the Beaufort Formation (Pliocene) Meighen Island, Arctic Canada. In: *Current Research, Part B, Geological Survey of Canada, Paper 91-1B*, pp. 461-468.

Gajewski, K. and G.M. MacDonald, 2004: Palynology of North American Arctic Lakes. In: *Long Term Environmental Change in Arctic and Antarctic Lakes* [R. Pienitz, M.S.V. Douglas and J.P. Smol (eds.)]. Springer, Netherlands, pp. 89-116.

Gard, G., 1986: Calcareous nannofossil biostratigraphy north of 80° latitude in the eastern Arctic Ocean. *Boreas*, **15**, 217-229.

Gard, G., 1987: Late Quaternary calcareous nannofossil biostratigraphy and sedimentation patterns—Fram Strait, Arctica. *Paleoceanography*, **2**, 219-229.

Gard, G., 1993: Late Quaternary coccoliths at the North Pole—Evidence of ice-free conditions and rapid sedimentation in the central Arctic Ocean. *Geology*, **21**, 227-230.

Geirsdottir, A., Miller, G.H., Axford, Y. and Olafsdottir, S., in press, Holocene and latest Pleistocene climate and glacier fluctuations in Iceland. *Quaternary Science Reviews*.

Gervais, B.R., G.M. MacDonald, J.A. Snyder, and C.V. Kremenetski, 2002: *Pinus sylvestris* treeline development and movement on the Kola Peninsula of Russia—Pollen and stomate evidence. *Journal of Ecology*, **90**, 627-638.

Goetcheus, V.G., and H.H. Birks, 2001: Full-glacial upland tundra vegetaion preserved under tephra in the Beringia National Park, Seward Peninsula, Alaska. *Quaternary Science Reviews*, **20(1-3)**, 135-147.

Goetz, S.J., M.C. Mack, K.R. Gurney, J.T. Randerson, and R.A. Houghton, 2007: Ecosystem responses to recent climate change and fire disturbance at northern high latitudes—Observations and model results contrasting northern Eurasia and North America. *Environmental Research Letters*, **2**, 045031, doi:10.1088/1748-9326/2/4/045031

Goodfriend, G.A., J. Brigham-Grette, G.H. Miller, 1996: Enhanced age resolution of the marine quaternary record in the Arctic using aspartic acid racemization dating of bivalve shells. *Quaternary Research*, **45**, 176-187

Goosse, H., H. Renssen, A. Timmermann, and R.A. Bradley, 2005: Internal and forced climate variability during the last millennium—A model-data comparison using ensemble simulations. *Quaternary Science Reviews*, **24**, 1345-1360.

Gradstein, F.M., J.G.Ogg, and A.G. Smith (eds.), 2004: *A Geologic Time Scale*. Cambridge University Press, Cambridge, 589 pp.

Grice, K., W.C.M. Klein Breteler, S. Schoten, V. Grossi, J.W. de Leeuw, and J.S. Sinninge Damste, 1998: Effects of zooplankton herbivory on biomarker proxy records. *Paleoceanography*, **13**, 686-693.

Grootes, P.M., M. Stuiver, J.W.C. White, S. Johnsen, and J. Jouzel, 1993: Comparison of oxygen isotope records from the GISP2 and GRIP Greenland Ice cores. *Nature*, **366**, 522-555.

Grove, J.M., 1988: *The Little Ice Age*. Methuen, London, 498 pp.

Grudd, H., K.R. Briffa, W. Karlén, T.S. Bartholin, P.D. Jones, and B. Kromer, 2002: A 7400-year tree-ring chronology in northern Swedish Lapland—Natural climatic variability expressed on annual to millennial timescales. *The Holocene*, **12**, 657-666.

Gudina, V.D. Kryukov, L.K. Levchuk and L.A. Sudkov, 1983: Upper-Pleistocene sediments in north-eastern Taimyr. *Bulletin of Commission on Quaternary Researches,* **52**, 90-97 (in Russian).

Haeberli, W., G.D. Cheng, A.P. Gorbunov,and S.A. Harris, 1993: Mountain permafrost and climatic change. *Permafrost and Periglacial Processes,* **4(2),** 165-174.

Hammarlund, D., L. Barnekow, H.J.B. Birks, B. Buchardt, and T.W.D. Edwards, 2002: Holocene changes in atmospheric circulation recorded in the oxygen-isotope stratigraphy of lacustrine carbonates from northern Sweden. *The Holocene*, **12**, 339-351.

Hannon, G.E. and M.J. Gaillard, 1997: The plant-macrofossil record of past lake-level changes. *Journal of Paleolimnology*, **18**, 15-28.

Hantemirov, R.M. and S.G. Shiyatov, 2002: A continuous multi-millennial ring-width chronology in Yamal, northwestern Siberia. *The Holocene,* **12(6),** 717-726.

Harrison, S., P. Braconnot, C. Hewitt, and R.J. Stouffer, 2002: Fourth International Workshop of the Palaeoclimate Modelling Inter- comparison Project (PMIP): Launching PMIP Phase Ii. *EOS*, **83**, 447-447.

Harrison, S.P., D. Jolly, F. Laarif, A. Abe-Ouchi, B. Dong, K. Herterich, C. Hewitt, S. Joussaume, J.E. Kutzbach, J. Mitchell, N. de Noblet, and P. Valdes, 1998: Intercomparison of simulated global vegetation distributions in response to 6 kyr BP orbital forcing. *Journal of Climate*, **11**, 2721-2742.

Harrison, S.P., J.E. Kutzbach, I.C. Prentice, P.J. Behling, and M.T. Sykes, 1995: The response of northern hemisphere extratropical climate and vegetation to orbitally induced changes in insolation during the last interglaciation. *Quaternary Research*, **43**(2), 174-184.

Haywood, A.M., P. Dekens, A.C. Ravelo, and M. Williams, 2005: Warmer tropics during the mid-Pliocene? Evidence from alkenone paleothermometry and a fully coupled ocean-atmosphere GCM. *Geochemistry, Geophysics, Geosystems*, **6**, Q03010, doi:10.1029/2004GC000799.

Haywood, A.M. and P.J. Valdes, 2004: Modeling Pliocene warmth: contribution of atmosphere, oceans and cryosphere. *Earth and Planetary Science Letters*, **218,** 363-377.

Haywood, A.M. and P.J. Valdes, 2006: Vegetation cover in a warmer world simulated using a dynamic global vegetation model for the Mid-Pliocene. *Palaeogeography, Palaeoclimatology, Palaeoecology*, **237**, 412-427.

Helmke, J.P. and H.A. Bauch, 2003: Comparison of glacial and interglacial conditions between the polar and subpolar North Atlantic region over the last five climatic cycles. *Paleoceanograph*, **18(2),** 1036, doi:10.1029/2002PA000794

Henrich R. and K.-H. Baumann, 1994: Evolution of the Norwegian current and the

Scandinavian ice sheets during the past 2.6 m.y.: evidence from ODP Leg 104 biogenic carbonate and terrigenous records. *Palaeogeography, Palaeoclimatology, Palaeoecology,* **108,** 75-94.

Herbert, T.D., 2003: *Alkenone paleotemperature determinations*. In: *Treatise in Marine Geochemistry*, [Elderfield, H. and K.K. Turekian (eds.)]. Elsevier, Amsterdam, pp. 391-432.

Heusser, L. and J. Morley, 1996: Pliocene climate of Japan and environs between 4.8 and 2.8 Ma: a joint pollen and marine faunal study. *Marine Micropaleontology*, **27,** 85-106.

Hewitt, C.D. and J.F.B. Mitchell, 1998: A Fully Coupled GCM Simulation of the Climate of the Mid-Holocene. *Geophysical Research Letters*, **25**, 361-364.

Hoffmann, G., M. Werner, and M. Heimann, 1998: Water isotope module of the ECHAM atmospheric general circulation model—A study on timescales from days to several years. *Journal of Geophysical Research*, **103**, 16,871-16,896.

Holland, M.M. and C.M. Bitz, 2003: Polar amplification of climate change in coupled models. *Climate Dynamics*, **21**, 221-232.

Holland, M.H., C.M., Bitz, and B. Tremblay, 2006: Future abrupt reductions in the summer Arctic sea ice. *Geophysical Research Letters*, **33**, L23503, doi:10.1029/2006GL028024.

Huber, C., M. Leuenberger, R. Spahni, J. Flückiger, J. Schwander, T. F. Stocker, S. Johnsen, A. Landals, and J. Jouzel, 2006: Isotope calibrated Greenland temperature record over Marine Isotope Stage 3 and its relation to CH4. *Earth and Planetary Science Letters*, **243**, 504-519.

Hughen, K., J.Overpeck, R.F. Anderson, K.M. and Williams, 1996: The potential for palaeoclimate records from varved Arctic lake sediments: Baffin Island, Eastern

Canadian Arctic. In: *Lacustrine Environments. Palaeoclimatology and Palaeoceanography from Laminated Sediments* [Kemp, A.E.S. (ed.)]. Geological Society, London, Special Publications 116, pp. 57-71.

Hughes, M.K. and H.F. Diaz, 1994: Was there a ‘Medieval Warm Period’ and if so, where and when? *Journal of Climatic Change*, **265**, 109-142.

Huybers, P., 2006: Early Pleistocene glacial cycles and the integrated summer insolation forcing. *Science*, *313*, 508-511.

Hyvärinen, H., 1976: Flandrian pollen deposition rates and tree-line history in northern Fennoscandia. *Boreas,* **5(3),** 163-175.

Ilyashuk, E.A, B.P. Ilyashuk, D. Hammarlund, and I. Larocque, 2005: Holocene climatic and environmental changes inferred from midge records (Diptera: Chironomidae, Chaoboridae, Ceratopogonidae) at Lake Berkut, southern Kola Peninsula, Russia. *Holocene*, **15**, 897-914.

Imbrie, J. and N.G. Kipp, 1971: A new micropaleontological method for Quantitative Paleoclimatology: Application to a late Pleistocene Caribbean Core. In: *The Late Cenozoic Glacial Age*,. [Turekian, K.K. (ed.)]. Yale Univeristy Press, New Haven, CT, pp. 71-181.

Imbrie, J., A. Berger, E.A. Boyle, S.C. Clemens, A. Duffy, W.R. Howard, G. Kukla, J. Kutzbach, D.G. Martinson, A. McIntyre, A.C. Mix, B. Molfino, J.J. Morley, L.C. Peterson, N.G. Pisias, W.L. Prell, M.E. Raymo, N.J. Shackleton, and J.R. Toggweiler, 1993: On the structure and origin of major glaciation cycles. 2. The 100,000-year cycle. *Paleoceanography*, **8**, 699-735.

IPCC, 1990: *Climate Change: The IPCC scientific assessment*, [Houghton,J.T., G.J. Jenkins, and J.J. Ephraums, (eds.)]. Cambridge University Press, Camridge.

IPCC, 2007: Summary for Policymakers. In: *Climate Change 2007: The Physical Science Basis — Contribution of Working Group I to the Fourth Assessment Report of the Intergovernmental Panel on Climate Change*, [Solomon, S., D. Qin, M. Manning, Z. Chen, M. Marquis, K.B. Averyt, M.Tignor and H.L. Miller (eds.)]. Cambridge University Press, Cambridge, United Kingdom and New York, 996 pp.

Iversen, J., 1944: *Viscum*, *Hedera* and *Ilex* as climatic indicators. A contribution to the study of past-glacial temperature climate. Geologiska Foreningens Forhandlingar, .**66**, 463-483.

Jacoby, G.C. and R.D. D'Arrigo, 1995: Tree ring width and density evidence of climatic and potential forest change in Alaska. *Global Biogeochemical Cycles*, **9(2)**, 227-234.

Jakobsson, M., and R. Macnab, 2006: A comparison between GEBCO sheet 5.17 and the International Bathymetric Chart of the Arctic Ocean (IBCAO) version 1.0. *Marine Geophysical Researches*, **27(1),** 35-48.

Jakobsson, M., R. Løvlie, H. Al-Hanbali, E. Arnold, J. Backman, and M. Mörth, 2000: Manganese color cycles in Arctic Ocean sediments constrain Pleistocene chronology. *Geology*, **28**, 23-26.

Jansen, E., E. Bleil, R. Henrich, L. Kringstad, and B. Slettemark, B., 1988: Paleoenvironmental changes in the Norwegian Sea and the northeast atlantic during the last 2.8 m.y.: deep sea drilling project/ocean drilling program sites 610, 642, 643 and 644. *Paleoceanography,* **3,** 563-581.

Jansen, E., J. Overpeck, K.R. Briffa, J.-C. Duplessy, F. Joos, V. Masson-Delmotte, D. Olago, B. Otto-Bliesner, W.R. Peltier, S. Rahmstorf, R. Ramesh, D. Raynaud, D. Rind, O. Solomina, R. Villalba, and D. Zhang, 2007: Palaeoclimate. In: *Climate Change 2007—The Physical Science Basis. Contribution of Working Group I to the Fourth Assessment Report of the Intergovernmental Panel on Climate Change*, [Solomon, S., D. Qin, M.

Manning, Z. Chen, M. Marquis, K.B. Averyt, M. Tignor, and H.L. Miller (eds.)]. Cambridge University Press, Cambridge, U.K., and New York.

Jenkyns, H.C., A. Forster, S. Schouten, and J.S. Sinninghe Damsté, 2004: High temperatures in the Late Cretaceous Arctic Ocean. *Nature*, **432(7019)**, 888-892.

Jennings, A., K. Knudsen, M. Hald, C. Hansen, and J. Andrews, 2002: A mid-Holocene shift in Arctic sea-ice variability on the East Greenland Shelf. *The Holocene*, **12**, 49-58.

Jiang D., H. Wang, Z. Ding, X. Lang, H. Drange, 2005: Modeling the middle Pliocene climate with a global atmospheric general circulation model. *Journal of Geophysical Research,* **110**, D14107, doi:10.1029/2004JD005639.

Johnsen, S., H. Clausen, W. Dansgaard, K. Fuhrer, N. Gundestrup, C. Hammer, P. Iversen, J. Jouzel, B. Stauffer, and J. Steffensen, 1992: Irregular glacial interstadials recorded in a new Greenland ice core. *Nature*, **359**, 311-313.

Johnsen, S.J., D. Dahl-Jensen, W. Dansgaard, and N. Gundestrup, 1995: Greenland palaeotemperatures derived from GRIP bore hole temperature and ice core isotope profiles. *Tellus*, **47B**, 624-629.

Johnsen, S.J., W. Dansgaard, and J.W.C. White, 1989: The origin of Arctic precipitation under present and glacial conditions. *Tellus*, **41B**, 452-468.

Jones, P.D., K.R. Briffa, T.P. Barnett, and S.F.B. Tett, 1998: High-resolution palaeoclimatic records for the last millennium: interpretation, integration and comparison with General Circulation Model control-run temperatures. *Holocene*, **8**, 455-471.

Jouzel, J., V. Masson-Delmotte, O. Cattani, G. Dreyfus, S. Falourd, G. Hoffmann, B. Minster, J. Nouet, J. M. Barnola, J. Chappellaz, H. Fischer, J.C. Gallet, S. Johnsen, M. Leuenberger, L. Loulergue, D. Luethi, H. Oerter, F. Parrenin, G. Raisbeck, D. Raynaud, A. Schilt, J.

Schwander, E. Selmo, R. Souchez, R. Spahni, B. Stauffer, J.P. Steffensen, B. Stenni, T.F. Stocker, J.L. Tison, M. Werner, and E.W. Wolff, 2007: Orbital and Millennial Antarctic Climate Variability over the Past 800,000 Years. *Science*, **317**, 793-796, doi:10.1126/science.1141038.

Jouzel, J., R.B. Alley, K.M. Cuffey, W. Dansgaard, P. Grootes, G. Hoffmann, S.J. Johnsen, R.D. Koster, D. Peel, C.A. Shuman, M. Stievenard, M. Stuiver, and J. White, 1997: Validity of the temperature reconstruction from water isotopes in ice cores. *Journal of Geophysical Research*, **102**, 26471-26487.

Joynt, E.H., III and A.P. Wolfe, 2001: Paleoenvironmental inference models from sediment diatom assemblages in Baffin Island lakes (Nunavut, Canada) and reconstruction of summer water temperature. *Canadian Journal of Fisheries and Aquatic Sciences*, **58**, 1222-1243.

Kaakinen, A. and M. Eronen, 2000: Holocene pollen stratigraphy indicating climatic and tree-line changes derived from a peat section at Ortino, in the Pechora lowland, northern Russia. *The Holocene*, **10**, 611-620.

Kageyama, M., O. Peyron, S. Pinot, P. Tarasov, J. Guiot, S. Joussaume, and G. Ramstein, 2001: The Last Glacial Maximum climate over Europe and western Siberia: a PMIP comparison between models and data. *Climate Dynamics*, **17**, 23-43.

Kandiano, E.S. and H.A. Bauch, 2007: Phase relationship and surface water mass change in the Northeast Atlantic during Marind Isotope Stage 11 (MIS11). *Quaternary Research*, **68(3),** 445-455

Kaplan, J.O., N.H. Bigelow, P.J. Bartlein, T.R. Christiansen, W. Cramer, S.P. Harrison, N.V. Matveyeva, A.D. McGuire, D.F. Murray, I.C. Prentice, V.Y. Razzhivin, B. Smith, D.A. Walker, P.M. Anderson, A.A. Andreev, L.B. Brubaker, M.E. Edwards, A.V. Lozhkin, and J.C. Ritchie, 2003: Climate change and arctic ecosystems II—Modeling paleodata-model comparisons, and future projections. *Journal of Geophysical Research*, **108(D19)**, *8171*, doi:10.1029/2002JD002559.

Kaplan, M.R. and A.P. Wolfe, 2006: Spatial and temporal variability of Holocene temperature trends in the North Atlantic sector. *Quaternary Research*, **65**, 223-231.

Kapsner, W.R., R.B. Alley, C.A. Shuman, S. Anandakrishnan, and P.M. Grootes, 1995: Dominant influence of atmospheric circulation on snow accumulation in Greenland over the past 18,000 years. *Nature*, **373**, 52-54.

Karlén, W., 1988: Scandinavian glacial and climate fluctuations during the Holocene. *Quaternary Science Reviews*, **7**, 199-209.

Kaspar, F., N. Kühl, U. Cubasch, and T. Litt, 2005: A model-data-comparison of European temperatures in the Eemian interglacial, *Geophysical Research Letters*, **32**, L11703, doi:10.1029/2005GL022456.

Kaufman, D.S., T.A. Ager, N.J. Anderson, P.M. Anderson, J.T. Andrew, P.J. Bartlein, L.B. Brubakerg, L.L. Coats, L.C. Cwynar, M.L. Duvall, A.S. Dyke, M.E. Edwards, W.R. Eisner, K. Gajewski, A. Geirsdóttir, F.S. Hu, A.E. Jennings, M.R. Kaplan, M.W. Kerwin, A.V. Lozhkin, G.M. MacDonald, G.H. Miller, C.J. Mock, W.W. Oswald, B.L. Otto-Bliesver, D.F. Porinchu, K. Ruüland, J.P. Smol, E.J. Steig, and B.B. Wolfe, 2004: Holocene thermal maximum in the western Arctic (0–180°W). *Quaternary Science Reviews*, **23**, 529-560.

Kaufman, D.S. and J. Brigham-Grette, 1993: Aminostratigraphic correlations and paleotemperature implications, Pliocene-Pleistocene high sea level deposits, northwestern Alaska. *Quaternary Science Reviews*, **12**, 21-33.

Kellogg, T.B., 1977: Paleoclimatology and paleo-oceanography of the Norwegian and Greenland seas: the last 450,000 years. *Marine Micropaleontology*, **2,** 235-249.

Kerwin, M., J.T. Overpeck, R.S. Webb, A. DeVernal, D.H. Rind and R.J. Healy, 1999: The role of oceanic forcing in mid-Holocene northern hemisphere climatic change. *Paleoceanography* **14**, 200-210.

Kirk-Davidov, D.B., D.P. Schrag, and J.G. Anderson, 2002: On the feedback of stratospheric clouds on polar climate. *Geophysical Research Letters*, **29(11)**, 1556.

Kitoh, A.. and S. Murakami, 2002: Tropical Pacific Climate at the mid-Holocene and the Last Glacial Maximum simulated by a coupled ocean-atmosphere general circulation model, *Paleoceanography*, **17**, 1-13

Knutson, T.R., T.L. Delworth, K.W. Dixon, I.M. Held, J. Lu, V. Ramaswamy, M.D. Schwarzkopf, G. Stenchikov, and R.J. Stouffer, 2006: Assessment of twentieth-century regional surface temperature trends using the GFDL CM2 coupled models. *Journal of Climate*, **19(9)**, 1624-1651.

Koç, N. and E. Jansen, 1994: Response of the high-latitude Northern Hemisphere to climate forcing—Evidence from the Nordic Seas. *Geology*, **22**, 523-526.

Koç, N., E. Jansen, and H. Haflidason, 1993: Paleooceanographic reconstruction of surface ocean conditions in the Greenland, Iceland and Norwegian Seas through the last 14 ka based on diatoms. *Quaternary Science Reviews*, **12**, 115-140.

Koerner, R.M., 2005: Mass Balance of glaciers in the Queen Elizabeth Islands, Nunavut, Canada. *Annals of Glaciology,* **42(1),** 417-423.

Koerner, R.M. and D.A. Fisher, 1990: A record of Holocene summer climate from a Canadian high-Arctic ice core. *Nature*, **343**, 630-631.

Korhola, A., H. Olander, and T. Blom, 2000: Cladoceran and chironomid assemblages as quantitative indicators of water depth in sub-Arctic Fennoscandian lakes. *Journal of Paleolimnology*, **24**, 43-54.

K**orty**, R.L., K.A. Emanuel, and J.R. Scott, 2008: Tropical cyclone-induced upper-ocean mixing and climate: Application to equable climates. *Journal of Climate,* **21(4)**, 638-654.

Kremenetski, C.V., L.D. Sulerzhitsky, and R. Hantemirov, 1998: Holocenehistory of the northern range limits of some trees and shrubs in Russia. *Arctic and Alpine Research,* **30**, 317-333.

Kukla, G.J., 2000: The last interglacial. *Science,* **287**, 987–988.

Kump, L.R. and D. Pollard, 2008: Amplification of Cretaceous Warmth by Biological Cloud Feedbacks. *Science,* **11,(5873)**, 195, doi:10.1126/science.1153883.

Kvenvolden, K.A., 1988: Methane hydrate—a major reservoir of carbon in the shallow geosphere? *Chemical Geology,* **71**, 41–51.

Kvenvolden, K.A., 1993: A primer on gas hydrates. In: *The Future of Energy Gases*, [Howel, D.G. (Ed)]. U.S. Geological Survey Professional Paper 1570, pp. 279-291.

Lamb, H.H., 1977: *Climate History and the Future. Climate—Past, Present and Future*. Metheun, London, vol. 2, 835 pp.

Lambeck, K., Y. Yokoyama, and T. Purcell, 2002: Into and out of the Last Glacial Maximum: sea-level change during oxygen isotope stages 3 and 2. *Quaternary Science Reviews*, **21**, 343-360.

Larocque, I. and R.I. Hall, 2004: Holocene temperature estimates and chironomid community composition in the Abisko Valley, northern Sweden. *Quaternary Science Reviews*, **23**, 2453-2465.

Lauritzen, S.-E., 1996: Calibration of speleothem stable isotopes against historical records: a Holocene temperature curve for north Norway?. In: *Climatic Change: the Karst Record* [Lauritzen, S.-E. (Ed.)] Vol. 2 Karst Waters Institute Special Publication, Charles Town, West Virginia, pp. 78-80.

Lauritzen, S.E. and J. Lundberg, 1998: Rapid temperature variations and volcanic events during the Holocene from a Norwegian speleothem record. Past Global Changes and their Significance for the Future. Volume of Abstracts, IGBP-PAGES, Bern 00, p. 88.

LeGrande, A.N., and G.A. Schmidt, 2006: Global gridded data set of the oxygen isotopic composition in seawater. *Geophysical. Research Letters*, **33**, L12604, doi:10.1029/2006GL026011.

Lemke, P., J. Ren, R.B. Alley, I. Allison, J. Carrasco, G. Flato, Y. Fujii, G. Kaser, P. Mote, R.H. Thomas, and T. Zhang, 2007: Observations: Changes in Snow, Ice and Frozen Ground. In: *Climate Change 2007: The Physical Science Basis—. Contribution of Working Group I to the Fourth Assessment Report of the Intergovernmental Panel on Climate Change*, [Solomon, S., D. Qin, M. Manning, Z. Chen, M. Marquis, K.B. Averyt, M. Tignor and H.L. Miller (eds.)]. Cambridge University Press, Cambridge and New York, 996 pp.

Leng, M.J. and J.D. Marshall, 2004: Palaeoclimate interpretation of stable isotope data from lake sediment archives. *Quaternary Science Reviews*, **23**, 811-831.

Levac, E., A. de Vernal, and W.J. Blake, 2001: Sea-surface conditions in northernmost Baffin Bay during the Holocene—Palynological evidence. *Journal of Quaternary Science*, **16**, 353-363.

Levy, L.B., D.S. Kaufman, and A. Werner, 2003: Holocene glacier fluctuations, Waskey Lake, northeastern Ahklun Mountains, southwestern Alaska. *Holocene*, **14**, 185-193.

Ling, F. and T.J. Zhang, 2007: Modeled impacts of changes in tundra snow thickness on ground thermal regime and heat flow to the atmosphere in Northernmost Alaska. *Global and Planetary Change* **57(3-4)**, 235-246.

Lisiecki, L.E. and M.E. Raymo, 2005: A Pliocene-Pleistocene stack of 57 globally distributed benthic d^{18}O records. *Paleoceanography*, **20**, PA1003, doi:10.1029/2004PA001071.

Lisiecki, L.E. and M.E. Raymo, 2007: Plio-Pleistocene climate evolution—Trends and transitions in glacial cycle dynamics. *Quaternary Science Reviews*, **26**, 56-69.

Loutre, M.F., 2003: Clues from MIS 11 to predict the future climate – a modeling point of view. *Earth and Planetary Science Letters*, **212(1-2),** 213-224

Lozhkin, A.V. and P.M. Anderson, 1995: The last interglaciation of northeast Siberia. *Quaternary Research*, **43,** 147-158.

Lozhkin, A.V. and P,M. Anderson, 1996: A late Quaternary pollen record from Elikchan 4 Lake, northeast Siberia. *Geology of the Pacific Ocean,* **12**, 6-9-616.

Lozhkin, A.V., P.M. Anderson, W.R. Eisner, L.G. Ravako, D.M. Hopkins, L.B. Brubaker, P.A. Colinvaux, and M.C. Miller, 1993: Late Quaternary lacustrine pollen records from southwestern Beringia. *Quaternary Research,* **9**, 314-324.

Lozhkin, A.V., P.M. Anderson, T.V. Matrosova, and P.S. Minyuk, 2007: The pollen record from El'gygytgyn Lake: implications for vegetation and climate histories of northern Chukotka since the late middle Pleistocene. *Journal of Paleolimnology,* **37(1),** 135-153.

Lubinski, D.J., S.L. Forman, and G.H. Miller, 1999: Holocene glacier and climate fluctuations on Franz Josef Land, Arctic Russia, 80°N. *Quaternary Science Reviews*, **18**, 85-108.

Luckman, B.H., 2007: Dendroclimatology. In: *Encyclopedia of Quaternary Science* [Elias, S.

(ed.)] **1**, 465-475.

MacDonald, G.J., 1990: Role of methane clathrates in past and future climates. *Climatic Change*, **16(3)** 247-281.

MacDonald, G.M., T. Edwards, K. Moser, and R. Pienitz, 1993: Rapid response of treeline vegetation and lakes to past climate warming. *Nature*, **361**, 243-246.

MacDonald, G.M., B.R. Gervais, J.A. Snyder, G.A. Tarasov, and O.K. Borisova, 2000a: Radiocarbon dated *Pinus sylvestris* L. wood from beyond treeline on the Kola Peninsula, Russia. *The Holocene*, **10**, 143-147.

MacDonald, G.M., K.V. Kremenetski, and D.W. Beilman, D.W., 2007: Climate change and the northern Russian treeline zone. *Philosophical Transactions of the Royal Society B*, doi:10.1098/rstb.2007.2200.

MacDonald, G.M., A.A. Velichko, C.V. Kremenetski, O.K. Borisova, A.A. Goleva, A.A. Andreev, L.C. Cwynar, R.T. Riding, S.L. Forman, T.W.D. Edwards, R. Aravena, D. Hammarlund, J.M. Szeicz,and V.N. Gattaulin, 2000b: Holocene treeline history and climate change across northern Eurasia. *Quaternary Research*, **53**, 302-311.

Macdonald, R.W. and J.M. Bewers, 1996: Contaminants in the arctic marine environment: priorities for protection. *ICES Journal of Marine Science,* **53**, 537-563.

Mahowald, N. M., D. R. Muhs, S. Levis, P. J Rasch, M. Yoshioka, C. S. Zender, and C. Luo, 2006: Change in atmospheric mineral aerosols in response to climate: Last glacial period, preindustrial, modern, and doubled carbon dioxide climates, *ournal of. Geophysical Research*, **111**, D10202, doi:10.1029/2005JD006653

Manabe, S. and R.J. Stouffer, 1980: Sensitivity of a global climate model to an increase of CO_2 in the atmosphere. *Journal of Geophysical Research*, **85(C10)**, 5529-5554.

Mann, M.E., R.S. Bradley, and M.K. Hughes, 1998: Global-scale temperature patterns and climate forcing over the past six centuries. *Nature,* **392**, 779-787.

Mann, D.H., D.M. Peteet, R.E. Reanier, and M.L. Kunz, 2002: Responses of an arctic landscape to Late glacial and early Holocene climatic changes: The importance of moisture: *Quaternary Science Reviews*, **21**, 997-1021, doi: 10.1016/S0277-3791(01)00116-0.

Mann, M.E., and P.D. Jones,2003: Global surface temperatures over the past two millennia. *Geophysical Research Letters,* **30(15)**, 1820, doi:10.1029/2003GL017814

Mann, M.E., A. Zhang, M.K. Hughes, R.S. Bradley, S.K. Miller, S. Rutherford, and S. Ni, F., **in press**: Proxy-based Reconstructions of Hemispheric and Global Surface Temperature Variations over the past Two Millennia. *Proceedings of the National Academy of Sciences.*

Marchant, D.R., and G.H. Denton, 1996: Miocene and Pliocene paleoclimate of the Dry Valleys region, southern Victoria Land: A geomorphological approach. *Marine Micropaleontology,* **27,** 253-271.

Marincovitch, L., Jr. and A.Y. Gladenkov, 2000: New evidence for the age of Bering Strait. *Quaternary Science Reviews,* **20(1-3),** 329-335.

Marlowe I.T., J.C. Green, A.C. Neal, S.C. Brassell, G. Eglinton, P.A. Course, 1984: Long-chain (N-C37-C39) alkenones in the prymnesiophyceae - distribution of alkenones and other lipids and their taxonomic significance. *British Phycological Journal,* **19(3),** 203-216.

Marotzke, J., 2000: Abrupt climate change and thermohaline circulation—Mechanisms and predictability. *Proceedings of the National Academy of Sciences, U.S.A.,* **97(4)**, 1347-1350.

Marshall, S.J. and P.U. Clark, 2002: Basal temperature evolution of North American ice sheets and implications for the 100-kyr cycle. *Geophysical Research Letters*, **29(24),** 2214.

Martinson, D.G. and M. Steele, 2001: Future of the Arctic sea ice cover—Implications of an Antarctic analog. *Geophysical Research Letters*, **28**, 307-310.

Masson-Delmotte, V., J. Jouzel, A. Landais, M. Stievenard, S.J. Johnsen, J.W.C. White, M.A. Werner, A. Sveinbjornsdottir, and K. Fuhrer, 2005: GRIP deuterium excess reveals rapid and orbital-scale changes in Greenland moisture origin. *Science*, **309**, 118-121.

Mathieu, R., D. Pollard, J.E. Cole, J.W.C. White, R.S. Webb, and S.L. Thompson, 2002: Simulation of stable water isotope variations by the GENESIS GCM for modern conditions. *Journal of Geophysical Research*, **107**, doi:10.1029/2001JD900255.

Matthews, J.V., Jr., C.E. Schweger, and J. Janssens, 1990: The last (Koy-Yukon) interglaciation in the northern Yukon—Evidence from unit 4 at Chijee's Bluff, Bluefish Basin. *Geographie physique et Quaternaire*, **44**, 341-362.

Mayewski, P.A., L.D. Meeker, M.S. Twickler, S.I. Whitlow, Q. Yang, W.B. Lyons, and M. Prentice, 1997: Major features and forcing of high-latitude Northern Hemisphere atmospheric circulation using a 110,000-year-long glaciochemical series. *Journal of Geophysical Research*, **102**, 26,345-26,366.

Maximova, L.N. and V.E. Romanovsky, 1988: A hypothesis of the Holocene permafrost evolution. *Proceedings of the Fifth International Conference on Permafrost*, Norwegian Institute of Technology, Trondheim, Norway, 102-106.

McGhee, R., 2004: *The last imaginary place; a human history of the Arctic world*. Key Porter, Ontario, 296 pp.

McKenna, M.C., 1980. Eocene paleolatitude, climate and mammals of Ellesmere Island. *Paleogeography, Paleoclimatology and Paleoecology*, **30**, 349-362.

McLaughlin, F., E. Carmack, R. Macdonald, A.J. Weaver, and J. Smith, 2002: The Canada Basin, 1989–1995—Upstream events and far-field effects of the Barents Sea. *Journal of Geophysical Research*, **107(C7)**, 3082, doi:10.1029/2001JC000904.

McManus, J.F., 2004: A great grand-daddy of ice cores. *Nature*, **429**, 611-612.

Meehl, G.A., T.F. Stocker, W.D. Collins, P. Friedlingstein, A.T. Gaye, J.M. Gregory, A. Kitoh, R. Knutti, J.M. Murphy, A. Noda, S.C.B. Raper, I.G. Watterson, A.J. Weaver and Z.-C. Zhao, 2007: Global Climate Projections. In: *Climate Change 2007: The Physical Science Basis — Contribution of Working Group I to the Fourth Assessment Report of the Intergovernmental Panel on Climate Change*, [Solomon, S.,D. Qin, M. Manning, Z. Chen, M. Marquis, K.B. Averyt, M. Tignor and H.L. Miller (eds.)]. Cambridge University Press, Cambridge, United Kingdom and New York, pp. 747-845.

Meeker, L.D. and P.A. Mayewski, 2002: A 1400-year high-resolution record of atmospheric circulation over the North Atlantic and Asia. *Holocene*, **12**, 257-266.

Meier, M.F., M.B. Dyurgerov, U.K. Rick, S. O'Neel, W.T. Pfeffer, R.S. Anderson, S.P. Anderson, and A.F. Glazovsky, 2007: Glaciers Dominate Eustatic Sea-Level Rise in the 21st Century. *Science*, **317(5841)**, 1064-1067 doi: 10.1126/science.1143906

Miller, G.H., A.P. Wolfe, J.P. Briner, P.E. Sauer, and A. Nesje, 2005: Holocene glaciation and climate evolution of Baffin Island, Arctic Canada. *Quaternary Science Reviews*, **24**, 1703-1721.

Moberg, A., D.M. Sonechkin, K. Holmgren, N.M. Datsenko, and W. Karlen, 2005: Highly variable northern hemisphere temperatures reconstructed from low- and high-resolution proxy data. *Nature*, **433**, 613-617.

Montoya, M., H. von Storch, and T.J. Crowley, 2000: Climate Simulation for 125 kyr BP with a Coupled Ocean–Atmosphere General Circulation Model. *Journal of Climate*, **13**, 1057-1072.

Moran, K., J. Backman, H. Brinkhuis, S.C. Clemens, T. Cronin, G.R. Dickens, F. Eynaud, J. Gattacceca, M. Jakobsson, R.W. Jordan, M. Kaminski, J. King, N. Koc, A. Krylov, N. Martinez, J. Matthiessen, D. McInroy, T.C. Moore, J. Onodera, M. O'Regan, H. Palike, B. Rea, D. Rio, T. Sakamoto, D.C. Smith, R. Stein, K. St. John, I. Suto, N. Suzuki, K. Takahashi, M. Watanabe, M. Yamamoto, J. Farrell, M. Frank, P. Kubik, W. Jokat, and Y. Kristoffersen, 2006: The Cenozoic palaeoenvironment of the Arctic Ocean. *Nature*, **441**, 601-605.

Morison, J., K. Aagaard, and M. Steele, 2000: Recent environmental changes in the arctic. *Arctic*, **53(4)**, 359-371.

Muhs, D.R. and J.R. Budahn, 2006: Geochemical evidence for the origin of late Quaternary loess in central Alaska. *Canadian Journal of Earth Science*, **43**, 323-337

Muller, P.J., G. Kirst, G. Ruhland, I. von Storch, and A. Rossell-Mele, 1998: Calibration of the alkenone paleotemperature index UkÌ37 based on core-tops from the eastern South Atlantic and the global ocean (60°N–60°S). *Geochimica et Cosmochimica Acta*, **62**, 1757-1772.

National Research Council, 2006: *Surface temperature reconstructions for the last 2,000 years.* National Academies Press, Washington, DC. 160pp.

Naurzbaev, M.M., E.A. Vaganov, O.V. Sidorova, and F.H. Schweingruber, 2002: Summer temperatures in eastern Taimyr inferred from a 2427-year late-Holocene tree-ring chronology and earlier floating series. *The Holocene*, **12**, 727-736.

Nelson, R.E., and Carter, L.D. 1991. Preliminary interpretation of vegetation and paleoclimate in northern Alaska during the late Pliocene Colvillian marine transgression. In: *Geologic studies in Alaska*, [Bradley, D.C. and A.B. Ford (eds.)]. U.S.Geological Survey Bulletin 1999, pp. 219-222.

Nesje, A., J. Bakke, S.O. Dahl, O. Lie, and J.A. Matthews, 2008: Norwegian mountain glaciers in the past, present and future. *Global and Planetary Change*, **60**, 10-27.

Nesje, A. , J.A. Matthews, S.O. Dahl, M.S. Berrisford, and C. Andersson, 2001: Holocene glacier fluctuations of Flatebreen and winter precipitation changes in the Jostedalsbreen region, western Norway, based on glaciolacustrine records. *The Holocene*, **11,** 267-280.

Nørgaard-Pedersen, N., N. Mikkelsen, and Y. Kristoffersen, 2007a: Arctic Ocean record of last two glacial-interglacial cycles off North Greenland/Ellesmere Island—Implications for glacial history. *Marine Geology*, **244(2007)**, 93-108.

Nørgaard-Pedersen, N., N. Mikkelsen, S.J. Lassen, Y. Kristoffersen, and E. Sheldon, 2007b: Reduced sea ice concentrations in the Arctic Ocean during the last interglacial period revealed by sediment cores off northern Greenland. *Paleoceanography*, **22**, PA1218, doi:10.1029/2006PA001283.

Nørgaard-Pedersen, N., R.F. Spielhagen, H. Erlenkeuser, P.M. Grootes, J. Heinemeier, and J. Knies, 2003: The Arctic Ocean during the Last Glacial Maximum—Atlantic and polar domains of surface water mass distribution and ice cover. *Paleoceanography*, **18**, 8-1 to 8-19.

Nørgaard-Pedersen, N., R.F. Spielhagen, J. Thiede, and H. Kassens, 1998: Central Arctic surface ocean environment during the past 80,000 years. *Paleoceanography*, **13**, 193-204.

Nürnberg, D. and R. Tiedemann, 2004: Environmental changes in the Sea of Okhotsk during the last 1.1 million years. *Paleoceanography*, **19**, PA4011.

O'Brien, S.R., P.A. Mayewski, L.D. Meeker, D.A. Meese, M.S. Twickler, and S.I.Whitlow, 1995: Complexity of Holocene climate as reconstructed from a Greenland ice core. *Science,* **270**, 1962-1964.

Obata, A., 2007: Climate-carbon cycle model response to freshwater discharge into the North Atlantic. *Journal of Climate*, **20(24)** 5962-5976.

Ogilvie, A.E.J. and T. Jónsson, 2001: "Little Ice Age" Research: A Perspective from Iceland. *Climate Change,* **48**, 9-52.

Ogilvie, A.E.J. and I. Jónsdóttir, 2000. Sea ice, climate and Icelandic fisheries in historical times. *Arctic,* **53(4)**, 383-394.

Ohkouchi, N., T.I. Eglinton, L.D. Keigwin, and J.M. Hayes, 2002: Spatial and temporal offsets between proxy records in a sediment drift. *Science*, **298**, 1224-1227.

Oswald, W.W.,L.B. Brubaker, and P.M. Anderson, 1999, Late Quaternary vegetational history of the Howard Pass area, northwestern Alaska. *Canadian Journal of Botany,* **77(4)**, 570-581

Oswald, W.W., L.B. Brubaker, F.S. Hu, and G.W. Kling, 2003: Holocene pollen records from the central Arctic Foothills, northern Alaska—Testing the role of substrate in the response of tundra to climate change. *Journal of Ecology*, **91**, 1034-1048

Otto-Bliesner, B.L., C.D. Hewitt, T.M. Marchitto, E. Brady, A. Abe-Ouchi, M. Crucifix, S. Murakami, and S.L. Weber, 2007: Last Glacial Maximum ocean thermohaline circulation: PMIP2model inter-comparisons and data constraints. *Geophysical Research Letters*, **34**, L12706, doi:10.1029/2007GL029475.

Otto-Bliesner, B.L., S.J. Marshall, J.T. Overpeck, G.H. Miller, A. Hu, and CAPE Last Interglacial Project members, 2006, Simulating Arctic climate warmth and icefield retreat in the Last Interglaciation. *Science*, **311**, 1751-1753, doi:10.1126/science.1120808

Overpeck, J., K. Hughen, D. Hardy, R. Bradley, R. Case, M. Douglas, B. Finney, K. Gajewski, C. Jacoby, A. Jennings, S. Lamoureux, A. Lasca, G. MacDonald, J. Moore, M. Retelle, S. Smith, A. Wolfe, and G. Zielinski, 1997: Arctic environmental change of the last four centuries. *Science*, **278**, 1251-1256.

Pagani, M., K. Caldeira, D. Archer, and J.C. Zachos, 2006: An Ancient Carbon Mystery. *Science*, **314**, 1556 - 1557 doi: 10.1126/science.1136110

Pearson, P.N., B.E. van Dongen, C.J. Nicholas, R.D. Pancost, S. Schouten, J.M. Singano, and B.S. Wade, 2007: Stable warm tropical climate through the Eocene Epoch. *Geology*, 35, 211-214.

Peterson, B.J., R.M. Holmes, J.W. McClelland, C.J. Vorosmarty, R.B. Lammers, A.I. Shiklomanov, I.A. Shiklomanov, and S. Rahmstorf, 2002: Increasing river discharge to the Arctic Ocean. *Science*, **298**, 2171-2173.

Peterson, B.J., J. McClelland, R. Murry, R.M. Holmes, J.E. Walsh, and K. Aagaard, 2006: Trajectory shifts in the Arctic and subarctic freshwater cycle. *Science*, **313**, 1061-1066.

Pienitz, R., M.S.V. Douglas, and J.P. Smol (eds.), 2004: *Long-Term Environmental Change in Arctic and Antarctic Lakes*. Dordrecht, Germany: Springer, 579 pp.

Pienitz, R. and J.P. Smol, 1993: Diatom assemblages and their relationship to environmental variables in lakes from the boreal forest-tundra ecotone near Yellowknife, Northwest-Territories, Canada. *Hydrobiologia*, **269,** 391-404.

Pienitz, R., J.P. Smol, W.M. Last, P.R. Leavitt, and B.F. Cumming, 2000: Multi-proxy Holocene palaeoclimatic record from a saline lake in the Canadian Subarctic. *The Holocene,* **10(6)**, 673-686 doi:10.1191/09596830094935

Pierrehumbert, R.T., H. Brogniez, and R. Roca, 2007: On the relative humidity of the atmosphere. In: *The Global Circulation of the Atmosphere* [Schneider, T. and A. Sobel (eds.)]. Princeton University Press, Princeton, New Jersey, pp.143-185.

Peixoto, J.P. and A.H. Oort, 1992: *Physics of Climate*. American Institute of Physics, New York, 520 pp.

Pinot, S., G. Ramstein, S.P. Harrison, I.C. Prentice, J. Guiot, M. Stute. and S. Joussaume, 1999: Tropical paleoclimates of the Last Glacial Maximum: comparison of Paleoclimate Modelling Intercomparison Project (PMIP) simulations and paleodata. *Climate Dynamics,* **15**, 857-874.

Pisaric, M.F J., G.M. MacDonald, A.A Velichko, and L.C. Cwynar, 2001: The late-glacial and post-glacial vegetation history of the northwestern limits of Beringia, from pollen, stomates and tree stump evidence. *Quaternary Science Reviews,* **20,** 235-245.

Pollard, D. and S.L. Thompson, 1997: Climate and ice-sheet mass balance at the Last Glacial Maximum from the GENESIS Version 2 global climate model. *Quaternary Science Reiews,* **16**, 841-864

Polyak, L., W.B. Curry, D.A. Darby, J. Bischof, and T.M. Cronin, 2004: Contrasting glacial/interglacial regimes in the western Arctic Ocean as exemplified by a sedimentary record from the Mendeleev Ridge. *Palaeogeography, Palaeoclimatology, Palaeoecology,* **203**, 73-93.

Porter, S.C. and G.H. Denton, 1967: Chronology of neoglaciation. *American Journal of Science,* **165**, 177-210.

Poulsen, C.J., E.J. Barron, W.H. Peterson, and P.A. Wilson, 1999: A reinterpretation of mid-Cretaceous shallow marine temperatures through model-data comparison. *Paleoceanography,* **14(6)** 679-697.

Prahl, F.G., G.J. de Lange, M. Lyle, and M.A. Sparrow, 1989: Post-depositional stability of long-chain alkenones under contrasting redox conditions. *Nature*, **341**, 434-437.

Prahl, F.G., L.A. Muelhausen, and D.L. Zahnle, 1988: Further evaluation of long-chain alkenones as indicators of paleoceanographic conditions. *Geochimica et Cosmochimica Acta*, **52**, 2303-2310.

Prentice, I.C. and T. Webb III, 1998: BIOME 6000—Reconstructing global mid-Holocene vegetation patterns from palaeoecological records. *Journal of Biogeography*, **25**, 997-1005.

Rahmstorf, S., 1996: On the freshwater forcing and transport of the Atlantic thermohaline circulation. *Climate Dynamics*, **12**, 799-811.

Rahmstorf, S., 2002: Ocean circulation and climate during the past 120,000 years. *Nature*, **419**, 207-214.

Rasmussen, S.O., K.K. Andersen, A.M. Svensson, J.P. Steffensen, B.M. Vinther, H.B. Clausen, M.L. Siggaard-Andersen, S.J. Johnsen, L.B. Larsen, D. Dahl-Jensen, M. Bigler, R. Rothlisberger, H. Fischer, K. Goto-Azuma, M.E. Hansson, and U. Ruth, 2006: A new Greenland ice core chronology for the last glacial termination. *Journal of Geophysical Research*, **111**, D061202, doi:10.1029/2005JD006079.

Raymo, M.E., 1994: The initiation of northen hemisphere glaciation. *Annual Review of Earth and Planetary Sciences,* **22,** 353-383, doi:10.1146/annurev.ea.22.050194.002033

Raymo, M. E., 1997: The timing of major climate terminations, *Paleoceanography*, **12**, 577-585.

Raymo, M.E., B. Grant, M. Horowitz, and G.H. Rau, 1996: Mid-Pliocene warmth—Stronger greenhouse and stronger conveyer. *Marine Micropaleontology,* **27**, 313-326.

Raymo, M.E., L.E. Lisiecki, and K.H. Nisancioglu, 2006: Plio-Pleistocene ice volume, Antarctic climate, and the global δ^{18}O record. *Science*, **313**, 492-495.

Raymo, M.E., D.W. Oppo, and W. Curry, 1997: The mid-Pleistocene climate transition: A deep sea carbon isotopic perspective: *Paleoceanography*, **12,** 546-559.

Renssen, H., E. Driesschaert, M.F. Loutre, and T. Fichefet, 2006: On the importance of initial conditions for simulations of the Mid-Holocene climate. *Climate of the Past,* **2**, 91-97.

Renssen, H., H. Goosse, T. Fichefet, V. Brovkin, E. Dresschaert, and F. Wolk, 2005: Simulating the Holocene climate evolution at northern high latitudes using a coupled atmosphere–sea ice–ocean–vegetation model. *Climate Dynamics*, **24**, 23-43.

Reyes, A.V., G.C. Wiles, D.J. Smith, D.J. Barclay, S. Allen, S. Jackson, S. Larocque, S. Laxton, D. Lewis, P.E. Calkin, and J.J. Clauge, 2006: Expansion of alpine glaciers in Pacific North America in the first millennium A.D. *Geology,* **34**, 57-60.

Rignot, E. and R.H. Thomas, 2002: Mass balance of polar ice sheets. *Science* **297**, 1502-1506.

Rigor, I.G. and J.M. Wallace, 2004: Variations in the age of Arctic sea-ice and summer sea-ice extent. *Geophysical Research Letters*, **31**, L09401, doi:10.1029/2004GL019492.

Rimbu, N., G. Lohmann, and K. Grosfeld, 2007: Northern Hemisphere atmospheric blocking in ice core accumulation records from northern Greenland. *Geophysical Research Letters*, **34**, L09704, doi:10.1029/2006GL029175.

Ritchie, J.C., 1984: *Past and Present Vegetation of the Far Northwest of Canada*. University of

Toronto Press, Toronto, 251 pp.

Ritchie, J.C., L.C. Cwynar, and R.W. Spear, 1983: Evidence from northwest Canada for an early Holocene Milankovitch thermal maximum. *Nature,* **305,** 126-128.

Rivers, A.R., and A.H. Lynch, 2004: On the influence of land cover on early Holocene climate in northern latitudes. *Journal of Geophysical Research-Atmospheres,* **109(D21)**, D21114.

Roe, G.H. and M.R. Allen, 1999: A comparison of competing explanations for the 100,000-yr ice age cycle. *Geophysical Research Letters*, **26(15),** 2259-2262.

Rosell-Mele, A. and P. Comes, 1999: Evidence for a warm Last Glacial Maximum in the Nordic sea or an example of shortcomings in Uk37Ì and Uk37 to estimate low sea surface temperature? *Paleoceanography*, **14**, 770-776.

Rosell-Mele, A., G. Eglinton, U. Pflaumann, and M. Sarnthein, 1995: Atlantic core top calibration of the Uk37 index as a sea-surface temperature indicator. *Geochimica et Cosmochimica Acta*, **59**, 3099-3107.

Royer, D.L., 2006: CO2-forced climate thresholds during the Phanerozoic. *Geochimica et Cosmochimica Acta*, **70(23),** 5665-5675.

Royer, D.L., R.A. Berner, and J. Park, 2007: Climate sensitivity constrained by CO_2 concentrations over the past 420 million years. *Nature*, **446**, 530-532.

Ruddiman, W.F., 2003: Insolation, Ice Sheets and Greenhouse Gases. *Quaternary Science Reviews,* **22**, 1597.

Ruddiman, W.F., 2006: Ice-driven CO2 feedback on ice volume. *Climate of the Past*, **2**, 43-55.

Ruddiman, W.F.,N.J. Shackleton, and A. McIntyre, 1986: North Atlantic sea-surface temperatures for the last 1.1 million years. In: *North Atlantic Paleoceanography,* [Summerhayes, C.P. and N.J. Shackleton, (eds.)]. Geological Society of London, Special Publication, **21**, 155-173.

Rudels, B., L.G. Anderson, E.P. Jones, and G. Kattner, 1996: Formation and evolution of the surface mixed layer and halocline of the Arctic Ocean. *Journal of Geophysical Research*, **101**, 8807-8821.

Rühland, K., A. Priesnitz, and J.P. Smol, 2003: Evidence for recent environmental changes in 50 lakes the across Canadian Arctic treeline. *Arctic, Antarctic, and Alpine Research,* **35**, 110-23.

Salvigsen, O., S.L. Forman, and G.H. Miller, 1992: Thermophilous mollusks on Svalbard during the Holocene and their paleoclimatic implications. *Polar Research*, **11**, 1-10.

Salzmann, U., A.M. Haywood, D.J. Lunt, P.J. Valdes, and D.J. Hill, 2008: A new global biome reconstruction and data-model comparison for the Middle Pliocene. *Global Ecology and Biogeography*, **17**, 432-447.

Sauer, P.E., G.H. Miller, and J.T. Overpeck, 2001: Oxygen isotope ratios of organic matter in Arctic lakes as a paleoclimate proxy—Field and laboratory investigations. *Journal of Paleolimnology*, **25**, 43-64.

Schauer, U., B. Rudels, E.P. Jones, L.G. Anderson, R.D. Muench, G. Bjőrk, J.H. Swift, V. Ivanov, and A.-M. Larsson, 2002: Confluence and redistribution of Atlantic water in the Nansen, Amundsen and Makarov basins. *Annals of Geophysics*, **20**, 257- 273.

Schindler, D.W. and J.P. Smol, 2006: Cumulative effects of climate warming and other human activities on freshwaters of Arctic and subarctic North America. *Ambio,* **35**, 160-68.

Schlosser, P., B. Ekwurzel, S. Khatiwala, B. Newton, W. Maslowski, and S. Pfirman, 2000:

Tracer studies of the Arctic freshwater budget. In: *The Freshwater Budget of the Arctic Ocean* [Lewis, E.L. (ed.)]. Kluwer Academic Publishers, Norwell, Mass. pp. 453- 478.

Schlosser, P., R. Newton, B. Ekwurzel, S. Khatiwala, R. Mortlock, and R. Fairbanks, 2002: Decrease of river runoff in the upper waters of the Eurasian Basin, Arctic Ocean, between 1991 and 1996—Evidence from d^{18}O data. *Geophysical Research Letters*, **29(9)**, 1289, doi:10.1029/ 2001GL013135.

Schmidt, G.A., A.N. LeGrande, and G. Hoffman, 2007: Water isotope expressions of intrinsic and forced variability in a coupled ocean-atmosphere model. *Journal Geophyscial Research,* **112**, D10103, doi:10.1029/2006JD007781.

Schmittner, A., 2005: Decline of the marine ecosystem caused by a reduction in the Atlantic overturning circulation. *Nature*, **434**, 628-33.

Schneider, K.B. and B. Faro, 1975: Effects of sea ice on sea otters (*Enhydra lutris). Journal of Mammalogy*, **56,** 91-101.

Schouten, S., E.C. Hopmans, and J.S.S. Damsté, 2004: The effect of maturity and depositional redox conditions on archaeal tetraether lipid palaeothermometry. *Organic Geochemistry*, **35(5)**, 567-571

Schrag, D.P., J.F. Adkins, K. McIntyre, J.L. Alexander, D.A. Hodell, C.D. Charles, and J.F. McManus, 2002: The oxygen isotopic composition of seawater during the Last Glacial Maximum. *Quaternary Science Reviews*, **21(1-3)**, 331-342

Schulz, H., U. von Rad, and H. Erlenkeuser, 1998: Correlation between Arabian Sea and Greenland climate oscillations of the past 110,000 years: *Nature*, **393,** 54-57.

Scott, D.B., P.J. Mudie, V. Baki, K.D. MacKinnon, and F.E. Cole, 1989: Biostratigraphy and late Cenozoic paleoceanography of the Arctic Ocean—Foraminiferal, lithostratigraphic, and isotopic evidence. *Geological Society of America Bulletin*, **101**, 260-277.

Seager, R., D.S. Battisti, J. Yin. N. Gordon, N. Naik, A.C. Clement, and M.A. Cane, 2002: Is the Gulf Stream responsible for Europe's mild winters? *Quarterly Journal of the Royal Meteorological Society*, **128(586),** 2563-2586.

Seppä, H., 1996: Post-glacial dynamics of vegetation and tree-lines in the far north of Fennoscandia. *Fennia*, **174**, 1-96.

Seppä, H. and H.J.B. Birks, 2001: July mean temperature and annual precipitation trends during the Holocene in the Fennoscandian tree-line area—Pollen-based climate reconstructions. *The Holocene*, **11**, 527-539.

Seppä, H. and H.J.B. Birks, 2002: Holocene climate reconstructions from the Fennoscandian tree-line area based on pollen data from Toskaljavri. *Quaternary Research*, **57**, 191-199.

Seppä, H. and D. Hammarlund, 2000: Pollen-stratigraphical evidence of Holocene hydrological change in northern Fennoscandia supported by independent isotopic data. *Journal of Paleolimnology*, **24(1),** 69-79.

Seppä, H., H.J.B. Birks, A. Odland, A. Poska, and S. Veski, 2004: A modern pollen-climate calibration set from northern Europe—Developing and testing a tool for palaeoclimatological reconstructions. *Journal of Biogeography*, **31**, 251-267.

Seppä, H., L.C. Cwynar, and G.M. MacDonald, 2003: Post-glacial vegetation reconstruction and a possible 8200 cal. Yr BP event from the low arctic of continental Nunavut, Canada. *Journal of Quaternary Science*, **18**, 621-629.

Serreze, M.C. and J.A. Francis, 2006: The Arctic amplification debate. *Climatic Change*, **76**, 241-264.

Serreze, M.C., A.P. Barrett, A.G. Slater, M. Steele, J. Zhang, and K.E. Trenberth, 2007a: The large-scale energy budget of the Arctic. *Journal of Geophysical Research*, **112**, D11122, doi:10.1029/2006JD008230.

Serreze, M.C., A.P. Barrett, A.G. Slater, R.A. Woodgate, K. Aagaard, R.B. Lammers, M. Steele, R. Moritz, M. Meredith, and C.M. Lee, 2006: The large-scale freshwater cycle of the Arctic, *Journal of Geophysical Research-Oceans*, **111(C11),** C11010.

Serreze, M.C., M.M. Holland, and J. Stroeve, 2007b: Perspectives on the Arctic's shrinking sea ice cover. *Science*, **315**, 1533-1536.

Severinghaus, J.P. and E.J. Brook, 1999: Abrupt climate change at the end of the last glacial period inferred from trapped air in polar ice. *Science*, **286**, 930-934.

Severinghaus, J.P., T. Sowers, E.J. Brook, R.B. Alley and M.L. Bender. 1998: Timing of abrupt climate change at the end of the Younger Dryas interval from thermally fractionated gases in polar ice. *Nature*, **391(6663)**, 141-146.

Sewall, J.O. and L.C. Sloan, 2004: Disappearing Arctic sea ice reduces available water in the American west. *Geophysical Research Letters*, **31**, doi:10.1029/2003GL019133.

Sewall, J.O.and L.C. Sloan, 2001: Equable Paleogene climates: The result of a stable, positive Arctic Oscillation? *Geophysical Research Letters*, **28(19)**, 3693-3695.

Shackleton, N.J., 1967: Oxygen isotope analyses and paleotemperatures reassesssed. *Nature*, **215**, 15-17.

Shackleton, N.J., 1974: Attainment of isotopic equilibrium between ocean water and the benthonic foraminifera genus Uvigerina—Isotopic changes in the ocean during the last glacial. *Coll. Int. du CNRS*, **219**, 203-209.

Shellito, C. J., L.C. Sloan, and M. Huber, 2003: Climate model sensitivity to atmospheric CO_2 levels in the early-middle Paleogene. *Palaeogeography, Palaeoclimatology, Palaeoecology*, **193**, 113-123.

Shindell, D.T., G.A. Schmidt, M.E. Mann, D. Rind, and A. Waple, 2001: Solar forcing of regional climate change during the Maunder Minimum. *Science*, **294**, 2149-2152.

Shuman, C.A., R.B. Alley, S. Anandakrishnan, J.W.C. White, P.M. Grootes and C.R. Stearns, 1995: Temperature and accumulation at the Greenland Summit: comparison of high-resolution isotope profiles and satellite passive microwave brightness temperature trends. *Journal of Geophysical Research*, **100(D5),** 9165-9177.

Siegenthaler, U., T.F. Stocker, E. Monnin, E. Lüthi, J. Schwander, B. Stauffer, D. Raynaud, J.M. Barnola, H. Fischer, V. Masson-Delmotte, and J. Jouzel, 2005: Stable carbon cycle–climate relationship during the late Pleistocene. *Science*, **310,** 1313-1317, doi:10.1126/science.1120130

Sloan, L.C. and E.J. Barron, 1992: A comparison of eocene climate model results to quantified paleoclimatic interpretations. *Palaeogeography, Palaeoclimatology, Palaeoecology*, **93(3-4)**, 183-202

Sloan, L., T.J. Crowley, and D. Pollard, 1996: Modeling of middle Pliocene climate with the NCAR GENESIS general circulation model. *Marine Micropaleontology*, **27**, 51-61.

Sloan, L.C., and D. Pollard, 1998: Polar stratospheric clouds: A high latitude warming mechanism in an ancient greenhouse world. *Geophysical Research Letters*, **25(18),** 3517-3520.

Sluijs, A., U. Rohl, S. Schouten, H.J. Brumsack, F Sangiorgi, J.S.S. Damste, and H. Brinkhuis, 2008: Arctic late Paleocene-early Eocene paleoenvironments with special emphasis on the Paleocene-Eocene thermal maximum (Lomonosov Ridge, Integrated Ocean Drilling Program Expedition 302). *Paleoceanography*, **23(1)**, PA1S11.

Sluijs, A., S. Schouten, M. Pagani, M. Woltering, H. Brinkhuis, J.S.S. Damste, G.R. Dickens, M. Huber, G.J. Reichart, R. Stein, J. Matthiessen, L.J. Lourens, N. Pedentchouk, J. Backman and K. Moran, 2006: Subtropical arctic ocean temperatures during the Palaeocene/Eocene thermal maximum. *Nature*, **441**, 610-613.

Smith, L.C., G.M. MacDonald, A.A. Velichko, D.W. Beilman, O.K. Borisova, K.E. Frey, K.V. Kremenetski, and Y. Sheng, 2004: Siberian peatlands a net carbon sink and global methane source since the early Holocene. *Science*, **303(5656),** 353-356.

Smol, J.P., 1988: Paleoclimate proxy data from freshwater Arctic diatoms. *Internationale Vereinigung für Limnologie*, **23**, 837-44.

Smol, J.P., 2008: *Pollution of lakes and rivers—A paleoenvironmental perspective*. Blackwell Publishing, Oxford, U.K., 2nd ed., 280 pp.

Smol, J.P. and B.F. Cumming, 2000: Tracking long-term changes in climate using algal indicators in lake sediments. *Journal of Phycology*, **36**, 986-1011.

Smol, J.P. and M.S.V. Douglas, 2007a: From controversy to consensus—Making the case for recent climatic change in the Arctic using lake sediments. *Frontiers in Ecology and the Environment*, **5**, 466-474

Smol, J.P. and M.S.V. Douglas, 2007b: Crossing the final ecological threshold in high Arctic ponds. *Proceedings of the National Academy of Sciences, U.S.A.*, **104**, 12,395-12,397.

Solovieva, N., P.E. Tarasov, and G.M. MacDonald, 2005: Quantitative reconstruction of Holocene climate from the Chuna Lake pollen record, Kola Peninsula, northwest Russia. *The Holocene*, **15**, 141-148.

S**orvari**, S. and A. Korhola, 1998: Recent diatom assemblage changes in subarctic Lake Saanajarvi, NW Finnish Lapland, and their paleoenvironmental implications. *Journal of Paleolimnology*, **20(3),** 205-215.

Sorvari, S, A. Korhola, and R. Thompson, 2002: Lake diatom response to recent Arctic warming in Finnish Lapland. *Global Change Biology*, **8**, 171-181.

Sowers, T., Bender, M., Raynaud, D., 1989: Elemental and isotopic composition of occluded O_2 and N_2 in polar ice. *Journal of Geophysical Research-Atmospheres*, **94(D4),** 5137-5150.

Spencer, M.K., R.B. Alley and J.J. Fitzpatrick, 2006: Developing a bubble number-density paleoclimatic indicator for glacier ice. *Journal of Glaciology*, **52(178),** 358-364.

Spielhagen, R.F., K-H Baumann, H. Erlenkeuser, N.R. Nowaczyk, N. Nørgaard-Pedersen, C. Vogt, and D. Weiel, 2004: Arctic Ocean deep-sea record of northern Eurasian ice sheet history. *Quaternary Science Reviews*, **23(11-13)**, 1455-1483.

Spielhagen, R.F., G. Bonani, A. Eisenhauer, M. Frank, T. Frederichs, H. Kassens, P.W. Kubik, N. Nørgaard-Pedersen, N. R. Nowaczyk, A. Mangini, S. Schäper, R. Stein, J. Thiede, R. Tiedemann, and M. Wahsner, 1997: Arctic Ocean evidence for late Quaternary initiation of northern Eurasian ice sheets. *Geology*, **25(9)**, 783-786.

Spielhagen, R.F. and H. Erlenkeuser, 1994: Stable oxygen and carbon isotopes in planktic foraminifers from Arctic Ocean surface sediments—Reflection of the low salinity surface water layer. *Marine Geology*, **119(3/4)**, 227-250.

Spielhagen, R.F., H. Erlenkeuser, and C. Siegert, 2005: History of freshwater runoff across the Laptev Sea (Arctic) during the last deglaciation. *Global and Planetary Change*, **48(1-3)**, 187-207.

Stanton-Frazee, C., D.A. Warnke, K. Venz, D.A. Hodell, 1999: The stage 11 problem as seen from ODP site 982, In: *Marine Oxygen Isotope Stage 11 and Associated Terrestrial Records*, [R.Z. Poore, L. Burckle, A. Droxler, W.E. McNulty (eds.)]. U.S. Geological Survey Open-file Report 99-312, 1999, pp.75.

Steele, M. and T. Boyd, 1998: Retreat of the cold halocline layer in the Arctic Ocean. *Journal of Geophysical Research*, **103**, 10,419-10,435.

Stein, R., S.I. Nam, C. Schubert, C. Vogt, D. Fütterer, and J. Heinemeier, 1994: The last deglaciation event in the eastern central Arctic Ocean. *Science*, **264**, 692-696.

Stötter, J., M. Wastl, C. Caseldine, and T. Häberle, 1999: Holocene palaeoclimatic reconstruction in Northern Iceland—Approaches and results. *Quaternary Science Reviews*, **18**, 457-474.

Stroeve, J., M. Serreze, S. Drobot, S. Gearheard, M. Holland, J. Maslanik, W. Meier, and T. Scambos, 2008: Arctic Sea Ice Extent Plummets in 2007. *EOS, Transactions, American Geophysical Union*, **89(2)**, 13-14.

Sturm, M., T. Douglas, C. Racine, and G.E. Liston, 2005: Changing Snow and shrub conditions affect albedo with global implications. *Journal of Geophysical Research*, **110**, G01004, doi:10.1029/2005JG000013.

Svendsen, J.I. and J. Mangerud, 1997: Holocene glacial and climatic variations on Spitsbergen, Svalbard. *The Holocene*, **7**, 45-57.

Teece, M.A., J.M. Getliff, J.W. Leftley, R.J. Parkes, and J.R. Maxwell, 1998: Microbial degradation of the marine prymnesiophyte *Emiliania huxleyi* under oxic and anoxic conditions as a model for early diagenesis—Long chain alkadienes, alkenones and alkyl alkenoates. *Organic Geochemistry*, **29**, 863-880.

Thomas, D.J., J.C. Zachos, T.J. Bralower, E. Thomas, and S. Bohaty, 2002: Warming the fuel for the fire: Evidence for the thermal dissociation of methane hydrate during the Paleocene-Eocene thermal maximum. *Geology*, **30(12),** 1067-1070.

Thomsen, C., D.E. Schulz-Bull, G. Petrick, and J.C. Duinker, 1998: Seasonal variability of the long-chain alkenone flux and the effect on the Uk37 index in the Norwegian Sea. *Organic Geochemistry*, **28**, 311-323.

Toggweiler, J. R., 2008: Origin of the 100,000-year timescale in Antarctic temperatures and atmospheric CO2. *Paleoceanography*, **23**, PA2211, doi:10.1029/2006PA001405.

Troitsky, S.L.,1964: Osnoviye zakonomernosti izmeneniya sostava fauny po razrezam morskikh meshmorennykh sloev ust-eniseyskoy vpadiny i nishne-pechorskoy depressii. *Akademia NAUK SSSR, Trudy instituta geologii i geofiziki,* **9,** 48-65 (in Russian).

Vassiljev, J., 1998: The simulated response of lakes to changes in annual and seasonal precipitation—Implication for Holocene lake-level changes in northern Europe. *Climate Dynamics*, **14**, 791-801.

Vassiljev, J., S.P. Harrison, and J. Guiot, 1998: Simulating the Holocene lake-level record of Lake Bysjon, southern Sweden. *Quaternary Research*, **49**, 62-71.

Velichko, A.A., A.A. Andreev, and V.A. Klimanov, 1997: Climate and vegetation dynamics in the tundra and forest zone during the Late Glacial and Holocene. *Quaternary International*, **41/42**, 71-96.

Velichko, A.A., and V.P. Nechaev (eds), 2005: *Cenozoic climatic and environmental changes in Russia*. [H.E. Wright, Jr., T.A. Blyakharchuk, A.A. Velichko and Olga Borisova (eds. of English version)]. The Geological Society of America Special Paper, **382**, 226 pp.

Vinther, B.M., H.B. Clausen, S.J. Johnsen, S.O. Rasmussen, K.K. Andersen, S.L. Buchardt, D. Dahl-Jensen, I.K. Seierstad, M.L. Siggaard-Andersen, J.P. Steffensen, A. Svensson, J. Olsen, and J. Heinemeier, 2006: A synchronized dating of three Greenland ice cores throughout the Holocene. *Journal of Geophysical Research*, **111**, D13102, doi:13110.11029/12005JD006921.

Vörösmarty, C.J., L.D. Hinzman, B.J. Peterson, D.H. Bromwich, L.C. Hamilton, J.Morison, V.E. Romanovsky, M.Sturm, and R.S. Webb. 2001: The Hydrologic Cycle and its Role in Arctic and Global Environmental Change: A Rationale and Strategy for Synthesis Study. Fairbanks, Alaska: Arctic Research Consortium of the U.S., 84 pp.

Vörösmarty, C., L. Hinzman, and J. Pundsack, 2008: Introduction to special section on Changes in the Arctic Freshwater System: Identification, Attribution, and Impacts at Local and Global Scales. *Journal of Geophysical Research-Biogeosciences*, **113(G1)**, G01S91.

Walter, K.M., S.A. Zimov, J.P. Chanton, D. Verbyla, and F. S. Chapin, III, 2006: Methane Bubbling from Siberian Thaw Lakes as a Positive Feedback to Climate Warming. *Nature*, **443**, 71-75.

Walter K.M., M. Edwards S.A. Zimov G. Grosse F.S. Chapin, III, 2007: Thermokarst lakes as a source of atmospheric CH4 during the last deglaciation. *Science*, **318,(5850)**, 633-636.

Wang, Y.J., **H. Cheng, R. L. Edwards, Z. S. An, J. Y. Wu, C.-C. Shen, J. A. Dorale**, 2001: A high-resolution absolute-dated late Pleistocene monsoon record from Hulu Cave, China. *Science*, **294**, 2345-2348.

Weaver, A.J., C.M. Bitz, A.F. Fanning, and M.M. Holland, 1999: Thermohaline circulation—High latitude phenomena and the difference between the Pacific and Atlantic. *Annual Review of Earth and Planetary Sciences*, **27**, 231-285.

Weckström, J., A. Korhola, P. Erästö, and L. Holmström, 2006: Temperature patterns over the past eight centuries in northern Fennoscandia inferred from sedimentary diatoms. *Quaternary Research*, **66**, 78-86.

Weijers, J.W.H., S. Schouten, O.C. Spaargaren, and J.S.S. Damsté, 2006: Occurrence and distribution of tetraether membrane lipids in solid—Implications for the use of the TEX_{86} proxy and the BIT index. *Organic Geochemistry*, **37(12)**, 1680-1693.

Weijers, J.W.H., S. Schouten, A. Sluijs, H. Brinkhuis, and J.S.S. Damste, 2007: Warm arctic continents during the Palaeocene-Eocene thermal maximum. *Earth and Planetary Science Letters,* **261(1-2),** 230-238.

Werner, M., U. Mikolajewicz, M. Heimann, and G. Hoffmann, 2000: Borehole versus isotope temperatures on Greenland—Seasonality does matter. *Geophysical Research Letters,* **27**, 723-726.

Whitlock, C. and M.R. Dawson, 1990: Pollen and vertebrates of the early Neogene Haughton Formation, Devon Island, Arctic Canada. *Arctic*, **43(4)**, 324-330.

Wiles, G.C., D.J. Barclay, P.E. Calkin, and T.V. Lowell, 2008: Century to millennial-scale temperature variations for the last two thousand years indicated from glacial geologic records of Southern Alaska. *Global and Planetary Change*, **60,** 15-125.

Williams, C..J., A.H. Johnson, B.A. LePage, D.R. Vann and T. Sweda, 2003: Reconstruction of Tertiary Metasequoia Forests II. Structure, Biomass and Productivity of Eocene Floodplain Forests in the Canadian Arctic, *Paleobiology,* **29**, 271-292.

Wohlfahrt, J., S.P. Harrison, and P. Braconnot, 2004: Synergistic feedbacks between ocean and vegetation on mid- and high-latitude climates during the Holocene. *Climate Dynamics*, **22**, 223-238.

Wohlfarth, B., G. Lemdahl, S. Olsson, T. Persson, I. Snowball, J. Ising, and V. Jones, 1995: Early Holocene environment on Bjornoya (Svalbard) inferred from multidisciplinary lake sediment studies. *Polar Research*, **14**, 253-275.

Wooller, M.J., D. Francis, M.L. Fogel, G.H. Miller, I.R. Walker, and A.P.Wolfe, 2004: Quantitative paleotemperature estimates from delta O-18 of chironomid head capsules preserved in arctic lake sediments. *Journal of Paleolimnology*, **31(3),** 267-274.

Wuchter, C., S. Schouten, M.J.L. Coolen, and J.S.S. Damsté, 2004: Temperature-dependent variation in the distribution of tetraether membrane lipids of marine Crenarchaeota—Implications for TEX86 paleothermometry. *Paleoceanography*, **19(4)**, PA4028

Zachos, J.C., Dickens, G.R., Zeebe, R.E., 2008: An early Cenozoic perspective on greenhouse warming and carbon-cycle dynamics. *Nature*, **451** (7176), 279-283.

Zachos, Z., P. Pagani, L. Sloan, E. Thomas, and K. Billups, 2001: Trends, rhythms, and aberrations in global climate 65 Ma to present. *Science*, **292**, 686-693.

Zazula G.D., D.G. Froese, C.E. Schweger, R.W. Mathewes, A.B. Beaudoin, A.M. Telka, C.R. Harington, and J.A. Westgate, 2003: Ice-age steppe vegetation in east Beringia - tiny plant fossils indicate how this frozen region once sustained huge herds of mammals. *Nature*, **423**, 603-603.